Stress Induced Failure in Materials Subjected to Extremal Heat Fluxes

by

Dominic S. Napolitano

B.S.E. in Mechanical Engineering and Applied Mechanics,
University of Pennsylvania, May 1993

Submitted to the Department of Mechanical Engineering in Partial Fulfillment of the Requirements for the Degree of

Master of Science in Mechanical Engineering

at the

MASSACHUSETTS INSTITUTE OF TECHNOLOGY

June, 1995

Signature of Author.....
Department of Mechanical Engineering
May, 12 1995

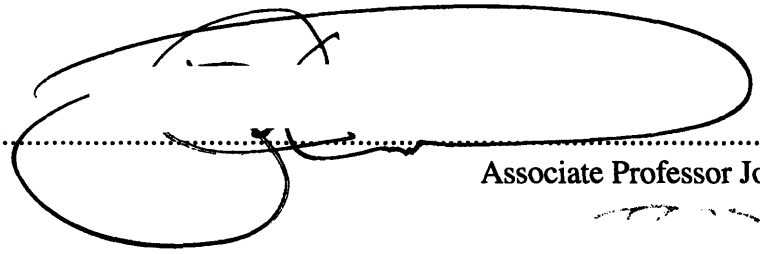

Certified by.....
Associate Professor John H. Lienhard V
Thesis Supervisor

Accepted by.....
Professor Ain A. Sonin
Chairman, Department Committee on Graduate Studies

For Josephine

Acknowledgments

This thesis work was supported and facilitated by many people. I would like to thank the members of the Defense Nuclear Facilities Safety Board (Mr. John T. Conway, Dr. A.J. Eggenberger, Mr. John W. Crawford, Jr., Mr. Joseph J. DiNunno, and Dr. Herbert John Cecil Kouts) for sponsoring my education at MIT. I am grateful for the opportunity.

I wish to thank my advisor, Dr. John H. Lienhard V, for the thoughtful guidance he provided for this work. His advice significantly shaped the thesis' structure and content.

I also want to thank my colleagues in the Heat Transfer Laboratory: Aaron Flores, Marc Hodes, James Moran, Tolga Ozgen, Andreas Pfahnl, and Sheit Chen, for their insightful suggestions and, of course, for the debates that we so often had.

Stress Induced Failure in Materials Subjected to Extremal Heat Fluxes

by
Dominic S. Napolitano

Submitted to the Department of Mechanical Engineering on May, 12 1995 in partial fulfillment of the requirements for the degree of Master of Science in Mechanical Engineering

Abstract

In 1992, Massachusetts Institute of Technology researchers demonstrated that heat fluxes of up to 400 MW/m^2 can be dissipated by liquid jets. These studies indicated that the mechanical strength of a material limits achievable heat flux. This conclusion is the impetus for the present thesis.

To use the results of the jet heat transfer research for design, tools are needed to evaluate candidate materials. Analytical and numerical models are developed here for this purpose. Localized and uniform surface heating configurations are examined. The models consider both elastic and plastic behaviors. The effects of temperature dependent properties are also incorporated. These models are used to evaluate candidate materials. A design methodology is developed. It explains which models are appropriate to a particular design and which steps are necessary for design.

Heat flux values that induce elastic and plastic failure of candidate materials are determined. A key conclusion reached by this thesis is that extremal heat fluxes generally induce plastic material behavior. Plastic behavior offers significant thermal stress relief. It is shown, that plasticity can be incorporated into design if deflections are maintained below the thickness of the material. Design recommendations and stress correlations are established based on these limits.

Another important conclusion of this thesis is that material performance rankings must consider the effect on strength variations across a temperature gradient. Simple figure of merit systems, based on uniform heating, can yield specious results.

Two material ranking systems- one for elastic design and one for plastic design- are developed in this thesis. These ranking systems show that, generally, elastic designs should incorporate materials with high thermal conductivities. At extremal heat flux levels, where plastic deformation occurs, the ranking systems indicate that mechanical strength becomes more important than thermal conductivity.

Thesis Supervisor: John H. Lienhard V
Title: Associate Professor of Mechanical Engineering

Table of Contents

List of Tables

List of Figures

Nomenclature

I. Coordinate System Variables

x,y,z - Cartesian coordinates
r,θ,z - cylindrical coordinates

II. Roman Symbols

A	Maximum stagnation pressure of cooling jet
a	constant in the gaussian function exp(-ar^2) unless otherwise defined
b	radius of circular plate unless otherwise defined
D	Bending rigidity
E	Young's modulus
E_T	Secant modulus
G	Shear modulus
ierfc	integral of the error function
k	thermal conductivity
M_r	bending moment in r per unit length
M_T	thermal moment
M_θ	bending moment in θ per unit length
N_r	in plane force in r per unit length
N_T	thermal force
N_{Tcr}	thermal stress buckling criteria
N_θ	in plane force in θ per unit length
n	plasticity strain hardening index
p	plasticity strength coefficient
ro	the constant in the gaussian expression exp(-ar^2) for cooling jet
r_i	radius of cooling jet stagnation zone
T	temperature rise over reference temperature
T_o	reference temperature
T_t	temperature
$\hat{T}_t$	non-linear component of temperature distribution
T_c	minimum temperature of body
T_h	maximum temperature of body
T_n	the integral over the thickness of a body of the temperature multiplied by the thickness variable
T_{cold}	minimum temperature rise in body
T_{hot}	maximum temperature rise in body
Q	Heat flux
q	pressure distribution
u	displacement in radial direction
u°	displacement of mid-plane in radial direction
v	displacement in tangential direction
v°	displacement of mid-plane in tangential direction

w	deflection; displacement in transverse direction

II. Greek Symbols

α	coefficient of linear thermal expansion
α_t	thermal diffusivity
δ	conducting length of a finite element
ε_i	strain in i direction
ε_l	linear strain component of ε_i
ε_n	non-linear strain component of ε_i
ϕ	potential function, second derivative of which is stress
γ_{ii}	shear strain component ij
ν	Poisson's ratio
σ_{ii}	stress component in ij
$\sigma_{1.2.3}$	principal stress components
σ_p	stress in material undergoing plastic deformation
σ_y	yield strength
σ_u	ultimate strength
$\sigma_{1.2.iet}$	principal stress due to cooling jet
$\sigma_{1.2.t}$	principal stress due to temperature gradient
τ_{ii}	shear stress component ij
ψ	potential function, derivative of which is displacement

Chapter 1

Introduction

The need to dissipate large heat fluxes has continuously increased since the Industrial Revolution. Technological developments in the nuclear and aerospace industries augmented this need. In recent times, many engineering systems can be conceived of whose heat removal requirements are not met by contemporary technology. Rapid advances in electronics have established a trend toward smaller systems with higher power densities. Advanced neutron sources, fusion systems, and some accelerator units all require the removal of heat fluxes larger than what present heat exchanger technology can accommodate.

Contemporary heat transfer research aims to meet the needs of extreme heat flux systems. Research efforts include developments in micro-configured boiling, micro-channel heat exchangers, and liquid jet impingement. Cooling jets are the subject of this study.

In 1992, Massachusetts Institute of Technology researchers (Liu and Lienhard) demonstrated that heat fluxes of up to 400 MW/m^2 can be dissipated by liquid jets[1]. This value is approximately 6.3 times the flux at the Sun's surface. Before this work, the highest heat flux achieved was 337 MW/m^2 [2].

Liu and Lienhard indicated that the mechanical strength of materials limits increasing heat flux levels. This study begins where the Liu and Lienhard study left off. It focuses on how and why materials fail under extreme heat fluxes. The goal is to establish which type of materials and heating configuration characteristics allow high heat fluxes to be achieved.

This thesis has three components. First, one dimensional thermal stress models are considered. These determine which parameters and scenarios should be included in more

---

[1]Liu, Xin, *Liquid Jet Impingement Heat Transfer and its Potential Applications at Extremely High Heat Fluxes,* Ph.D Thesis, M.I.T., Cambridge, MA, 1992.
[2]*Ibid.*

complicated models. These variables include transient heating, plasticity, end restraints, and material temperature dependence.

The second element of this thesis considers the case of heating a small region on a material's surface. Previous work in this area includes: simple hot spot stress models,[3] X-ray diffraction heat load solutions[4], and various welding studies[5]. The hot spot models are used in this thesis as a first estimate of localized thermal stresses. Kushnir's work on inclined monochromators provides accurate analytical solutions of the temperature distribution in a rectangular beam subjected to a flux loading. Welding studies comprise the bulk of past localized heating research. The reference provided is a good summary document. It is suggested for further reading. However, welding studies are highly case specific. They are not easily translatable to the scenarios examined in this thesis.

Localized heating problems are examined with both analytical and numerical tools. The analytical models are based on classical plate theory. Classical theory is readily applicable to problems involving both thermal and mechanical loads. These models are used to describe the heat flux limits on candidate materials which behave elastically. Numerical models are employed to account for non-linear material behavior - temperature dependence and plasticity. They help determine the heat fluxes which cause inelastic failure.

The last area of this study concerns uniformly heating a material's surface. Analytical and numerical models are used to describe the elastic and plastic limits on heat flux. Previous work in this area includes the development of a ranking system for material performance under steady state and transients conditions[6]. The rankings are limited to elastic materials at uniform temperatures. Therefore, at extreme heat flux levels these rankings must be used with caution.

---

[3]Johns, D.J., *Thermal Stress Analyses*, Pergamon Press Ltd, 1960.
[4]Kushnir, Vladimir, *Temperature Distribution, Deformations, and X-ray Diffraction in the Inclined Heat Load Monochromator: Analytical Solutions*, Rev. Sci. Instrum., 65, November 1994.
[5]Hetnarski, R.B., *Thermal Stresses, Vol. I.*, Elsevier Science Publishers B.V., 1986.
[6]Abou, et. al., *Magnetic Fusion Energy Plasma Interactive and High Heat Flux Components, Vol. 2*, UCLA/PPG-815, DOE Office of Fusion Energy, June 1984.

Chapter 2

Generalization of Past Experiments - Framework for Models

2.1 Description of Heating Configuration

The Liu and Lienhard experimental apparatus is shown in figure 2.1. A 1 mm thick plate, fixed on all edges, is heated by the plasma arc of a 21.8 kW AIRCO-3A/DDR245 TIG welder. The plate is cooled by a water jet from a 34 MPa piston pump. The jet exits a cylindrical plenum 1.4 m long and .19 mm in diameter. The jet stagnation pressure ranges from 2.06 to 8.97 MPa. Its temperature is approximately 20 C [7].

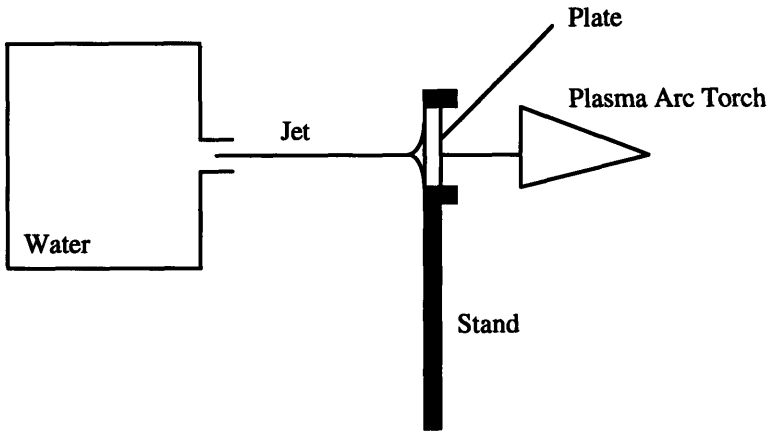

Figure 2.1: Experimental Setup for the Liu and Lienhard Experiment

A portion of the plate is expected to melt. A liquid pool results as shown in figure 2.2. At the base of the pool, the plate temperature equals the melting point temperature. The minimum plate temperature ranges from 20-100 C depending on the heat flux.

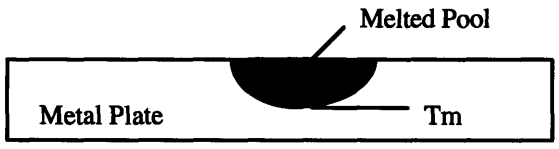

Figure 2.2: Schematic of melted region in metal plate used in Liu and Lienhard experiment. Tm is melting temperature.

[7]Liu, Xin, *Liquid Jet Impingement Heat Transfer and its Potential Applications at Extremely High Heat Fluxes*, Ph.D Thesis, M.I.T., Cambridge, MA, 1992.

The region of interest for the thermal stress analysis is the unmelted portion. This study focuses on stress failures. Melting should not occur in a structure. Consequently, the case shown in figure 2.2 is not considered in the design models developed in this thesis. Instead a solid 1 mm thick plate, heated to its melting point and cooled on its base, provides the general heating configuration for this thesis.

2.2 General Framework for Models

2.2.1 Temperature Distribution and Anisotropic Behavior of Materials

In Cartesian coordinates, temperature distributions in the Liu and Lienhard experiment are the result of a transient three dimensional heating process. In cylindrical coordinates it is reasonable to assume that the heat flux loading varies only in the radial direction - resulting in a two dimensional temperature distribution (along the radius and through the thickness of the plate). The simplification offered by cylindrical coordinates will be used throughout this thesis.

As will be discussed in Chapter 4, when the radius of the heated region is much larger than the plate thickness, it can be assumed that the temperature varies linearly through the plate thickness. Thus, the simplified version of the Liu and Lienhard experiment is a two dimensional temperature model with a linear temperature variation through the depth of the plate.

It is necessary to discuss a basic proof in thermal stress analysis before continuing. Timoshenko and Goodier have proven that in steady state, a two dimensional, homogeneous, isotropic, and unrestrained material will not experience thermal stresses. Additionally, temperature distributions which vary linearly in x, y, z coordinates will not result in thermal stresses.[8]

These proofs are for a Cartesian coordinate system. A two dimensional temperature distribution which satisfies Laplace's equation in cylindrical coordinates may still yield thermal stresses. Additionally, if end restraints exist or if temperature varies non-linearly through the body, thermal stresses arise. Non-linearities may be the result of either anisotropies, including material temperature dependence, or thermal transients.

---

[8] Timoshenko, S., and Goodier, J.N., *Theory of Elasticity*, The Maple Press Company, 1951.

2.2.2 Material Properties

A material which transmits an extermal heat flux will have a very large temperature gradient across its thickness. Consequently, material property values may vary significantly in the body. The properties of importance include thermal conductivity, thermal diffusivity, the thermal expansion coefficient, Young's modulus, and the yield and ultimate strengths.

Four candidate materials have been chosen for detailed analysis in this thesis. Two refractory materials - molybdenum and tungsten - are examined. These metals were used in the Liu and Lienhard experiments, thus their behavior under extreme heat fluxes is known in a qualitative sense. They are high strength materials with high melting points - desirable characteristics in extreme environments. However, molybdenum is ductile and tungsten is brittle. The results for these materials are used to illustrate how high temperature metals behave and also to distinguish between brittle and ductile behavior.

Stainless Steel 304 L and Aluminum 6061 are also examined. Both of the materials are widely used in structural design. However, these materials were chosen to illustrate key points. Stainless steel is a high strength metal but it has a low thermal conductivity. Aluminum is a low strength metal, but it has a high conductivity. Actually, in this thesis the thermal conductivity of Aluminum 6061 has been over-estimated. The thermal conductivity of pure aluminum is used to describe the alloy. The behaviors of steel and aluminum help to answer the question of whether thermal or mechanical properties are more important for transmitting extreme heat fluxes.

2.2.3 Plane Strain and Plane Stress Assumptions

The solution of the three dimensional thermal stress equations is difficult to obtain analytically. If the problem satisfies either the conditions of plane stress or plane strain, its complexity can be reduced to a system involving only two dimensions.

Plane strain occurs in a body when the *strain* in one direction is zero. This condition is satisfied when the body is fixed in one plane or when the body's length in one direction is large enough so that a small change in length maintains the strain at approximately zero.

A problem arises when plane strain is used to describe the stress field in a free body. In this case, the boundary conditions require the ends to be free of tractions, yet simultaneously plain strain requires a normal traction on the plate's ends equivalent to $E\alpha T$. To satisfy the boundary conditions, the solution of an isothermal problem with tractions of $-E\alpha T$ on the plate ends must be superimposed upon the thermal solution to get a meaningful answer. This problem can be dealt with using Saint-Venant's (see Boley for a discussion of this method).[9]

The plane strain hypothesis simplifies the equations of equilibrium (see Gatewood)[10]. If the strain in the z direction (plate thickness) is zero, the components of the Cauchy stress tensor become:

$$\sigma_{xx}=f_1(x,y) \quad \sigma_{yy}=f_2(x,y) \; \sigma_{xy}=f_3(x,y) \; \sigma_{xz}=\sigma_{yz}=0 \qquad (2.1)$$
$$\sigma_{zz}=\upsilon(\sigma_{xx}+\sigma_{yy}) - E\alpha T$$

where the functions are determined by solving the equilibrium equations with the appropriate boundary conditions.

These simplifications hold only when the mechanical loads and the temperature distribution in a body are independent of the direction in which the strain is zero. Thus, for the case of plane strain, the temperature can be an arbitrary function of two directions.

Plane stress occurs when the *stress* in one direction is zero. If the stress in the z direction (plate thickness) is zero, the components of the Cauchy stress tensor acting in the z direction simplify to:

$$\sigma_{zz}=\sigma_{xz}=\sigma_{yz}=0 \qquad (2.2)$$

The condition for plane stress is satisfied when a body is very thin in one direction compared to the body's length in the other two directions. When this occurs the stresses in the smallest direction can be neglected. However, plane stress is restrictive in its allowable temperature distributions. Substitution of the above stress tensor components into the stress compatibility equations yields the statement that the temperature can only be a function of the direction in which the stress is zero or a linear function of this

[9]Boley, B.A., *Theory of Thermal Stress*, John Wiley and Sons, Inc., 1960.
[10]Gatewood, B.E., *Thermal Stresses*, McGraw-Hill, Inc., 1957.

direction and an arbitrary function of another direction. An exception to this rule is discussed in section 4.2.2.

In this study, both the assumption of plane stress and plane strain are used to model the heated plate. In the literature, plane stress is used to provide a convenient way to solve the equilibrium equations. However, it is possible to convert plane stress solutions to plane strain solution by a simple set of variable transformations. To see this, examine the expressions for strain under both assumptions:

Plane Strain	Plane Stress
$\varepsilon_x = \frac{1-\nu^2}{E}(\sigma_x - \frac{\sigma_y \nu}{1-\nu})$	$\varepsilon_x = \frac{1}{E}(\sigma_x - \sigma_y \nu)$
$\varepsilon_y = \frac{1-\nu^2}{E}(\sigma_y - \frac{\sigma_x \nu}{1-\nu})$	$\varepsilon_y = \frac{1}{E}(\sigma_y - \sigma_x \nu)$ (2.3)
$\gamma_{xy} = \frac{\tau_{xy}}{G}$	$\gamma_{xy} = \frac{\tau_{xy}}{G}$

Comparing these two sets of equations, it is obvious that to convert plane stress solutions to plane strain solutions one needs only to substitute the quantities E and ν for the variables $E/(1-\nu^2)$ and $\nu/(1-\nu)$. A similar comparison between the stress equations shows that α in plane stress solutions must also be converted to $\alpha(1+\nu)$ for plain strain[11].

[11]Boley, B.A., *Theory of Thermal Stress*, John Wiley and Sons, Inc., 1960.

Chapter 3

One Dimensional Models

One dimensional temperature and stress field models yield a first approximation for the actual case. The purpose of this section is to determine which heating configurations and parameters should be considered in this study.

The following chapter considers a rectangular parallelepiped with insulated ends. A temperature gradient is imposed across the plate thickness. First, the steady state case with and without the effects of temperature dependent conductivity is considered. The second portion of this chapter examines transient and plastic behaviors..

Conclusions are drawn concerning the relative importance of the transient versus the steady state case and the influence of material properties on elastic and plastic failure.

3.1 Body in Steady State with Isotropic Material Properties

This case is shown in figure 3.1 with boundary conditions. The ends of the slab are insulated, so the temperature varies in y only. The solution to Laplace's is:

$$T_t(y) = \frac{T_h - T_c}{2}\frac{y}{H} + \frac{T_h + T_c}{2} \tag{3.1}$$

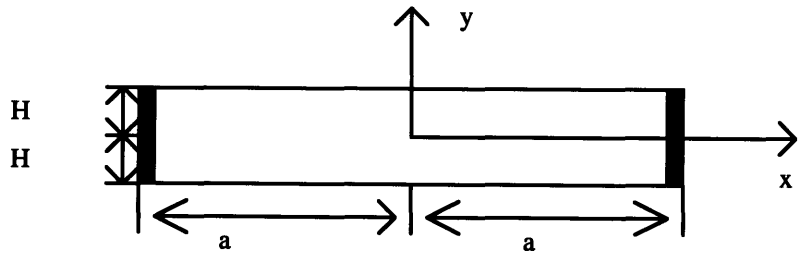

Figure 3.1:Beam with insulated ends, basis for one dimensional model.

Boundary Conditions:

$$\frac{dt}{dx}_{x=a} = \frac{dt}{dx}_{x=-a} = 0$$
$$T_t(y = H) = T_h$$
$$T_t(y = -H) = T_c$$

The beam shown in figure 3 satisfies the plane stress hypothesis explained in section 2.2.3. Consequently, the only stress component for an arbitrary temperature function of y is along the x-axis of the body. The stress compatibility equations (see Gatewood)[12] can then be solved for the stress in x:

$$\sigma_{xx} = -E\alpha T + C_1 + C_2 y \tag{3.2}$$

Where C1 and C2 are constants determined by the boundary conditions. Johns[13] solves this equation assuming that the beam in neither restricted in bending nor axial expansion, *i.e.*, a free beam. The results is:

$$\sigma_{xx} = -E\alpha T + \frac{1}{2H}\int_{-H}^{H} E\alpha T dy + \frac{3y}{2H^3}\int_{-H}^{H} E\alpha T y dy \tag{3.3}$$

If the plate is restrained in bending, the last term goes to zero. If the plate's axial expansion is restrained, the second term is zero. If the plate is free and the temperature is a linear function of y, as in figure 3, the complete stress equation evaluates to zero.

The body in figure 3 will not be thermally stressed if it is unrestrained. Stresses will arise if it is restrained in either bending or axial expansion. The table below illustrates stress results for a number of materials when restrained. The stress value shown is the maximum stress in the body. Figures 3.2-3.4 show example stress fields in molybdenum for the three types of restraints.

---

[12]Gatewood, B.E., *Thermal Stresses*, McGraw-Hill, Inc., 1957.
[13]Johns, D.J., *Thermal Stress Analyses*, Pergamon Press Ltd, 1960.

Material	Melting Point (K)	Flux (MW)	Stress (MPa) if: free	ends restrained	bending restrained	fully restrained	Yield at STP (MPa)
molybdenum	2883	207.2	0	-774	-777	-1551	380
tungsten	3660	585.9	0	-3374	-3384.2	-6758.3	197
aluminum 6010	993	154	0	-293.2	594.9	-590.6	300
stainless steel 304L	1670	31.1	0	-1962	3954	-3940	415

Table 3.1: Results of one dimensional stress models for four materials. Maximum flux is based on a temperature difference of the melting temperature minus the cooling temperature of 20 C. STP refers to standard temperature and pressure.

Table 3.1 illustrates a number of important points. First, unrestrained beams are not stressed. Second, if the material is restrained in either bending or compression, thermal stresses are very large in comparison to the yield strength. Therefore, plastic deformation is expected to occur when restrained materials are heated to their respective melting temperatures.

Regarding the Liu and Lienhard experiment, the one dimensional models suggest that beams may have locally yielded in the region of the hot spot. This will be examined more closely in the following two chapters.

Fig. 3.2: Stress in axial restrained molybdenum.

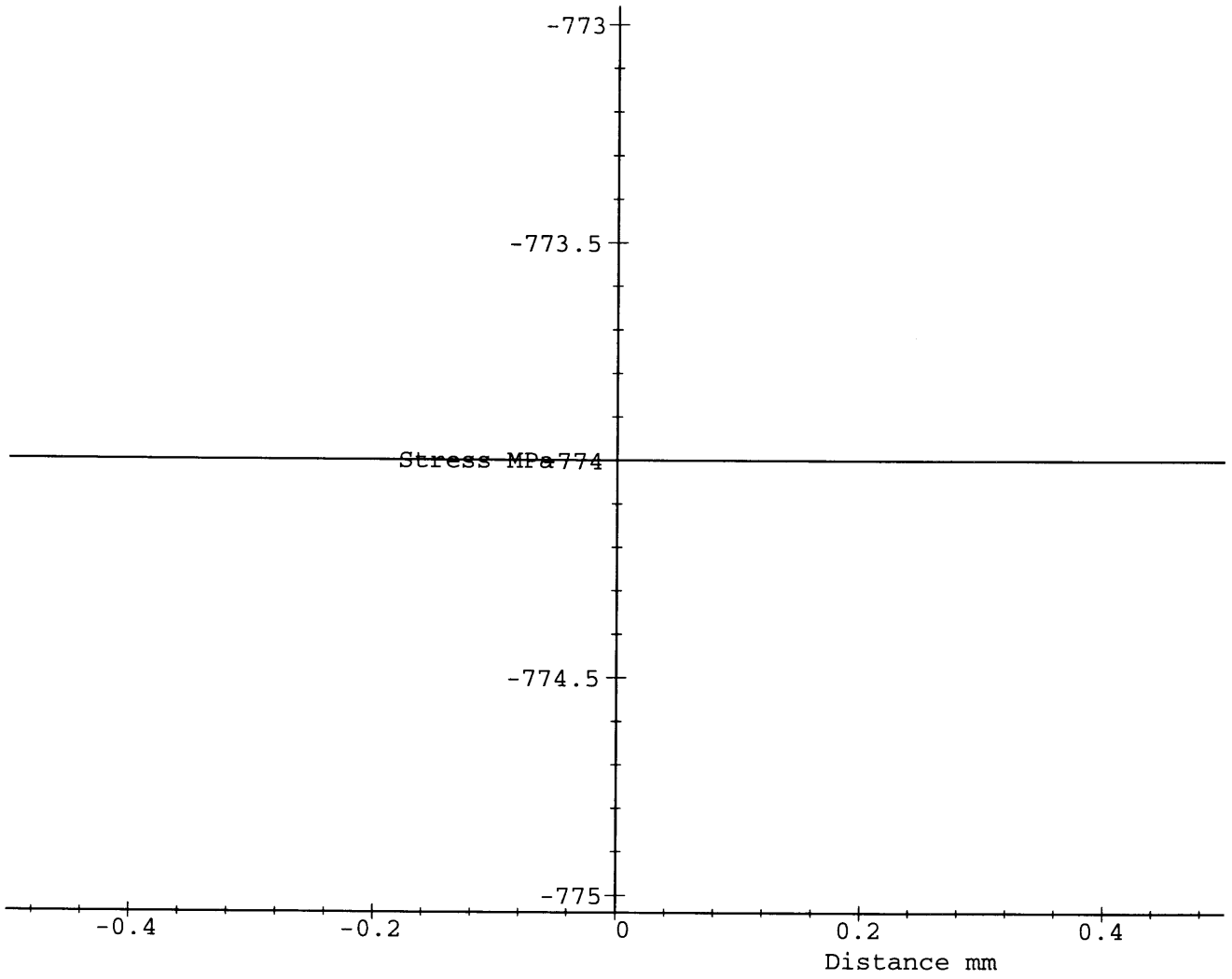

Fig. 3.3: Stress in bending restrained molybdenum

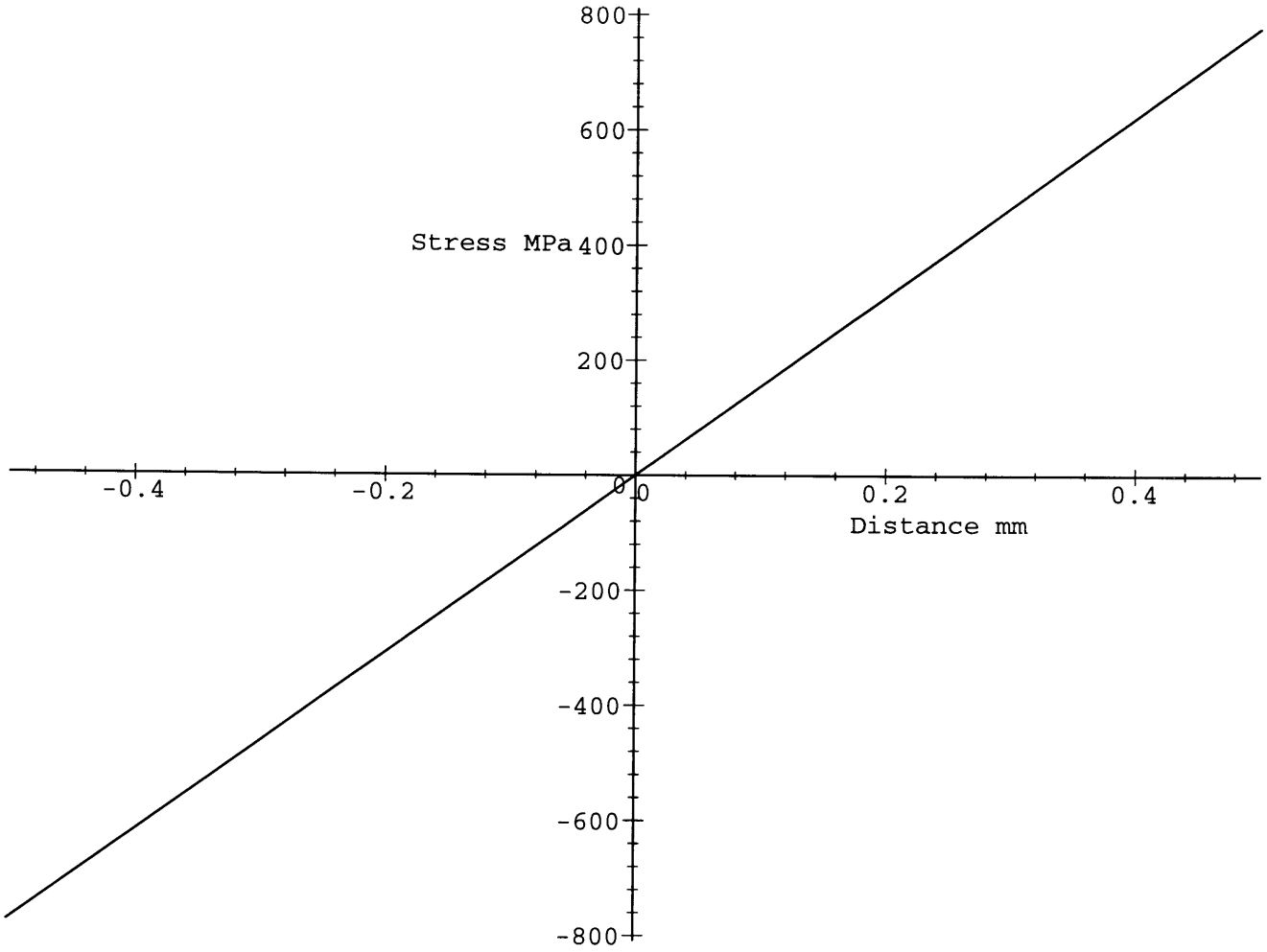

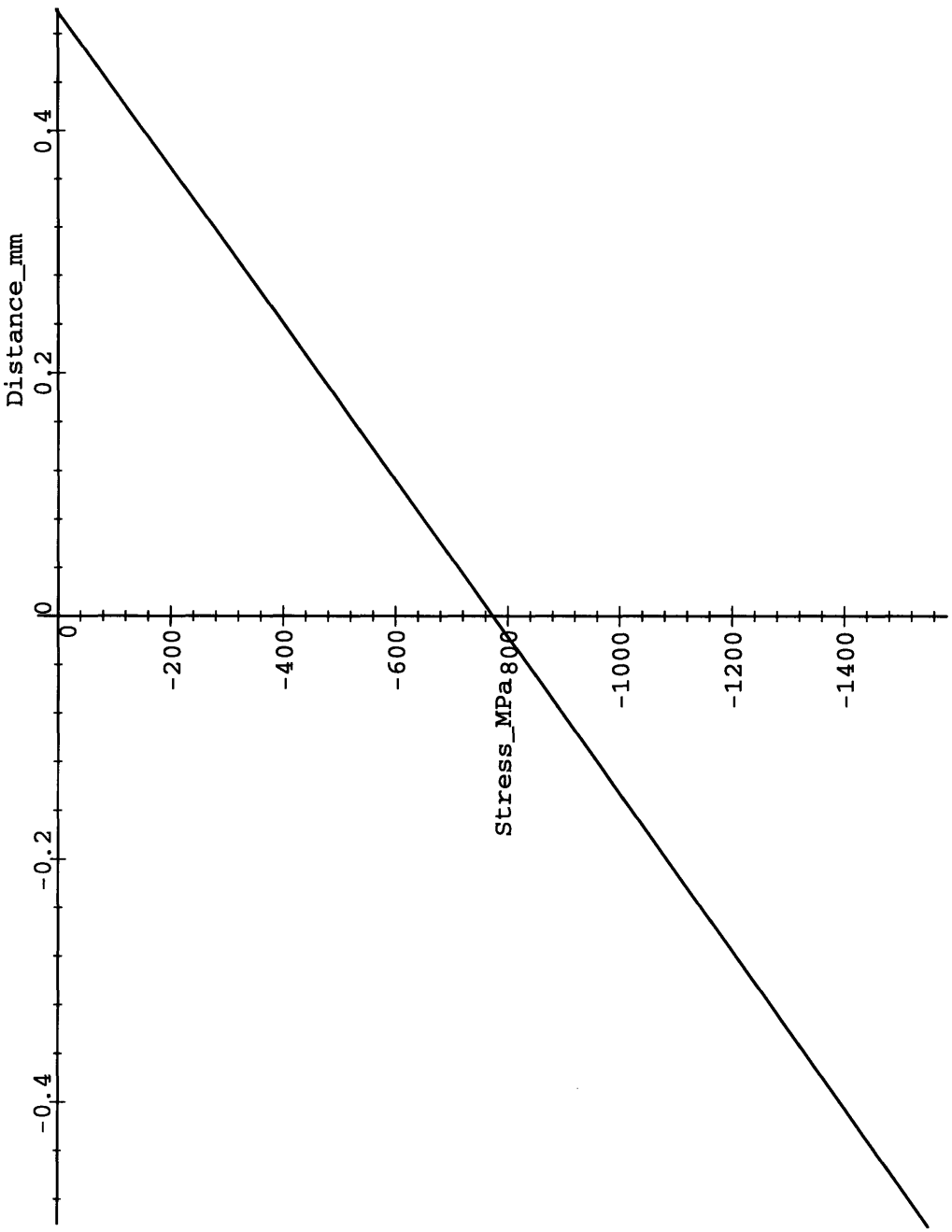

Fig. 3.4: Stress in fixed molybdenum.

3.2 Body in Steady State with Temperature Dependent Material Properties

This section lifts the restriction that the slab have homogeneous and isotropic material properties. Since material properties vary with temperature, a body subjected to a large temperature gradient will have non-uniform properties. In this case, the one dimensional Laplace equation for temperature becomes,

$$\frac{d}{dy}(k(T_t)\frac{dT_t}{dy}) = 0 \tag{3.4}$$

This equation can be solved easily once it is known how the conductivity varies with temperature. The general solution is given by Gebhart (albeit, with a change of coordinates) as,[14]

$$\int_{T_h}^{T} k(T_t)dT_t = \frac{y}{2H}\int_{T_h}^{T_c} k(T_t)dT_t \tag{3.5}$$

The stress equation (3.2) given above still holds. However, now both the Young's modulus and the thermal expansion coefficient are functions of the temperature. This must be accounted for in determining the constants. Equation (3.3) becomes[15]:

$$\sigma_{xx} = E(-\alpha T + \frac{\int_{-H}^{H} E\alpha T dy}{\int_{-H}^{H} E dy} + y\frac{\int_{-H}^{H} E\alpha T dy}{\int_{-H}^{H} Ey^2 dy}) \tag{3.6}$$

When equation 3.5 is substituted for the temperature in equation 3.6 it must also be substituted into the material property functions to eliminate the temperature variable in the stress equation. The difference between this section and the previous section is that now, the temperature is a non-linear function of y. Thermal stresses are expected in the free beam case.

These equations have been used to calculate the stress field in four materials as shown in table 3.2. As before, the table gives the value of the maximum stress. Figures 3.5-3.8

---

[14]Gebhart, B., *Heat Conduction and Mass Transfer*, McGraw-Hill, Inc., 1993.
[15]Goodier, J.N., *Thermal Stress*, Journal of Applied Mechanics, Trans. ASME, Vol.59, March 1937.

show example stress fields for free and restrained beams. The functional forms of the material properties have been found by curve fitting data given in handbooks to yield approximate functions (see appendix for equations).[16,17,18,19,20]

Material	Melting Point (K)	Flux (MW)	Stress (MPa) if: free	ends restrained	bending restrained	fully restrained	Yield Stress (MPa) at STP
molybdenum	2883	229.1	775	750	1000	-1200	380
tungsten	3660	759.3	840	4080	-4720	-7120	197
aluminum 6010	993	159.4	40	-450	-462	-850	300
stainless steel 304L	1670	36	700	3050	-3300	-5000	415

Table 3.2: Results for anisotropic one-dimensional models. Formulas for material property as given above.

Table 3.2 illustrates the importance of considering temperature dependent material variations. The three properties considered here are thermal conductivity, the modulus of elasticity, and the coefficient of linear thermal expansion. These parameters have opposing influences on the thermal stress level. Thus, the resultant stress can be higher or lower than the isothermal case depending on the material.

The variation in conductivity creates a non-linear temperature distribution which induces thermal stresses in the free beam. The expansion coefficient increases with temperature. It tends to augment the stress level. The Young's modulus decreases with temperature. This has the effect of decreasing stress levels.

The results show that the general effect of temperature dependent properties is to increase stress levels relative to the homogeneous case. This does not hold true for aluminum.

---

[16]Wilson, J.W., and Tietz, T.E., Behavior and Properties of Refractory Metals, Stanford University Press, 1965.
[17]Touloulcian, *et.al, Thermophysical Properties of Matter, Vol.I*, TPRC Data Series, 1979.
[18]Holt, John., *et. al., Structural Alloys Handbook*,Purdue University, 1993.
[19]*Handbook of Stainless Steel*, Peckner/Bernstein, 1977.
[20]*Metals Handbook, Vol.2*, Mechanical Testing, American Society for Metals, 1985.

These results illustrate that the effect of temperature dependent material properties is not ignorable for materials subjected to melting point temperatures.

Fig. 3.5: Stress in free molybdenum- temperature dependent properties.

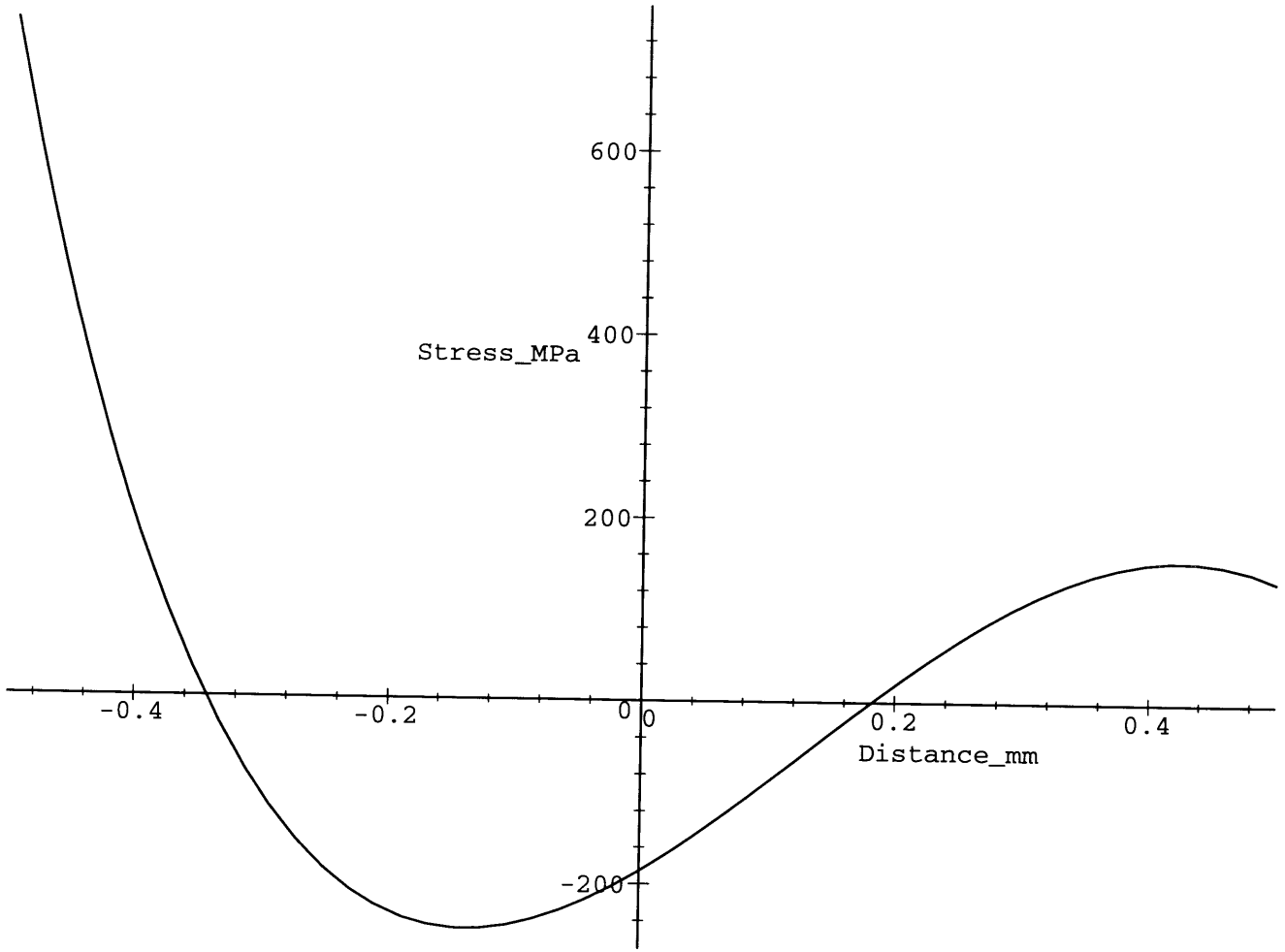

Fig. 3.6: Stress in axial restrained molybdenum- temperature dependent properties.

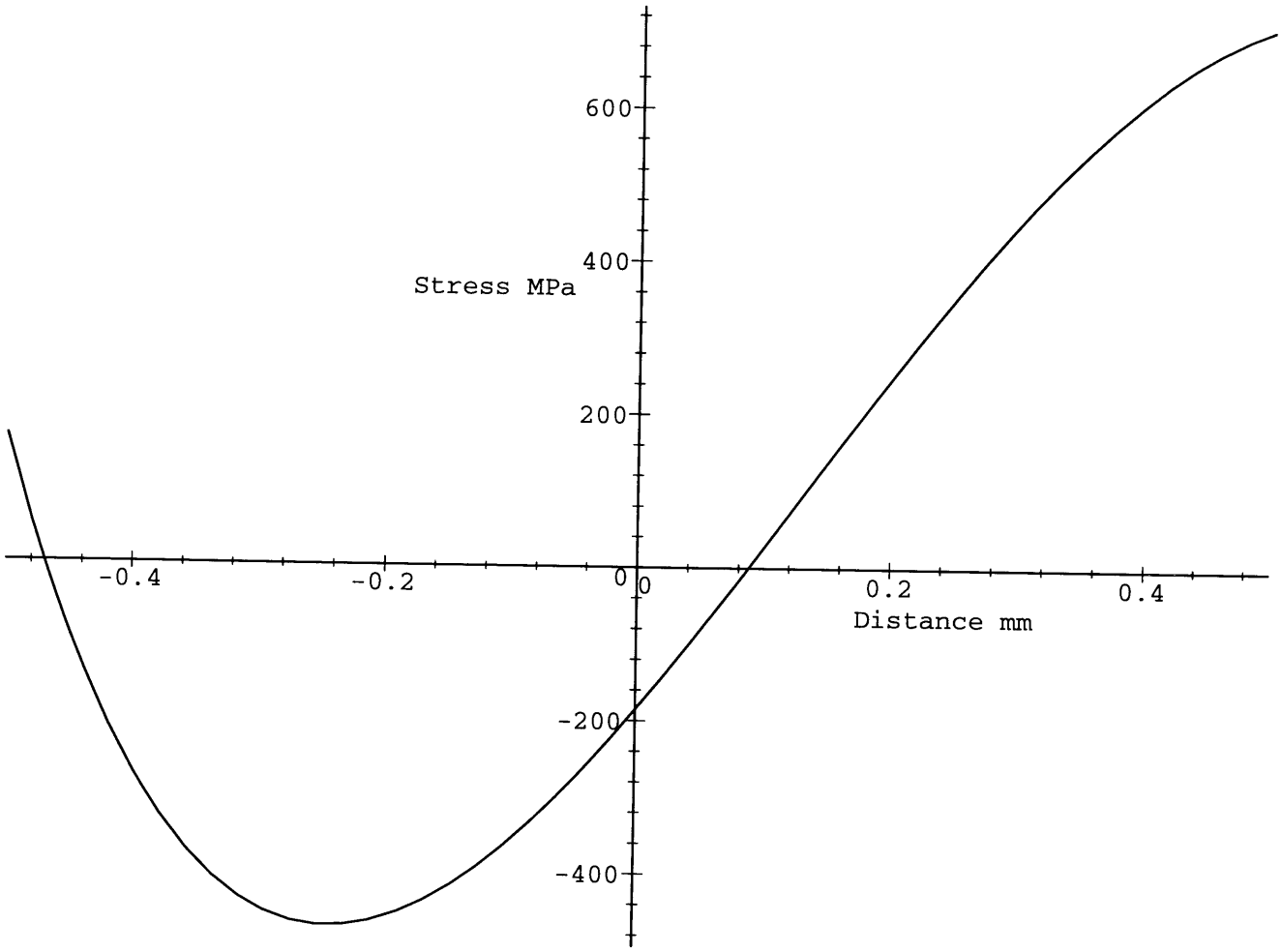

Fig. 3.7:Bending restrained molybdenum- temperature dependent properties.

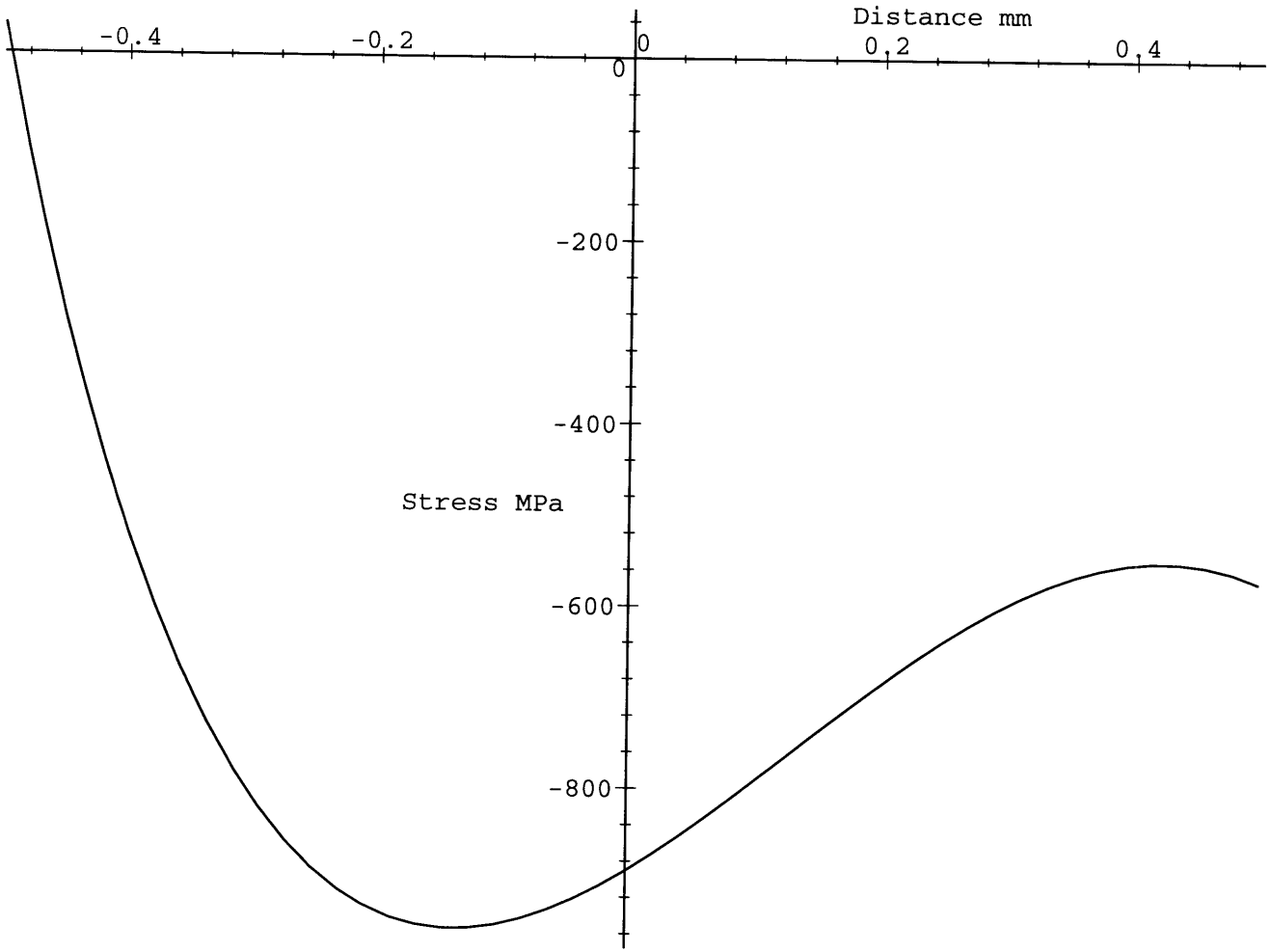

Fig 3.8: Stress in fixed molybdenum- temperature dependent properties.

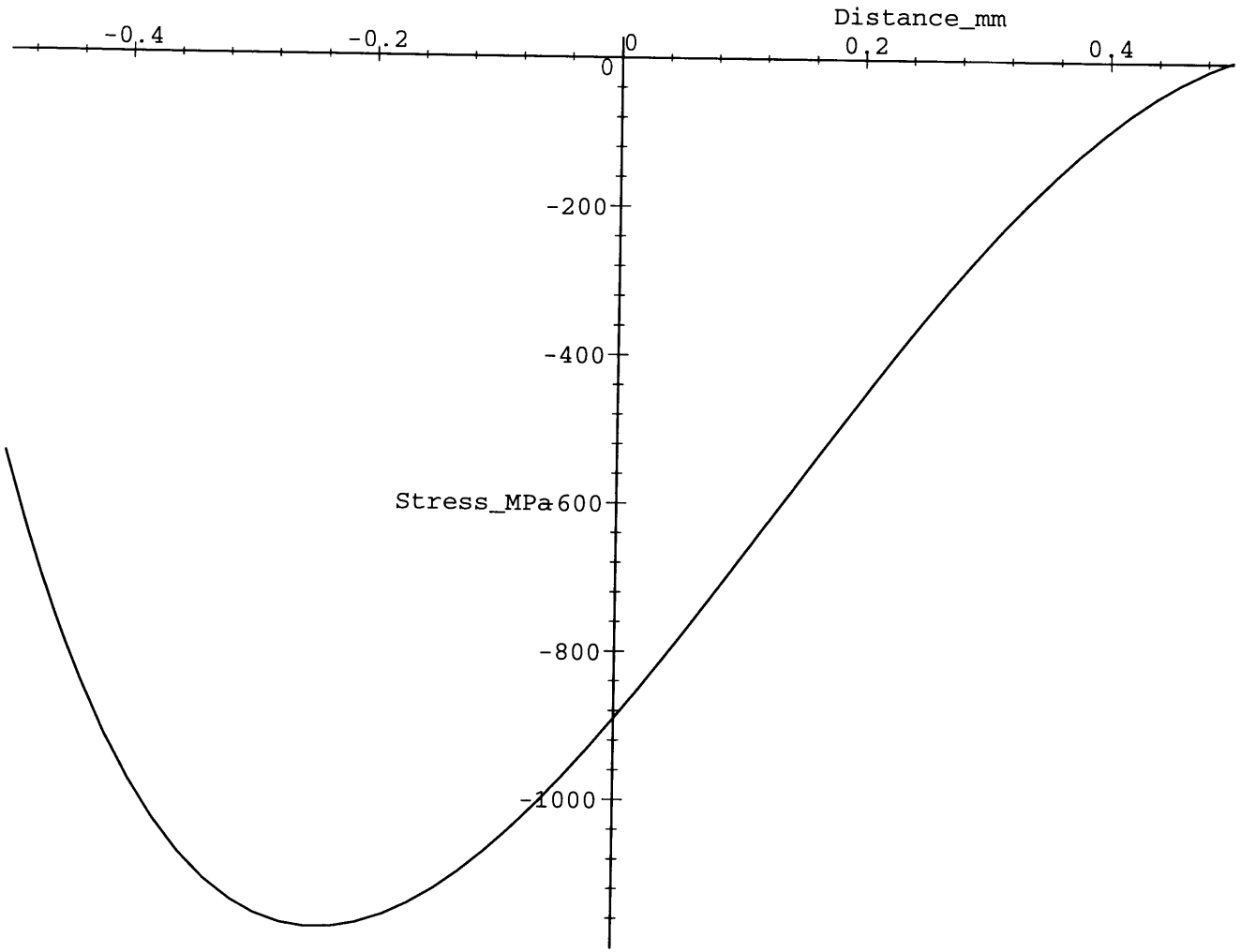

3.3 Transient Case

Non-linear temperature distributions cause thermal stresses. A body undergoing a transient heating process, will possess a non-linear temperature distribution. This section determines if transients are worth further consideration in more detailed models.

The plate and boundary conditions for this case are the same as given in figure 3.1 for times greater than zero seconds. At zero seconds, the plate is at a uniform temperature, To. The following equation describes the temperature as a function of y and t.

$$T_t(y,t) - To = \frac{T_h - T_c}{2}\frac{y}{H} + \frac{T_h - T_c}{2} + \sum_{n=0}^{\infty} F_n e^{-(n+.5)^2\pi^2\frac{\alpha_t t}{H}} \cos((n+\frac{1}{2})\pi\frac{y}{H})$$

where:

$$Fn = \frac{2}{H}\int_0^H (\frac{T_h - T_c}{2}\frac{y}{H} + \frac{T_h - T_c}{2})\cos((n+\frac{1}{2})\pi\frac{y}{H}dy \qquad (3.7)$$

The derivation of this equation follows the solution procedure for nonsymmetrical transient boundary conditions given in Mills[21]. Equation 3.3 determines the thermal stresses.

The results for molybdenum when free and fixed are shown in figures 3.9 and 3.10. Both figures illustrate that immediately after heating commences, thermal stresses reach a maximum. Therefore, one can conclude that transient thermal stresses are important for an imposed temperature boundary condition.

However, in the Liu and Lienhard experiment and in other high heat flux systems, it is not temperature but a flux which is imposed on the plate surface. Consider the case of a beam whose top surface is exposed to a flux and whose bottom surface is held at the reference temperature. Carslaw gives the solution for the change in temperature as a function of time (the coordinate system in the equation given below has been translated from the Carslaw solution so that the origin is at the center of the plate thickness):[22]

$$T = \frac{2Q(\alpha_t t)^{1/2}}{k}\sum_{n=0}^{\infty}(-1)^n\left[ierfc\frac{(4n+2)L - y - L}{2(\alpha_t t)^{1/2}} - ierfc\frac{(4n+2)L + y + L}{2(\alpha_t t)^{1/2}}\right] \qquad (3.8)$$

[21]Mills, A.F., *Heat Transfer*, Irwin, 1992.

[22]Carslaw, H.S. and Jaeger, J.C., *Conduction of Heat in Solids*, Oxford University Press, 1959.

The results for a 100 MW flux imposed upon both a free and a fixed molybdenum plate are shown in figures 3.11 and 3.12, respectively. The graphs show that in the free case, the thermal stresses are largest after heating commences but approach zero as the transient decays. In the fixed case, the magnitude of the thermal stresses increases with time, *i.e.*, as the temperature gradient increases. Thus, for a restrained beam exposed to a heat flux, transient non-linearities do not dominate the thermal stress problem. Instead, the temperature gradient, which increases with time, does. Consequently, the steady state case experiences higher thermal stresses than the transient. However, transients can still be important in brittle materials. This will be discussed in more detail below.

Fig 3.9: Transient stress in free molybdenum under ~2600 C temperature gradient.

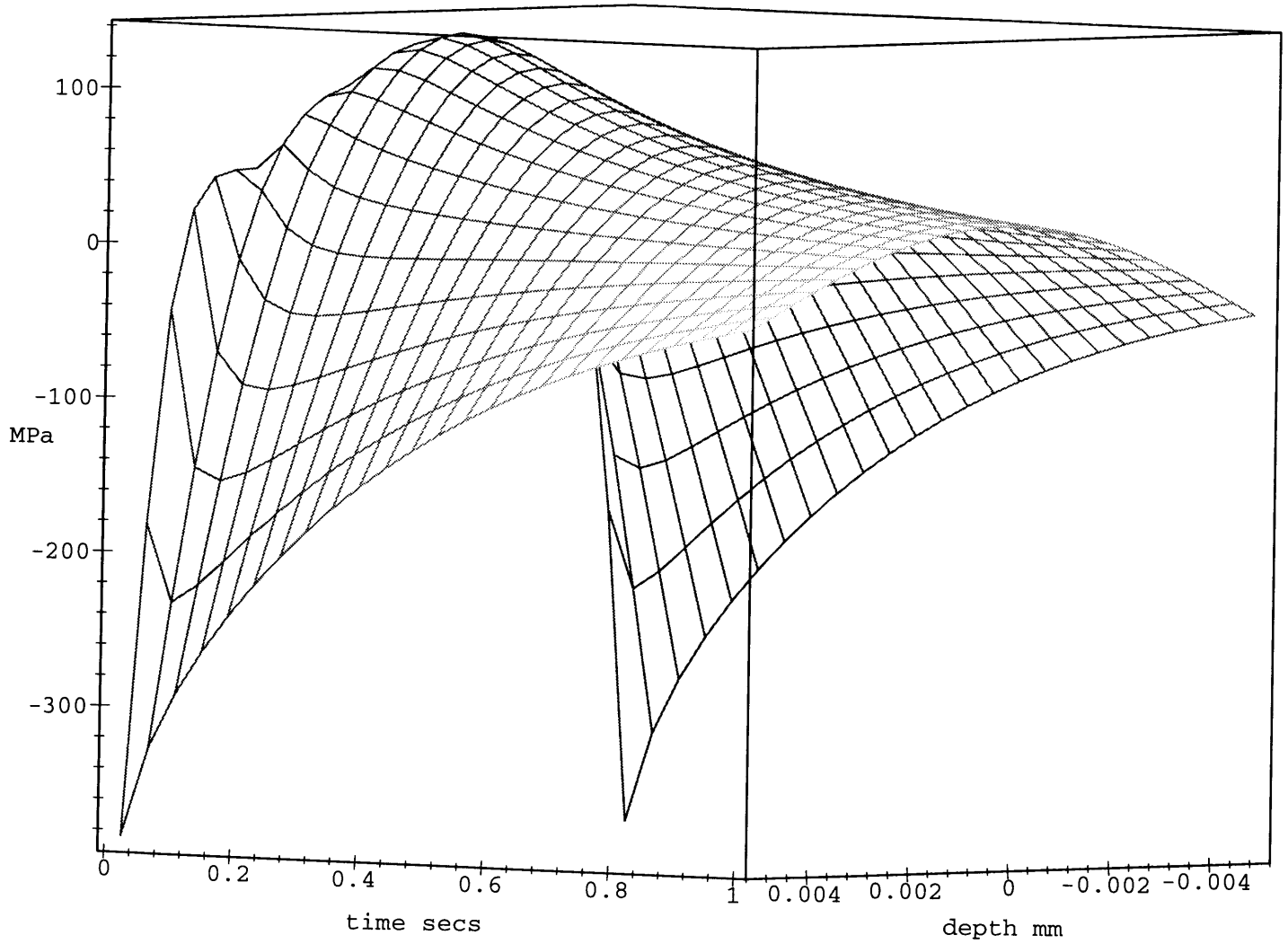

Fig. 3.10: Transient stress in fixed molybdenum under ~26000 C temperature gradient.

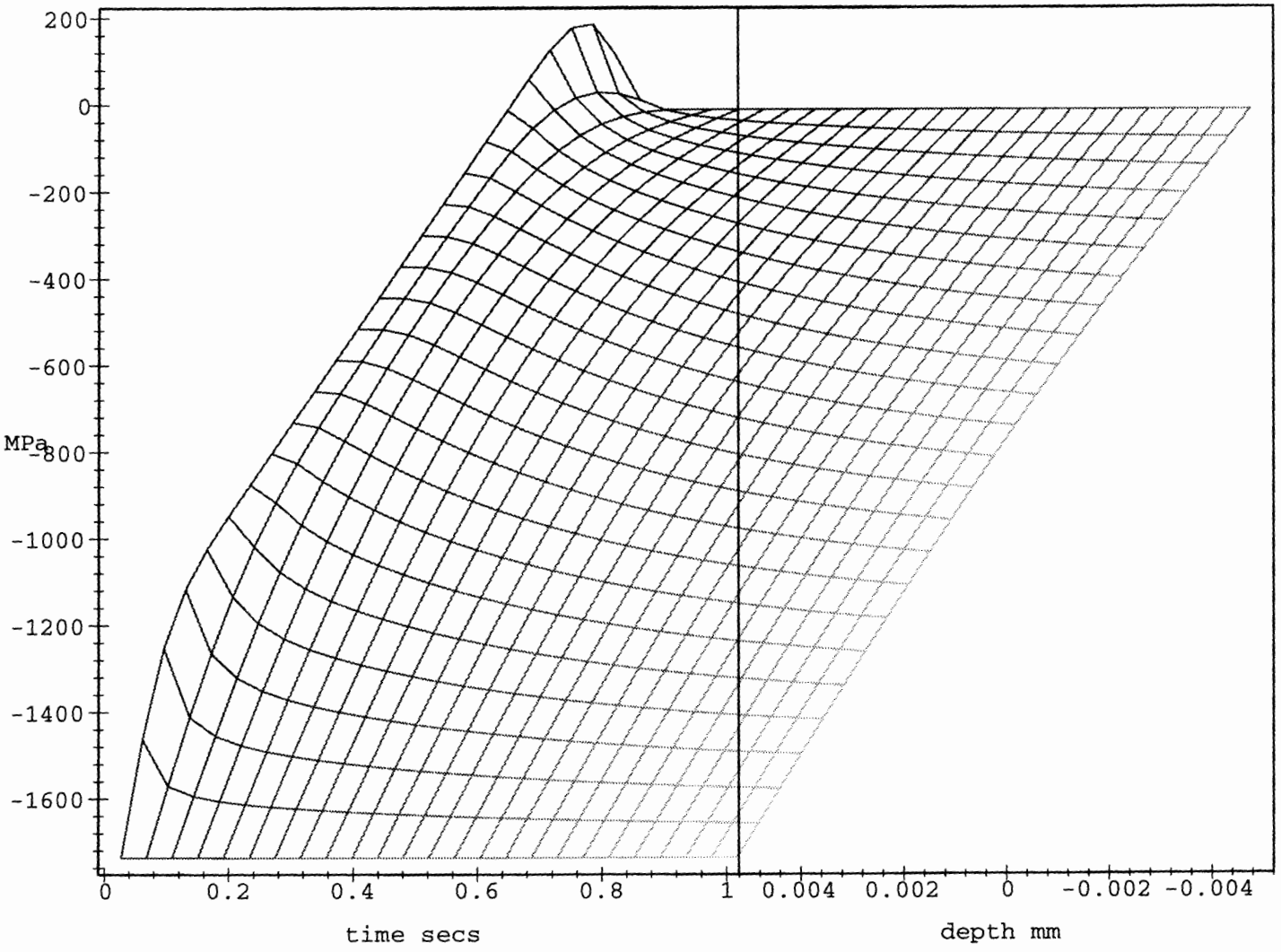

Fig.3.11:Transient stress in free molybdenum under 100 MW flux.

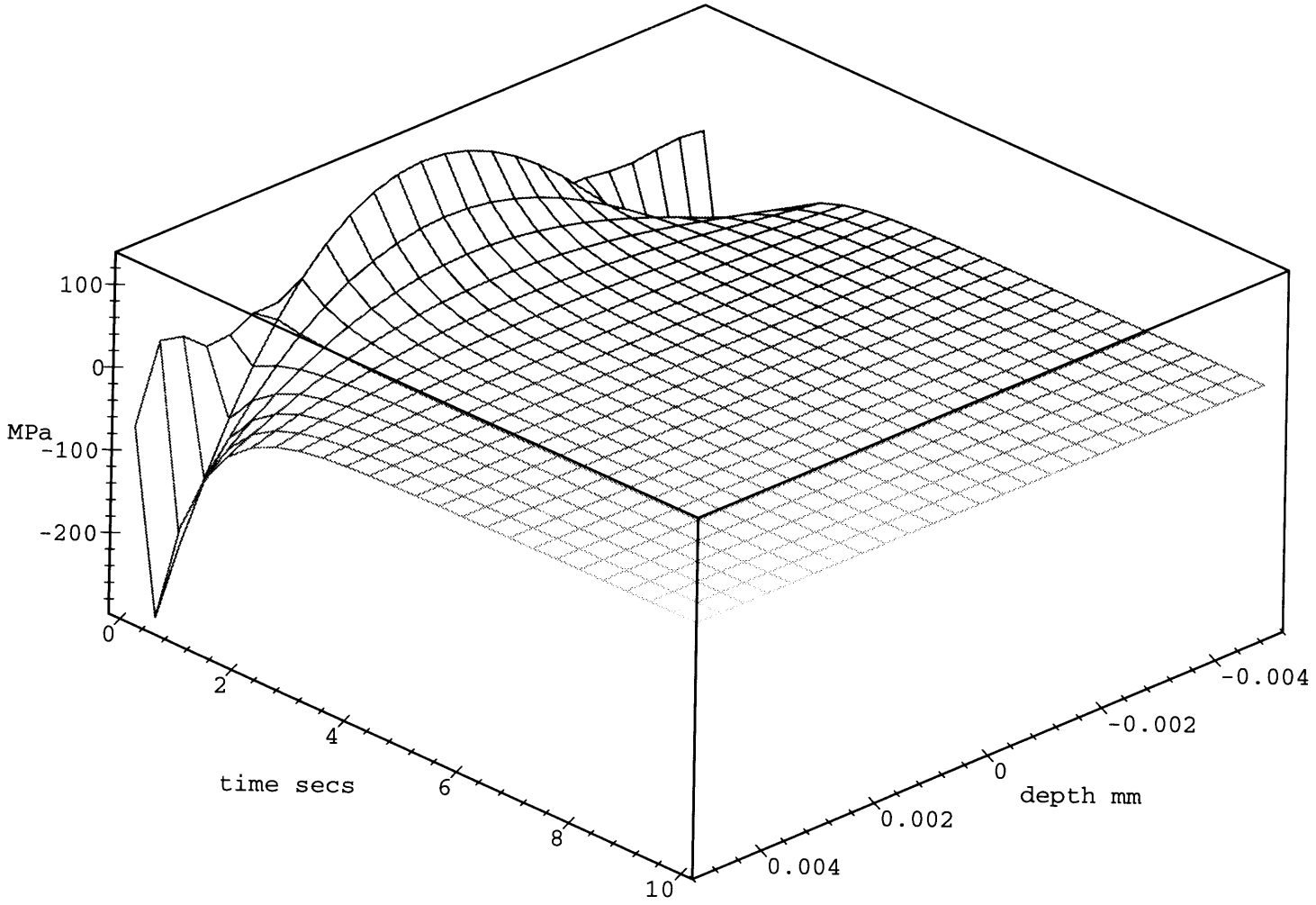

Fig.3.12:Transient stress in fixed molybdenum under 100 MW flux.

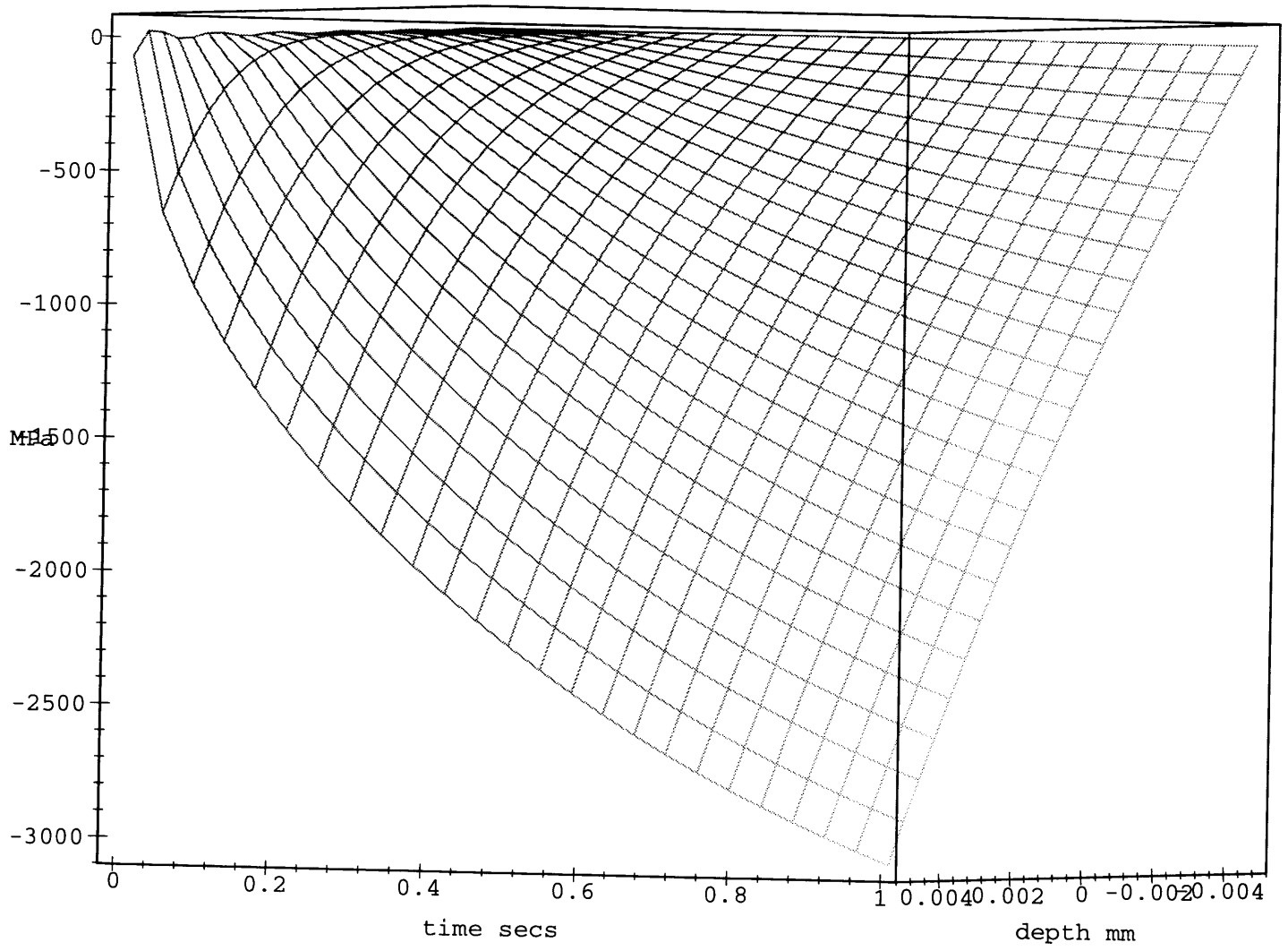

3.4 Plasticity

When a material is stressed to its yield strength, failure does not necessarily occur. A material "fails" if it no longer allows a system to function as designed.

Plastic deformation can result in substantial thermal stress relief. Further, if plastic deformations are kept small, i.e. small enough so that they do not inhibit the system from performing properly, the material will not fail even though the yield point has been surpassed.

The purpose of this section is to determine the temperature at which the ultimate strength of a material is reached. The heating configuration is identical to that of section 3.1. Gatewood describes an iterative procedure to account for plastic behavior in one dimensional models. He gives the following equations:[23]

$$\varepsilon = -\alpha T + e_c + e_b\left(\frac{y}{c} - 1\right) \qquad c = \frac{\int E_T y dA}{\int E_T dA}$$

$$e_c = \frac{\int \alpha E_T T dA}{\int E_T dA} \qquad E_T = \frac{\sigma}{\varepsilon}$$

$$e_b = \frac{\int \alpha E_T T\left(\frac{y}{c} - 1\right) dA}{\int E_T\left(\frac{y}{c} - 1\right)^2 dA} \qquad \int \sigma dA = 0$$

$$\int\left(\frac{y}{c} - 1\right)\sigma dA = 0$$

(3.9)

To use these equations, first assume values for *ec, eb,* and *c*. Find ε from the equations, find σ from the uniaxial stress-strain curve, and determine if equilibrium holds. The results for the candidate materials are given in table 3.3.

[23]Gatewood, B.E., *Thermal Stresses*, McGraw-Hill, Inc., 1957.

Material	Condition	strain/strain$_{max}$	T_{max}/T_{melt} (K)	Time to rupture
Molybdenum	bending restraints	1	2894/2894	< 1000 min
	fixed	1	2894/2894	
Tungsten	bending restraints	1	3050/3660	12 min
	fixed	1	3000/3660	
Stainless Steel	bending restraints	1	1300/1670	< 100 hrs
	fixed	1	1050/1670	
Aluminum	bending restraints	.36	993/993	< 500 hrs
	fixed	.36	993/993	

Table 3.3: Results of one-dimensional plastic analysis. Creep data also included. strain/strain$_{max}$ refers to the strain at the failure limit divided by the strain at the plastic limit. T_{max}/T_{melt} refers to the temperature at the failure limit divided by the melting temperature.

Section 3.1 suggests that yielding will occur well before the melting point of the material can be reached. The results show that very large temperature gradients can be attained if plastic deformation is allowed.

Creep results are also included in table 3.3. These results are based on the creep curves given in the references identified in footnotes 16-19. The creep times give a measure of the service time till rupture for elevated temperature applications.

3.5 Conclusions

The one dimensional models discussed in this chapter suggest a number of important points for both future modeling and design. First, a beam heated to its melting point will experience stresses which exceed its yield point. Thus, plastic material behavior is important to determine failure. In addition, these stress levels demand that failure criteria be well defined, e.g. large plastic deflections may be a better definition of failure than elastic yielding.

These models suggest that in the case of the Liu and Lienhard experiment, the metals experienced local yielding and plasticity in the vicinity of the melted pool. The following chapter will discuss localized stresses.

This chapter also illustrates that temperature dependent material behavior is an important parameter, especially in the case of the unrestrained beam. Future modeling efforts need to account for this element.

Transients also have a strong impact on stress levels if a temperature boundary condition is imposed. In this case, if failure occurs, it will occur almost immediately after heating begins. In contrast, if a flux boundary condition is applied to a restrained beam, the steady state case will experience the maximum stress levels.

From a design standpoint, these models indicate that materials should be elasticity restrained and/or be allowed to plastically deform. Flexibility can also be built into the system by either using a continuous vessel or by creating points which allow expansion, e.g. the circular loops in steam lines.

Chapter 4

Localized Heating Analytical Models - Elastic Regime

This chapter examines localized heating effects. The heating configuration of many high heat flux systems causes hot spots to develop on materials. Devices used to cool such systems, e.g. impinging jets, introduce localized mechanical loads. The Liu and Lienhard experiment is a good example of this. The primary goal of this chapter is to estimate the elastic limits of candidate materials. Correlations are also developed which determine the magnitude of thermal and mechanical stresses.

Membrane stresses in a beam subjected to a small hot spot are analyzed first. This establishes a first estimate of the effects of localized heating. However, the model is limited by its inability to account for temperature gradients through the plate's thickness.

A two dimensional beam model is introduced to account for this parameter. The beam is heated and cooled so that a large thermal gradient develops through the thickness. The temperatures along the top and bottom plate faces are defined by a gaussian function with its origin at the plate center. This model provides a framework for the temperature distribution assumptions used throughout the chapter.

The remainder of the chapter employs classical plate theory to analyze the combination of membrane and bending stresses. Attempts are made to determine the mechanical influence of end restraints and cooling jets.

The models in this chapter are limited by their inability to account for transients and the temperature dependence of material properties. This will be examined in later chapters using finite element techniques.

4.1 Circular Hot Spot on an Infinite Beam

This section estimates the stresses in an infinite plate with a circular hot spot of radius a. The model accounts for material property temperature dependence inside the hot spot.

The plate is subject to in-plane expansion inside and near the heated region. This induces compressive membrane stresses.

A potential function ψ which satisfies the stress compatibility equations can be defined in terms the x and y displacements (u and v respectively) as,

$$u = \frac{\partial \psi}{\partial x} \qquad v = \frac{\partial \psi}{\partial y} \tag{4.1}$$

Substituting equation 4.1 into the stress equilibrium equations, under assumptions of plane stress and zero body forces, yields[24],

$$\nabla^2 \psi = \frac{1+\nu}{1-\nu} \alpha T \tag{4.2}$$

The solution to ψ can then be substituted into the stress compatibility equations to determine the stress field. Goodier's solution for a circular hot spot of radius a is given below[25]:

$$\begin{aligned} \sigma_r = \sigma_\theta &= -\frac{E\alpha T}{2} && \text{inside hot spot} \\ \sigma_r = -\sigma_\theta &= -\frac{E\alpha T}{2}\left(\frac{a}{r}\right)^2 && \text{outside hot spot} \end{aligned} \tag{4.3}$$

These equations express the membrane stresses in an infinite beam. Equation 4.3 has been applied to the candidate materials. By expressing the material properties - E, α, and yield strength - as functions of temperature, the temperature at which the thermal stress equals the yield strength can be solved for. The results are given in Table 4.1.

---

[24]Johns, D.J., *Thermal Stress Analyses*, Pergamon Press Ltd, 1960.
[25]Goodier, J.N., *Thermal Stress*, Journal of Applied Mechanics, Trans. ASME, Vol.59, March 1937.

Material	Temperature (K)	Yield (MPa)	Diameter (mm)	Zero stress at (mm)
molybdenum	573	210	1	5
aluminum	496.5	91.3	1	5
tungsten	546	284.7	1	5
steel	487.4	304.3	1	5

Table 4.1: Results for circular hot spot model. 'Stress' refers to the maximum stress in the hot spot. 'Diameter' refers to the geometry of the hot spot. The term 'Zero stress at' refers to the distance from the center of the hot spot at which the thermal stresses approach zero (tolerance of 1 MPa).

Table 4.1 shows that for the circular hot spot, the membrane stresses are on the order of the yield strength. In comparison to the restrained cases reported in tables 3.1-2, the membrane stresses in table 4.1 are generally lower. This is due to the inverse relationship between temperature and Young's modulus. In chapter 3, properties were varied with temperature throughout the beam thickness. Here, properties are evaluated at the maximum temperature. Thus, the maximum stress is expected to decrease.

Additionally, the area of the plate influenced by the hot spot decreases to zero within five diameters. This suggests that failure will be centered near the point of localized heating.

This model has not accounted for the temperature gradient through the thickness of the plate. Such a gradient will introduce bending stresses. This issue will be considered in sections 4.2-4.4. Without, this gradient molybdenum achieves the highest temperature despite the fact that its yield strength is smaller than that of both tungsten and steel. Yield strength alone is not a good estimate of a material's performance. Instead the ratio between yield and the product of the linear expansion coefficient and Young's modulus should be considered. The importance and proper use of this ratio for ranking materials is discussed in section 4.3.3.5.

4.2 Beam with Localized Heating on Top and Bottom Faces

4.2.1 Heat Transfer Problem

Figure 4.1 shows a beam heated locally on it top surface. The temperature on the top face varies in both the x and z directions. The resultant steady state temperature distribution is three dimensional. If the temperature variation in the z direction is significantly small so

that the hot spot is no longer circular, as shown in the figure, the temperature field is approximately two dimensional. Alternatively, a thin slice of the beam midsection in the x-y plane can be approximated as having a two dimensional temperature distribution since the temperature variation in the z direction of the slice is negligible.

Figure 4.1 illustrates the geometry and boundary conditions for both cases. The slab is assumed to be in steady state. The resultant temperature distribution is two dimensional and non-linear through the thickness of the beam.

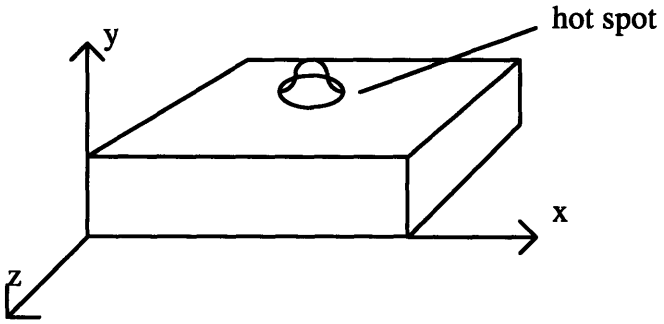

Figure 4.1: Beam with three dimensional hot spot on top surface.

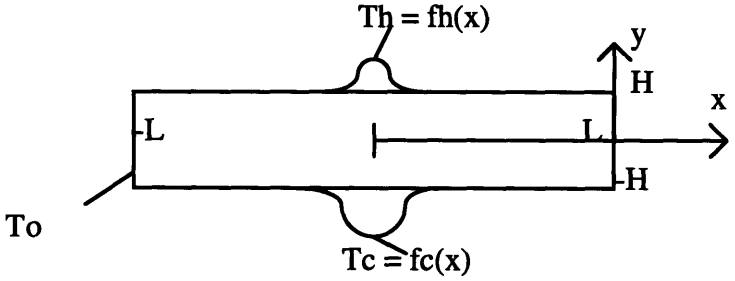

Figure 4.2: Model for local heating in a beam

Boundary Conditions:

$$T_t(x=L,y)=T_0$$

$$T_t(x=-L,y)=T_0$$

$$T(x,y=H)=T_h(x)=T_0+T_{hot}e^{-\frac{2x^2}{a^2}}$$

$$T_t(x,y=-H)=T_c(x)=T_0+T_{cold}e^{-\frac{2x^2}{a^2}} \qquad (4.1a)$$

where:

$$T_0=\frac{T_h(x=0)+T_c(x=0)}{2}$$

The governing equation for this case is:

$$\frac{\partial}{\partial x}(k(T_t)\frac{\partial T}{\partial x})+\frac{\partial}{\partial y}(k(T_t)\frac{\partial T}{\partial y})=0 \qquad (4.1)$$

This problem can be solved using separation of variables and superposition techniques (see appendix for solution). The final result for a beam heated to its melting temperature and cooled to one hundred degrees Celsius is shown in equation 4.3.

$$T=2\sum_{n=1}^{\infty}F_x\frac{1-(-1)^n}{2L}\frac{\sin(n\pi\frac{x}{L})}{\sinh(n\pi\frac{H}{L})}[T_h\sinh\frac{n\pi(y+H/2)}{L}-T_c\sinh\frac{n\pi(H/2-y)}{L}]$$

where: (4.2)

$$F_x=\int_0^L e^{-\frac{2(x-L/2)^2}{a^2}}\sin n\pi\frac{x}{L}dx$$

Figure 4.3 shows the temperature distribution in a body with a small portion of its top surface heated. Note that there is a nearly linear variation of temperature through the thickness. This observation suggests that it is possible to simplify equation 4.2 for the case of hot spots much larger than the thickness of the beam. This simplification is important for evaluating stresses as discussed below. Equation 4.3 illustrates how linearity can be accounted for (see boundary conditions in equation. 4.1a for definition of functions).

$$T=\frac{f_h(x)+f_c(x)}{H}y+\frac{f_h(x)-f_c(x)}{2} \qquad (4.3)$$

This equation is graphed in figure 4.4. Notice that the temperature distribution is very similar to that shown in figure 4.3, especially near the point of maximum temperature. The linear approximation is reasonable as long as the hot spot radius is at least an order of magnitude greater than the thickness (y direction) of the beam.

Forcing the temperature to vary linearly through y, the plate thickness, introduces an apparent contradiction. In section 2.2.1, it was stated that steady state two dimensional temperature distributions (Cartesian coordinates) do not induce thermal stresses.

However, when the steady state temperature field is approximated as linear in y, it no longer satisfies Laplace's equation, $\nabla^2 T = 0$. Consequently, although equation 4.3 approximates equation 4.2, the former yields thermal stresses while the latter does not.

This difficulty can be reconciled by recognizing that the initial problem included a temperature variation in z. Consider a small elemental volume of the beam shown in figure 4.1. Since the radius of the hot spot divided by the beam thickness is much larger than unity, the temperature variation in y is much larger than both the variations in x and z. Therefore,

$$\frac{\partial^2 T}{\partial y^2} >> \frac{\partial^2 T}{\partial x^2}$$
$$\frac{\partial^2 T}{\partial y^2} >> \frac{\partial^2 T}{\partial z^2} \qquad (4.4a)$$

so,

$$\nabla^2 T \approx \frac{\partial^2 T}{\partial y^2} \qquad (4.4b)$$

and thus for the steady state case the temperature field is dominated by a linear variation in y of the form,

$$T = ay + b + T_o \qquad (4.4c)$$

It is more accurate to describe the temperature field T as having both a linear and a small non-linear component such that,

$$T = (ay + b) + \hat{T}(x, y, z) + T_o \qquad (4.5)$$

This equation must satisfy Laplace's equation, and thus the Laplacian of $\hat{T}$ must be equal to zero. That is,

$$\nabla^2 \hat{T} = \left(\frac{\partial^2}{\partial x^2} + \frac{\partial^2}{\partial z^2}\right)\hat{T} + \frac{\partial \hat{T}^2}{\partial y^2} = 0 \qquad (4.6)$$

Since the first term of equation 4.6 does not equal zero, equation 4.4b does not equal zero, and so a plane stress condition exists even though the Laplacian of equation 4.5 is zero. In order words, the small non-linear component of the temperature in y, which is neglected in equation 4.3, allows the Laplacian of equation 4.5 to equal zero.

Additionally, the gradual variation of temperature in z (also neglected in 4.3) makes the temperature field three dimensional and thus causes thermal stresses to develop.

Therefore, equation 4.3 is a reasonable approximation of the temperature field in the beam. The small non-linear component of the temperature variation in y can be neglected since the hot spot radius is much larger than the plate thickness. The component of temperature in the z direction can be neglected since its variation is assumed to be small. With regard to stresses, in the original three dimensional case thermal stresses exist. When the z component is neglected in equation 4.2 these stresses are lost. When the linear approximation in y is made, stresses are re-introduced. Additionally, these stresses should approximate the actual stress field since the temperature distribution approximates the three dimensional case.

One point needs to be elaborated upon. The above discussion requires a gradual temperature variation in z (relative to that in x). If the variation in z and x are similar, stresses calculated on the basis of equation 4.3 will neglect the z component of the stress field. Such a calculation is equivalent to estimating membrane stresses (a material which has no resistance to bending) in a thin slice of the beam midsection (x-y plane). This is a poor stress estimate, but should describe the correct order of magnitude for thermal stresses (compare results of section 4.1 and 4.3). This difficulty can be removed by switching to a cylindrical coordinate system as will be done in section 4.3 and as describe in section 2.2.1.

4.2.2 Thermal Stress Problem

For a free beam, Boley provides an exact thermal stress solution.[26] The equation that must be solved is:

$$\frac{\partial^4\phi}{\partial y^4}+2\frac{\partial^4\phi}{\partial x^4\partial y^4}+\frac{\partial^4\phi}{\partial x^4}=\alpha E(\frac{\partial^2 T}{\partial y^2}+\frac{\partial^2 T}{\partial x^2}) \qquad (4.7)$$

with the boundary conditions:

$$\phi(y=\pm H)=\frac{\partial\phi}{\partial y}=0$$

[26]Boley, B.A., *Theory of Thermal Stress*, John Wiley and Sons, Inc., 1960.

This is the governing stress equation for the condition of plane stress. The Airy stress function ϕ is related to stress by the following:

$$\sigma_{xx} = \frac{\partial^2 \phi}{\partial y^2} \qquad \sigma_{zz} = \frac{\partial^2 \phi}{\partial x^2} \qquad \sigma_{xy} = \frac{\partial^2 \phi}{\partial x \partial y} \tag{4.8}$$

The solution provided by Boley assumes that the beam's length is much greater than its thickness ($\frac{H}{L} \langle\langle 1$), that the beam is in plane stress, and that it has an arbitrary temperature distribution in x and y which can be expressed in terms of a power series. The full solution is tedious and not easily evaluated for complex temperature distributions. However, in the case of a temperature linear in y, the solution becomes simple. The expression for the stress in x is:

$$\frac{\sigma_{xx}}{\alpha E} = \frac{(3H^2/4 - 5y^2)^2}{30} \frac{\partial^2 T}{\partial x^2} - \left(\frac{y^5}{60} - \frac{y^3 H^2/4}{30} + \frac{9yH^4/16}{700}\right) \frac{\partial^4 T}{\partial x^4} \tag{4.8}$$

The solutions for the stress in y and the shear can be found in Boley or in the Maple™ programs located in the appendix.

Table 4.2 shows the results for a free beam The beam length is 400 mm, and its thickness is 1 mm. The area of the hot spot covers 10 % of the beam length, measures from the origin to the edge. The cool spot also covers 10 % of the beam area but the minimum temperature is 100 C. Material properties for the beam are evaluated at the average temperature.

Material	Maximum Temperature (K)	Flux (MW)	% of Beam Length under Stress	σ_{xx} (MPa)
Molybdenum	2883	205.6	10	.6
Aluminum 6061	993	149.6	10	.8
Stainless Steel 304L	1670	24.9	10	4.6
Tungsten	3660	582.4	10	10

Table 4.2: Maximum stress levels in a 1 mm free beam heated to the melting point on a small portion of one side of the beam and cooled to 100 C on the opposite side. The hot and cool spots act across 10 % of the beam length.

The values shown in Table 4.2 are small compared to those reported in Table 4.1. The latter table reported results for a hot spot which acted on a minuscule portion of an infinite beam. A sharp gradient - a 100 % decrease in temperature - existed between the temperature inside and outside the hot spot. This gradient was responsible for the large membrane stresses. In the present case, the hot spot acts over a larger portion of the beam and gradually decreases its intensity over this area (see equation 4.2). Consequently, the stress levels are expected to be much less. However, this model will yield stresses on the same order of magnitude as those in table 4.1 for very small hot spots. Table 4.3 shows the maximum stresses for a stainless steel beam as the area of the hot spot increases.

Heated Area (% of Beam Length)	σ_{xx} (MPa)	σ_{vv} (MPa)
3	48.3	2
10	4.6	0
30	0.53	0

Table 4.3: Maximum stresses in x and y directions for stainless steel beam with the same properties and conditions as in Table 4.2.

This model is not representative of the Liu and Lienhard experiment. The beam analyzed here is free while in the experiment the beam was restrained. Section 3.1 showed that restraints increased the stress levels significantly.

The remainder of this chapter will examine the influence of end conditions for circular plates. Circular plates are analyzed for two reasons. The first has been discussed in section 2.2.1. Second, thermal stress problems with end restraints are more easily solved in cylindrical coordinates.

Fig.4.3: Hot spot on top surface of body

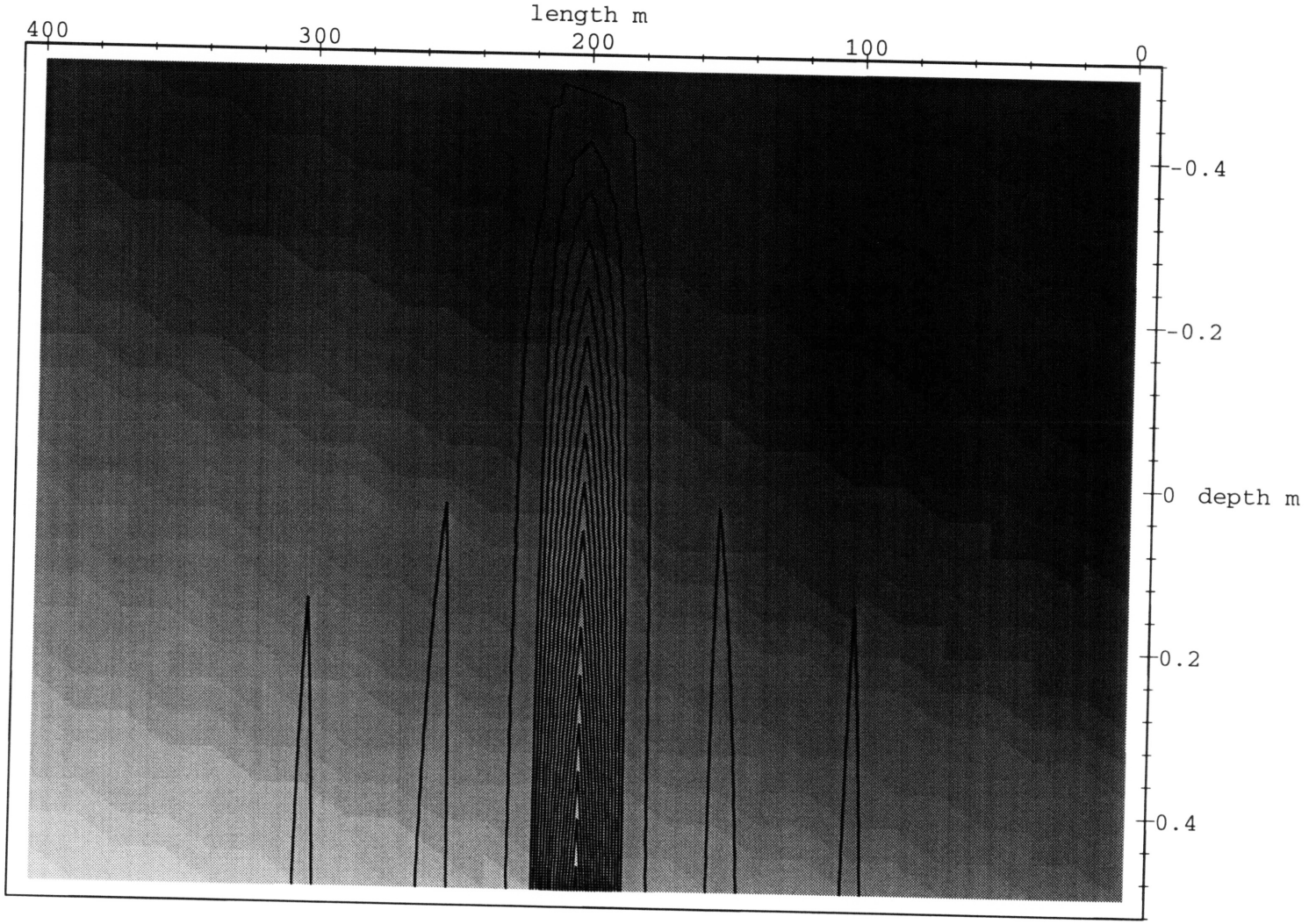

Fig.4.4: Hot spot linear approximation

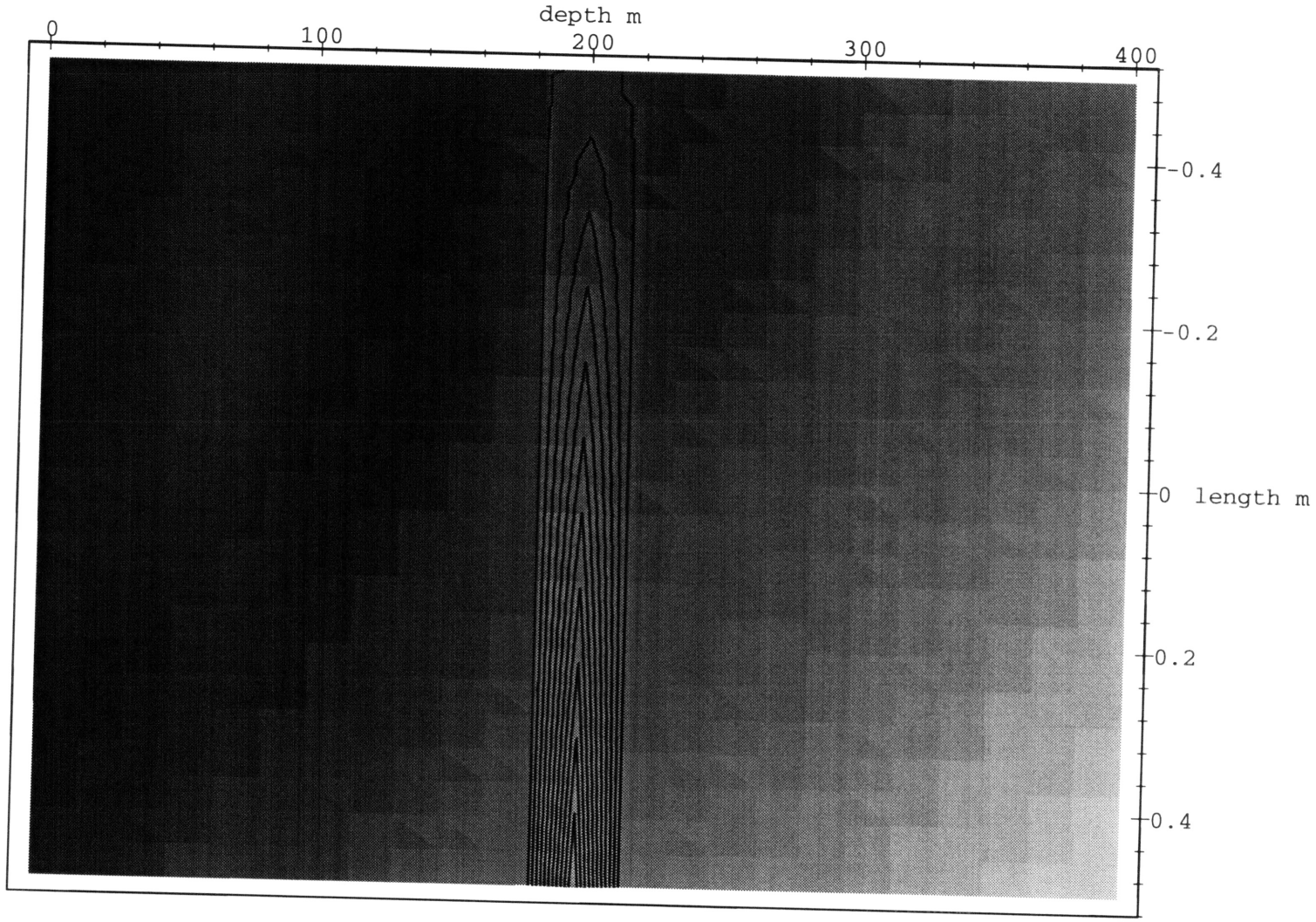

4.3 Simply Supported Circular Plate

4.3.1 Heat Transfer Problem

The circular plate shown in figure 4.5 provides the basis for this section. A simply supported plate is heated on its top surface, and cooled on its bottom surface to 100 C. The heating takes place on a small fraction of the plate surface. The temperature boundary condition at the top surface is represented by a normally distributed function of the radius. This boundary condition provides a more realistic approximation of actual localized heating cases than the previous model.

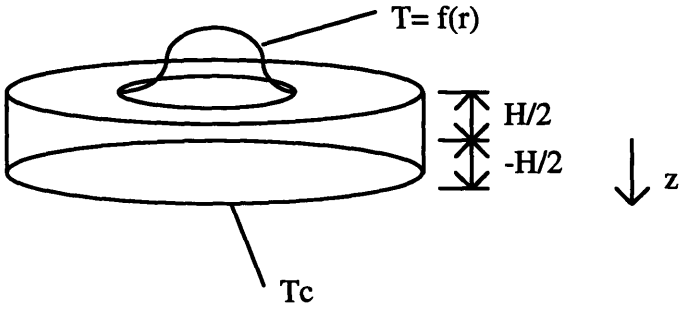

Figure 4.5: Diagram of locally heated circular plate
Graph not to scale.

The plate has an axisymmetric temperature field in r and z. Additionally, so long as the heating occurs in a region whose radius is an order of magnitude larger than the plate thickness (now in the z direction), the temperature can be assumed to be linear in z, as per the discussion of section 4.2.1. The temperature field is given by the following equation:

$$T = \frac{T_h(r) - T_c(r)}{H} z + \frac{T_h(r) + T_c(r)}{2} \tag{4.9}$$

The radial functions in equation 4.9 are normally distributed as in equation 4.2.

4.3.2 Thermal Stress Problem - Classical Plate Theory

Classical plate theory describes the membrane and bending stresses under the following assumptions:

(1) The plate's mechanical material properties are isotropic, homogeneous, and

temperature insensitive.

(2) Plane stress is assumed.

(3) Kirchhoff hypothesis - line elements perpendicular to the middle surface before thermal or mechanical loads are applied, remain straight and perpendicular to the middle surface after loads are applied.

(4) The strain-displacement relations can be described by linear terms only.

Assumption 1 is a principal limit of this analysis. Numerical methods are needed to remove this limitation for localized heating cases. This will be elaborated upon when finite element techniques are discussed.

The plane stress hypothesis results in a simplified stress tensor as discussed in section 2.2.3. However, it limits the analysis to thin plates and temperature distributions of the form T= T(z) or T= zT(r). The latter condition is satisfied by the plate described in section 4.3.1.

Assumptions 3 and 4 imply that the plate deflection must be smaller than the thickness of the plate and transverse strains must be small so that $\varepsilon_{zz} = \gamma_{rz} = \gamma_{\theta z} = 0$ is a good approximation to the actual case. Transverse strains will be appropriately small so long as the linear strain displacement relations hold, *i.e.*,

$$\begin{aligned} \varepsilon_{rr} &= \frac{\partial u}{\partial r} = \frac{\partial u^{\circ}}{\partial r} - z\frac{\partial^2 w}{\partial r^2} \\ \varepsilon_{\theta\theta} &= \frac{\partial v}{\partial \theta} = \frac{\partial v^{\circ}}{\partial \theta} - z\frac{\partial^2 w}{\partial \theta^2} \\ \gamma_{r\theta} &= \frac{\partial u^{\circ}}{\partial r} + \frac{\partial v^{\circ}}{\partial \theta} - 2z\frac{\partial^2 w}{\partial r \partial \theta} \end{aligned} \tag{4.10}$$

However, if transverse strains are not small then a non-linear term must be added to the above equations. The Von Karman theory helps describe stresses and strains in this case. In the Von Karman theory, the above equations (equation. 4.10) become[27]:

[27]Hetnarski, R.B., *Thermal Stresses, Vol. I.*, Elsevier Science Publishers B.V., 1986.

$$\varepsilon_{rr} = \frac{\partial u}{\partial r} = \frac{\partial u^{\circ}}{\partial r} - z\frac{\partial^2 w}{\partial r^2} + \frac{1}{2}\left(\frac{\partial w}{\partial r}\right)^2$$
$$\varepsilon_{\theta\theta} = \frac{\partial v}{\partial \theta} = \frac{\partial v^{\circ}}{\partial \theta} - z\frac{\partial^2 w}{\partial \theta^2} + \frac{1}{2}\left(\frac{\partial w}{\partial \theta}\right)^2 \qquad (4.11)$$
$$\gamma_{r\theta} = \frac{\partial u^{\circ}}{\partial r} + \frac{\partial v^{\circ}}{\partial \theta} - 2z\frac{\partial^2 w}{\partial r \partial \theta} + \frac{\partial w}{\partial r}\frac{\partial w}{\partial \theta}$$

Classical theory is no longer valid when the non-linear term is of the same order of magnitude as the linear terms. Both the small deflection and linear requirements are checked for the results given below. This check illustrates the limits of classical theory.

There are two governing equations in classical plate theory. The first, equation 4.12a, describes membrane stresses in the r-θ plane. The second, equation 4.12b, is associated with bending stresses and plate deflection.

$$\nabla^4 \phi = -\nabla^2 N_T$$
$$D\nabla^4 w = -\frac{1}{1-\nu}\nabla^2 M_T \qquad (4.12\ \text{a-b})$$

where:

$$N_T = E\alpha \int T dz$$
$$M_T = E\alpha \int T z dz \qquad (4.12\ \text{c})$$
$$D = \frac{Ed^3}{12(1-\nu^2)}$$

Solutions of equation 4.12b are available for a number of boundary conditions[28]. To solve equation 4.12a, it is necessary to recognize its similarity to the Airy stress function equation in two dimensions. It has the form[29]:

$$\nabla^4 \phi + E\alpha \nabla^2 T = 0 \qquad (4.13)$$

The general solution of this equation is available for circular plates[30]. Equation 4.12a can be manipulated into the form of equation 4.13 by substituting equation 4.12c into equation 4.12a to get,

---

[28]Ibid.

[29]Johns, D.J., *Thermal Stress Analyses*, Pergamon Press Ltd, 1960.

$$\nabla^4\phi + E\alpha\nabla^2\int Tdz = 0 \tag{4.14}$$

Consequently, the solutions to equation 4.13 can be used by replacing the temperature variable with the term $\int Tdz$.

4.3.3 Solution of the Governing Equations

Solutions to equations 4.12b (the bending stress equation) and 4.13 (the membrane stress equation) are provided by Johns[31]. The result for the former is,

$$w = \frac{1+\nu}{d}\left[\int_0^r \frac{F(r)}{r}dr - \int_0^b \frac{F(r)}{r}dr - \frac{(1-\nu)}{2(1+\nu)}F(b)\left(1-\frac{r^2}{b^2}\right)\right]$$

where: (4.15)

$$F(r) = \int_0^r \alpha T r dr$$

The thermal stresses can be found from the deflection equation (4.15) by introducing two additional functions[32]. These are,

$$M_r = \frac{-EH^3}{12(1-\nu^2)}\left(\frac{\partial^2 w}{\partial r^2} + \frac{\nu}{r}\frac{\partial w}{\partial r} + \frac{\nu}{r^2}\frac{\partial^2}{\partial\theta^2}\right) - M_T$$

$$M_\theta = \frac{-EH^3}{12(1-\nu^2)}\left(\nu\frac{\partial^2 w}{\partial r^2} + \frac{1}{r}\frac{\partial w}{\partial r} + \frac{1}{r^2}\frac{\partial^2}{\partial\theta^2}\right) - M_T \tag{4.17}$$

Johns gives a general solution for equation 4.13. This is solution is used with the substitution described in equation 4.14 to solve the governing equation for membrane stresses (4.12a). The solution is given below in terms of the second derivatives of r and θ.

---

[30]Ibid.

[31]Ibid.

[32]Hetnarski, R.B., *Thermal Stresses, Vol. I.*, Elsevier Science Publishers B.V., 1986.

$$Nr = \frac{\partial^2 \phi}{\partial r^2} = \frac{E\alpha}{r^2}\left[\frac{r^2}{b^2}\int_0^b r \int_{-H/2}^{H/2} T dz dr - \int_0^r r \int_{-H/2}^{H/2} T dz dr\right]$$
$$N_\theta = \frac{\partial^2 \phi}{\partial \theta^2} = \frac{E\alpha}{r^2}\left[\frac{r^2}{b^2}\int_0^b r \int_{-H/2}^{H/2} T dz dr + \int_0^r r \int_{-H/2}^{H/2} T dz dr - r^2 \int_{-H/2}^{H/2} T dz\right] \quad (4.18)$$

The thermal stresses are determined from equations 4.17-4.18 by the following equations[33],

$$\sigma_{rr} = \frac{N_r - N_T}{H} + \frac{12z}{H^3}(M_r + M_T) - \frac{E\alpha}{1-\nu}T$$
$$\sigma_{\theta\theta} = \frac{N_\theta - N_T}{H} + \frac{12z}{H^3}(M_\theta + M_T) - \frac{E\alpha}{1-\nu}T \quad (4.19a\text{-}b)$$

4.3.4 Thermal Stress Correlations

An important part of this study is to determine how variations in geometry, material properties, and heating configuration affect stress fields. The goal is to develop correlations for thermal stresses below the elastic limit.

This is done by varying the parameters which affect the thermal stress level and determining relationships between the variables. The base case is a material and heating configuration conforming to the following (this is not any particular material but a combination of the candidate materials):

Young's Modulus:	158 GPa
Linear Coefficient of Thermal Expansion:	$4.5*10^{-6}$
Plate Radius:	200 mm
Plate Thickness:	1 mm
Maximum Temperature:	1670 K
Percent of Plate Surface Area Heated:	9 % (a =.0075 m^{-2})
Calculated Maximum Principal Stress (σ_1):	-412.5 MPa
Calculated Minimum Principal Stress (σ_2):	-281.2 MPa

[33]Ibid.

This heating configuration has been chosen to satisfy the requirements discussed above, i.e. a 1 mm thick plate heated such that the heating radius is much larger than the thickness. The plate radius has been chosen based on the applicable limits of classical plate theory (see section 4.3.3.4). While this system is not reflective of the Liu and Lienhard experiment (the ratio of plate radius to thickness was much less), it is important for the more general issue of localized heating.

The results given below are the maximum values of the principal stresses in the material. Yield strength, and thus failure, is not considered. All results conform to the small deflection and linear stress-strain requirements as described in section 4.3.2.

A) Effect of Young's Modulus

Young's Modulus (GPa)	Classical Theory Valid?	σ_1 (MPa)	σ_2 (MPa)
25	Yes	-65.9	-44.5
50	Yes	-131.7	-89
158	Yes	-416.5	-281.2
200	Yes	-527.2	-356
250	Yes	-659	-445

Table 4.4: Relationship between maximum stresses and Young's Modulus. Note, all results conform to linear stress-strain relations.

The results show that the level of stress is linearly related to Young's Modulus. More specifically,

$$\sigma \propto E \tag{4.20}$$

B) Effect of Linear Coefficient of Thermal Expansion

Coefficient (10^{-6})	Classical Theory Valid?	σ_1 (MPa)	σ_2 (MPa)
1	Yes	-92.5	-62.5
2	Yes	-185	-125
4	Yes	-416.5	-281.2
6	Yes	-555	-375

Table 4.5: Relationship between maximum stresses and Coefficient of Linear Thermal Expansion. Note, all results conform to linear stress-strain relations.

As in the previous results, the level of stress is linearly related to the coefficient of linear thermal expansion, i.e.

$$\sigma \propto \alpha \tag{4.21}$$

C) Effect of Plate Thickness

Thickness (mm)	Classical Theory Valid?	σ_1 (MPa)	σ_2 (MPa)
1	Yes	-416.5	-281.2
2	Yes	-416.5	-281.2
4	Yes	-416.5	-281.2
6	Yes	-416.5	-281.2

Table 4.6: Relationship between maximum stresses and plate thickness. Note, all results conform to linear stress-strain relations.

Table 4.6 shows that the thermal stresses are independent of the plate thickness. This is expected since stresses are calculated assuming a linear variation of temperature through the thickness. As discussed in section 3.1 linear temperature variations in the z-direction (through the plate thickness) do not yield thermal stresses.

Mechanical stresses induced by the cooling jet are very sensitive to the plate thickness. This will be discussed in section 4.3.3.3.

D) Effect of Plate Radius

Diameter (mm)	% of Surface Area Heated	Classical Theory Valid?	σ_1 (MPa)	σ_2 (MPa)
100	18	Yes	-421	-292
150	12	Yes	-419.3	-287.7
200	9	Yes	-416.5	-281.2
300	6	Yes	-407	-262.7

Table 4.7: Relationship between maximum stresses and plate diameter. Note, all results conform to linear stress-strain relations.

This study has thus far limited itself to cases where the heating radius is much larger than the plate thickness. To satisfy this requirement, if the radius of a hot spot acts over 10 % of the beam radius, a 200 mm diameter beam is needed.

If the table data is fit to a polynomial, the following expressions result:

$$\sigma_1 = -.0002b^2 + .01b + 422$$
$$\sigma_2 = -.0004b^2 + .033b + 293.1 \qquad (4.22)$$

E) Effect of Temperature Gradient

Maximum Temperature (K)	Classical Theory Valid?	σ_1 (MPa)	σ_2 (MPa)
1670	Yes	-416.5	-281.2
835	Yes	-208.3	-140.6
417.5	Yes	-104.2	-70.3

Table 4.8: Relationship between maximum stresses and temperature. Note, all results conform to linear stress-strain relations. The minimum temperature is 20 C.

Table 4.8 shows that the temperature is linearly related to the stress. This is described by,

$$\sigma \propto T \qquad (4.23)$$

F) Effect of Heating Radius

% of Surface Area Heated	a (m^{-2})	Classical Theory Valid?	σ_1 (MPa)	σ_2 (MPa)
3.5	.003	Yes	-380.2	-209.2
6	.005	Yes	-407.5	-262.7
9	.0075	Yes	-416.5	-281.2
12	.01	Yes	-419.3	-287.7
18	.015	Yes	-420.9	-292.1

Table 4.9: Relationship between maximum stresses and hot spot radius. Note, all results conform to linear stress-strain relations. The value *a* refers to the decay rate of the gaussian temperature boundary condition shown in figure 17, i.e., e^{-2r^2/a^2}.

These results can be fit to an exponential function which relates the heating radius to the principal thermal stresses.

$$\sigma_1 = -420 + 195e^{-523a}$$
$$\sigma_2 = -291.4 + 370e^{-502a} \qquad (4.24)$$

The area of a plate subject to thermal stresses from a hot spot is directly proportionally to the size of the hot spot. Section 4.1 demonstrated that membrane stresses quickly die out outside of the hot spot. Classical theory agrees with this.

Figures 4.6-4.8 illustrate this. They show stress contours in a tungsten plate when a hot spot occupies 6,10, and 25 percent of the plate's area respectively. In all three cases stresses are felt throughout the plate. However, the steepest stress gradients occur inside the hot spot. By measuring the width of the stress contours, one observes that the areas of elevated stress levels are completely included within the hot spot.

Fig.4.6:Radial stress contours-6 % case

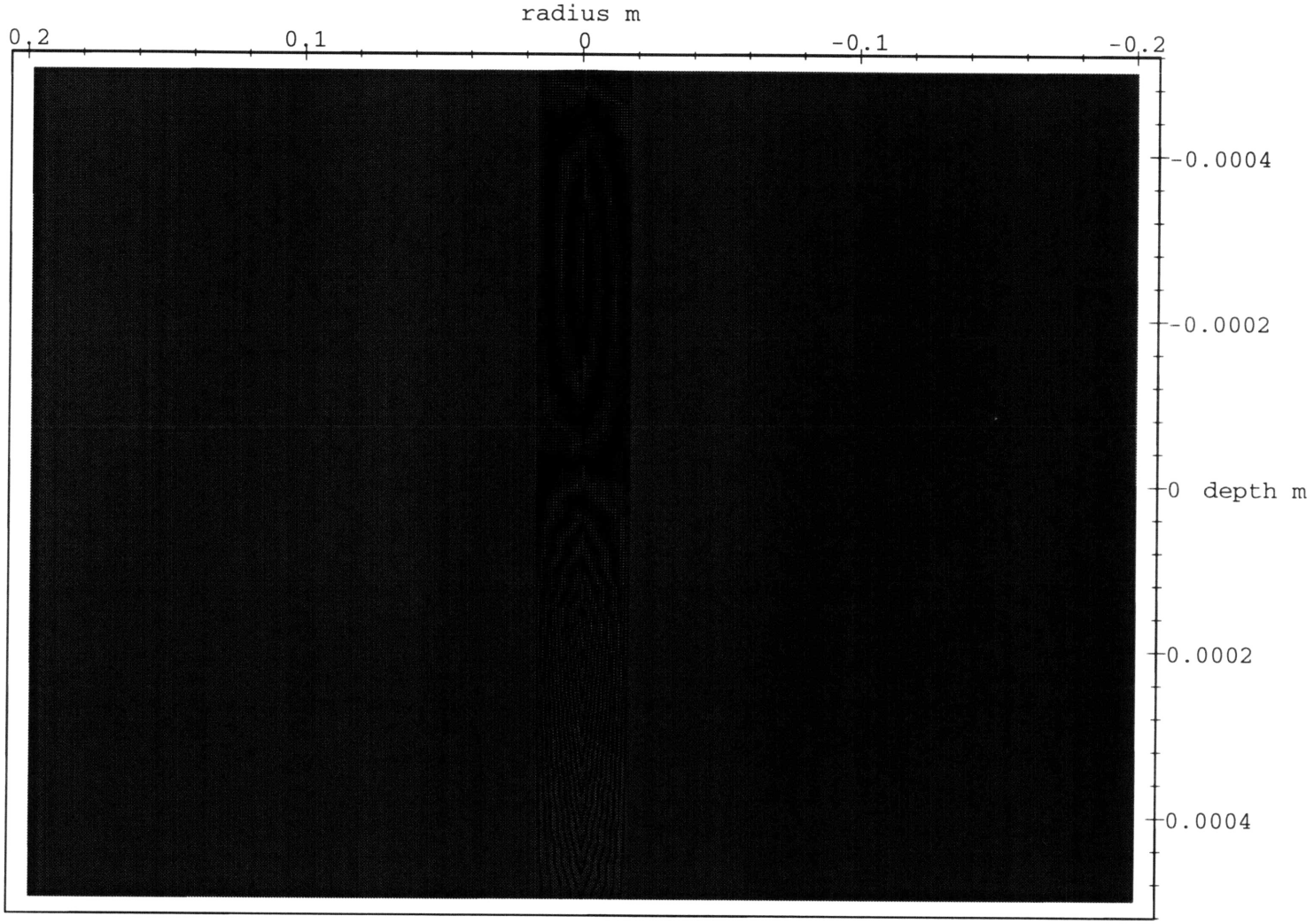

Fig.4.7:Radial stress contours- 10% case

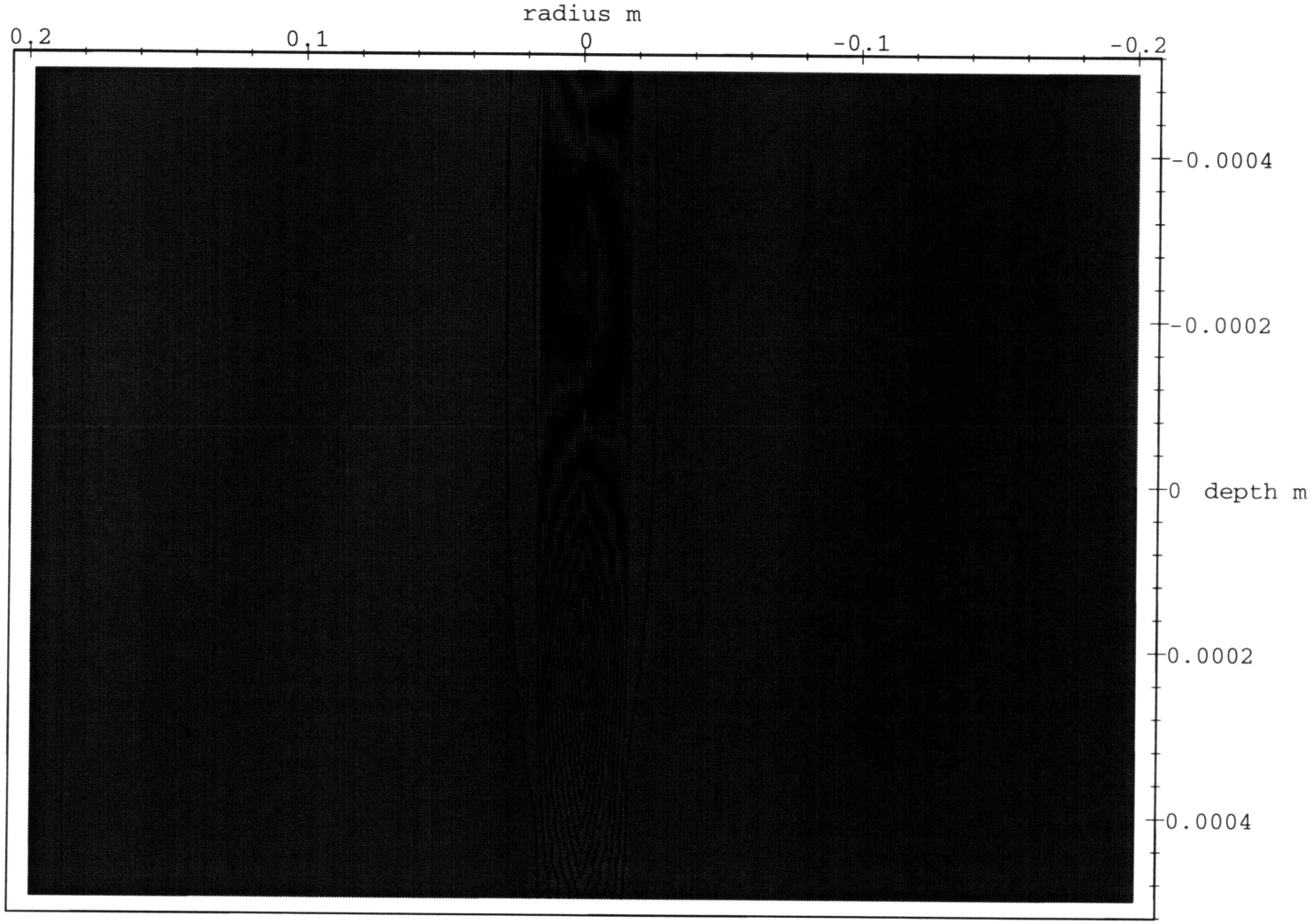

Fig.4.8:Radial stress contours- 22% case

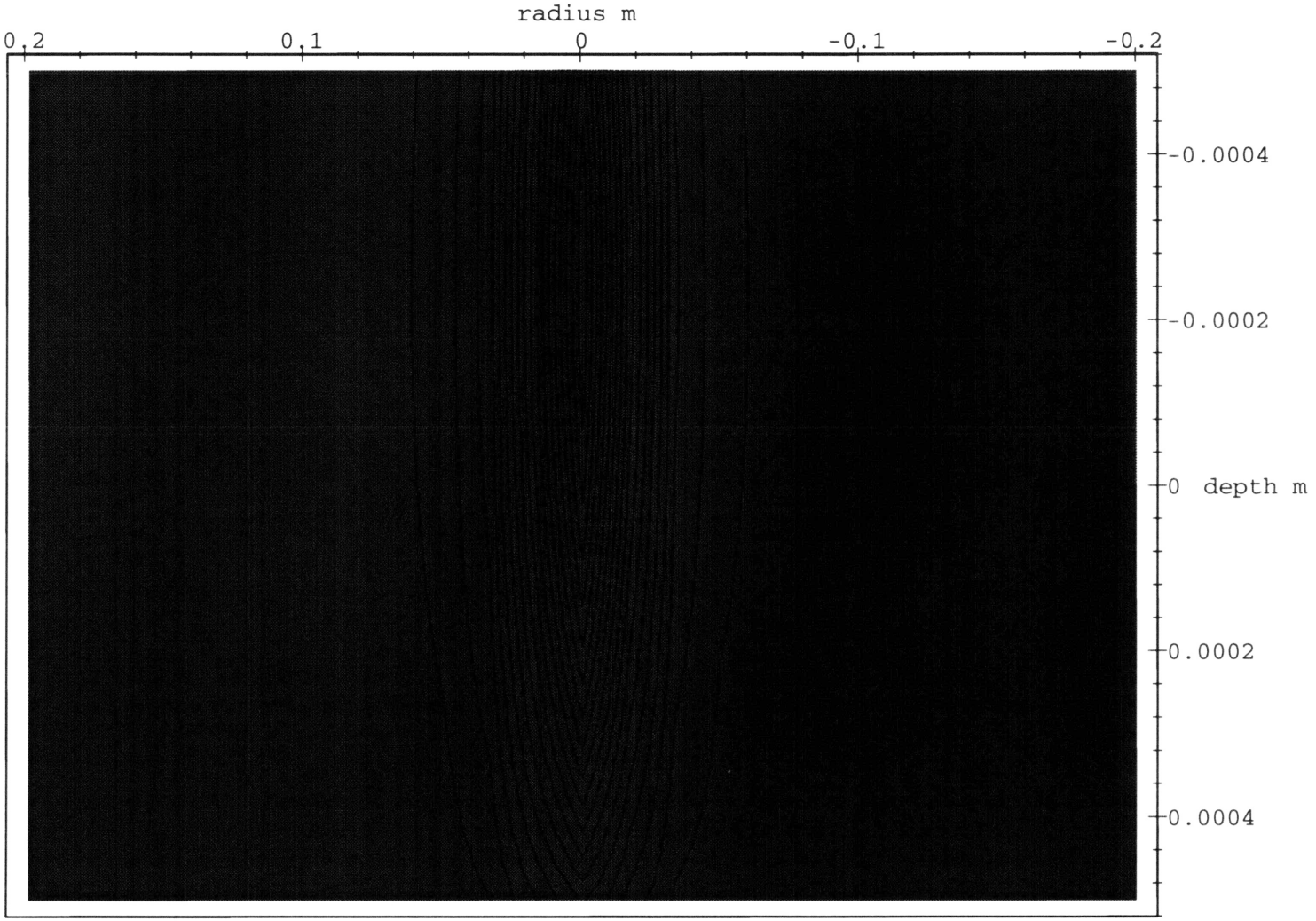

G) Final Correlation

Based on these results a correlation can be developed which describes the thermal stress intensity.

$$\sigma_{1t} = \frac{416.5}{2.94E14}\frac{E\alpha T}{1-\nu}\left[195e^{-523a} - 420\right]\left[-.0002b^2 + .01b + 422\right]$$
$$\sigma_{2t} = \frac{281.2}{1.36E14}\frac{E\alpha T}{1-\nu}\left[370e^{-502a} - 291.4\right]\left[-.0004b^2 + .033b + 293.1\right] \quad (4.25)$$

error: $<\pm 1\%$ {cumulative errors at limits of analysis}

These correlations are valid when:

$$.35m > b > .1m$$
$$\frac{\%b_{heated}}{d} >> 1$$
$$3\% < \%b_{heated} < 18\%$$
$$\sigma_{1,2} \leq \sigma_y$$

where $\%b_{heated}$ is the heating radius.

4.3.5 Influence of Cooling Jet on Stress Levels

In extreme heat flux systems cooled by impinging water jets, mechanical loading can be significant. Liu and Lienhard reported that for aluminum plates whose thickness were much less than 1 mm, jets caused plastic deformation[34]. This section considers the stresses due to cooling jets. As before, a correlation is developed to describe the maximum stress level caused by the jet.

Referring to equations 4.12a-b, for small deflections, the cooling jet only affects the bending stress equation, 4.12b. This equation can be modified to account for the mechanical load in the following manner[35],

---

[34]Liu, Xin and Lienhard V, J.H., *Extremely High Heat Flux Removal by Subcooled Liquid Jet Impingement*, HTD-Vol.217, ASME, 1992.
[35]Hetnarski, R.B., *Thermal Stresses, Vol. I.*, Elsevier Science Publishers B.V., 1986.

$$D\nabla^4 w = q - \frac{1}{1-\nu}\nabla^2 M_T \tag{4.26}$$

The term q is the pressure loading upon the plate due to the jet.

In cylindrical coordinates this equation can be solved for w by integrating the mechanical and thermal elements separately since,

$$\nabla^4 w = \frac{1}{r}\frac{d}{dr}\{r\frac{d}{dr}[\frac{1}{r}\frac{d}{dr}(r\frac{dw}{dr})]\} \tag{4.27}$$

Thus, by applying classical plate theory, from which equation 4.26 is derived, the calculated mechanical stresses can be superimposed upon the thermal stress results calculated in the previous section.

The governing equation for mechanical induced deflections is thus,

$$D\nabla^4 w = q(r) = Pe^{-r_o r^2} \tag{4.28}$$

with the edge boundary conditions:

Simply supported case	Fixed case	
$w = Mr = \frac{\partial^2 w}{\partial r^2} + \frac{\nu}{r}\frac{\partial w}{\partial r} = 0$	$w = \frac{dw}{dr} = 0$	(4.28a-b)

The form of the pressure function, q(r), has been chosen to model a gaussian decay of the jet pressure field. The term r_o is a constant which allows the gaussian function to approach zero within a specified tolerance. For example, if the jet has a diameter of 2 mm, an r_o term is calculated such that at the jet radius (1 mm), $q \to 0$. That is:

$$r_o = \lim_{q \to 0} \frac{-\ln\frac{q}{P}}{r_j^2} = \lim_{r \to 0} \frac{-\ln\frac{r}{P}}{r_j^2} \approx \frac{-\ln\frac{tolerance}{P}}{r_j^2} \tag{4.29}$$

where r_j is the radius of the jet.

The actual form of the gaussian decay function is based upon research performed by Liu and Lienhard[36]. Figure 4.9 provides more detail.

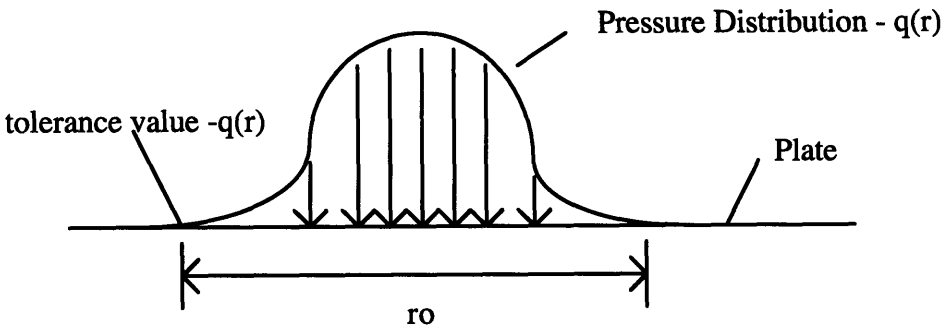

Figure 4.9: Pressure distribution due to impinging water jet.

Equation 4.27 has been solved for the boundary conditions given in 4.28 a-b. The solutions are as follows (see appendix):

$$w_{simple} = wp + \frac{r^2}{4} C2 + C4$$

where:

$$wp = \frac{\mathrm{Pr}^2}{16 D r_o}\left[e^1 - 2 + 2\ln r + \gamma(1) + \ln r_o\right]$$

$$\gamma(n) = \lim_{m \to \infty} \sum_{k=1}^{n} \frac{(\ln k)^n}{k} - \frac{(\ln m)^{n+1}}{n+1}$$

$$C2 = \frac{-P}{4 D r_o}\left[\gamma(1) + 2\ln b + \ln r_o + e^1 + \frac{1-\nu}{1+\nu}\right]$$

$$C4 = \frac{P b^2}{16 D r_o}\frac{3+\nu}{1+\nu}$$

(4.30)

[36]Liu, Xin, J.H. Lienhard V, and L.A. Gabour, *Stagnation-Point Heat Transfer During Impingement of Laminar Liquid Jets: Analysis Including Surface Tension*, Journal of Heat Transfer, Vol. 115, Feb. 1993.

$$w_{fixed} = wp + C2\frac{r^2}{4} + C4$$

where:

$$wp = \frac{\mathrm{Pr}^2}{16Dr_o}\left[e^1 - 2 + 2\ln r + \gamma(1) + \ln r_o\right]$$

$$C2 = \frac{-P}{4Dr_o}\left[e^1 - 1 + 2\ln b + \gamma(1) + \ln r_o\right]$$

$$C4 = \frac{Pb^2}{16Dr_o}$$

(4.31)

The stresses are given by the following expressions[37]:

$$M_{r=} \frac{\partial^2 w}{\partial r^2} + \frac{\nu}{r}\frac{\partial w}{\partial r} \qquad \sigma_{rr=} \frac{-6DM_r}{d^2}$$

$$M_\theta = \frac{1}{r}\frac{\partial w}{\partial r} + \nu\frac{\partial^2 w}{\partial r^2} \qquad \sigma_{\theta\theta} = \frac{-6DM_\theta}{d^2} \tag{4.32}$$

The maximum stress occurs at the center of the plate. This value can be found by substituting equation 4.29 into equations 4.32, and taking the limit as r approaches zero. This results in the following expressions for *both* fixed and simply supported plates:

$$\sigma_{rr\max} = \sigma_{\theta\theta\max} = \frac{3}{2}\frac{\mathrm{Pr}_j^2}{d^2}(1+\nu) \tag{4.33}$$

Therefore, the maximum values of the principal stresses are:

$$\sigma_1 = \sigma_{rr\max}$$
$$\sigma_2 = 0 \tag{4.34}$$

[37]Ugural, A.C. and Fenster, S.K., *Advanced Strength and Applied Elasticity*, Elsevier North Holland, 1981.

4.3.3.3 When do jet or thermal stresses dominate

The correlations developed in section 4.3.3.1 and 4.3.3.2 can be used to determine when either the thermal or the mechanical loading dominates the stress field for the extremal heat flux system.

Mechanical stresses dominate the problem when

$$\frac{\sigma_{1t}}{\sigma_{1jet}} \langle\langle 1 \tag{4.35}$$

Thermal stresses dominate the problem when

$$\frac{\sigma_{1t}}{\sigma_{1jet}} >> 1 \tag{4.36}$$

The correlations show that in cases where the plate thickness is less than .1 mm, mechanical stresses generally dominate the elastic problem. Additionally, large jets (radius > 6 mm) will dominate when a plate is 1 mm thick.

When the plate is 1 mm thick and the jet is small (radius < 2 mm), as is the case considered in this thesis, thermal stresses generally dominate the problem.

4.3.3.4 Applicability of Classical Plate Theory

As discussed in section 4.3.3.2, classical theory is not valid when large deflections occur or when the linear stress-strain relations do not adequately describe the material's strain. Deflection can be easily checked by comparing equations 4.15 and 4.30 to the thickness of the plate. The linear strain relations apply, if the quadratic terms in equation 4.11 are an order of magnitude less than the non-squared terms. Using these principles, the results can be checked for validity. The discussion below relates to the strain requirement. The maximum deflection is given by the constant terms in equations 4.15 and 4.30.

Correlations have been developed to determine the relationship between the parameters and the linear and non-linear strain components. The relationship is complex and not easily garnered from examining calculated results. Additionally, substituting Hooke's Law

($\sigma = E\varepsilon$) into the stress correlations (4.25 and 4.34) is not sufficient to describe the linear portion of the strain correlation. The stress correlations developed above describe only the maximum stress levels, they do not account for the stress field variations. The strain correlations need to describe this variation, as will be discussed below. However, a reasonable correlation can be developed by examining the components of the strain equations (4.11) term by term.

The correlations developed for the linear and non-linear strain components are shown below:

$$\varepsilon_l = \left[\frac{-0.00014227}{0.003485584}\right]\frac{\alpha T}{1-\nu} Lin_T$$

where:

$$Lin_T = \frac{a^2}{b^2}\left(d - e^{-.00005\frac{b^2}{a^2}} + \frac{b^2}{a^2}\right) + d\left(2 + e^{-.00005\frac{b^2}{a^2}} - \frac{a^2}{b^2}\right)$$
$$+\frac{z^2}{d^2}\left(1 - \frac{a^2}{r^2} + \left(\frac{a^2}{r^2}+1\right)e^{-2\frac{r^2}{a^2}}\right)$$
$$+\frac{z}{d}\left(1 + \frac{a^2}{r^2} - \left(\frac{a^2}{r^2}\right)e^{-2\frac{r^2}{a^2}}\right)$$

(4.37)

$$\varepsilon_n = \left[\frac{0.000016096}{0.001169579}\right]\left(\frac{\alpha T}{1-\nu}\right) Non_T$$

where:

$$Non_T = \frac{z}{d}\left(-r - \frac{a^2}{r}e^{-0.00005\frac{b^2}{a^2}} + \frac{a^2}{r} - r + \frac{a^2 r}{b^2}\right)$$
$$+\frac{z}{d}\left(-2r + 2a^2\left(\frac{1}{r} + \frac{r}{b^2} - \frac{e^{-0.00005\frac{b^2}{a^2}}}{r}\right)\right)$$
$$r + \frac{a^2}{r}e^{-2\frac{r^2}{a^2}} + \frac{a^2}{r} + \frac{a^2}{b^2}r$$

(4.38)

To check whether the non-linear strain component (ε_n) is of significance, it must be compared to the linear strain component (ε_l). If throughout the entire body, the linear strains are an order of magnitude larger than the non-linear strains, then the non-linear component can always be neglected. However, as shown in section 4.3.4, the portion of the material which is stressed is the region inside the hot spot. Thus, it is inside this area where the strains should be compared. The influence of non-linearities elsewhere is not of concern since the stresses outside the hot spot will be smaller than those inside the hot spot. To compare the non-linear and linear strain components, the correlations given above should be graphed as functions of r and z for a given set of α, T, ν, d, a and b values.

When these graphs are created for the base case (see section 4.3.4), the radius of the hot spot and plate diameter increase, the strains become more non-linear. This also holds for T, α, and ν. However, as the thickness increases, strain non-linearities decrease.

Table 4.10 lists the values of the important parameters for which classical theory is no longer applicable to the modified base case. In general, classical theory will not hold for very large thin plates with large hot spots. In these cases, the results of section 4.1 are more appropriate. Alternatively, a modified version of classical theory which accounts for large plate deflections can be used. When this is done, the bending rigidity of the plate can be approximated as zero.

Parameter	Value which makes strain non-linear
Plate Radius	> 0.35 m
Radius of hot spot as % of plate diameter	> 30 %
Coefficient of expansion	> 20
Maximum temperature	> 8300 K
Plate thickness	< 1mm

Table 4.10: Parameter values for which classical plate theory is no longer applicable to the base case described in section 4.3.4. Since the allowable temperature exceeds that of any known material, temperature is not a limiting parameter.

The following graphs illustrate how to determine if the linear stress-strain relations are applicable to the problem at hand. Figures 4.10-4.12 show the linear and non-linear strains and the difference between the two for the base case. Notice, that the non-linear

strain component has no effect except at the edges of the plate. In contrast, figures 4.13-4.15 show the same strain components for the case when the hot spot occupies 40 % of the plate. Notice that the plate is significantly affected by the non-linear strain terms.

The strain correlations listed above do not include strains due to the cooling jet. This is because strains induced by jet loading are insignificant compared to thermal strains when the jet radius is < 2 mm and the plate thickness is ≥ 0.5 mm. Since only small jets are considered, i.e., < 2 mm radii, and since only plates with thickness ≥ 1 mm are considered - lesser thicknesses invalidate classical theory- mechanical strains do not need to be included.

Fig.4.11:Linear strains when classical theory valid- base case

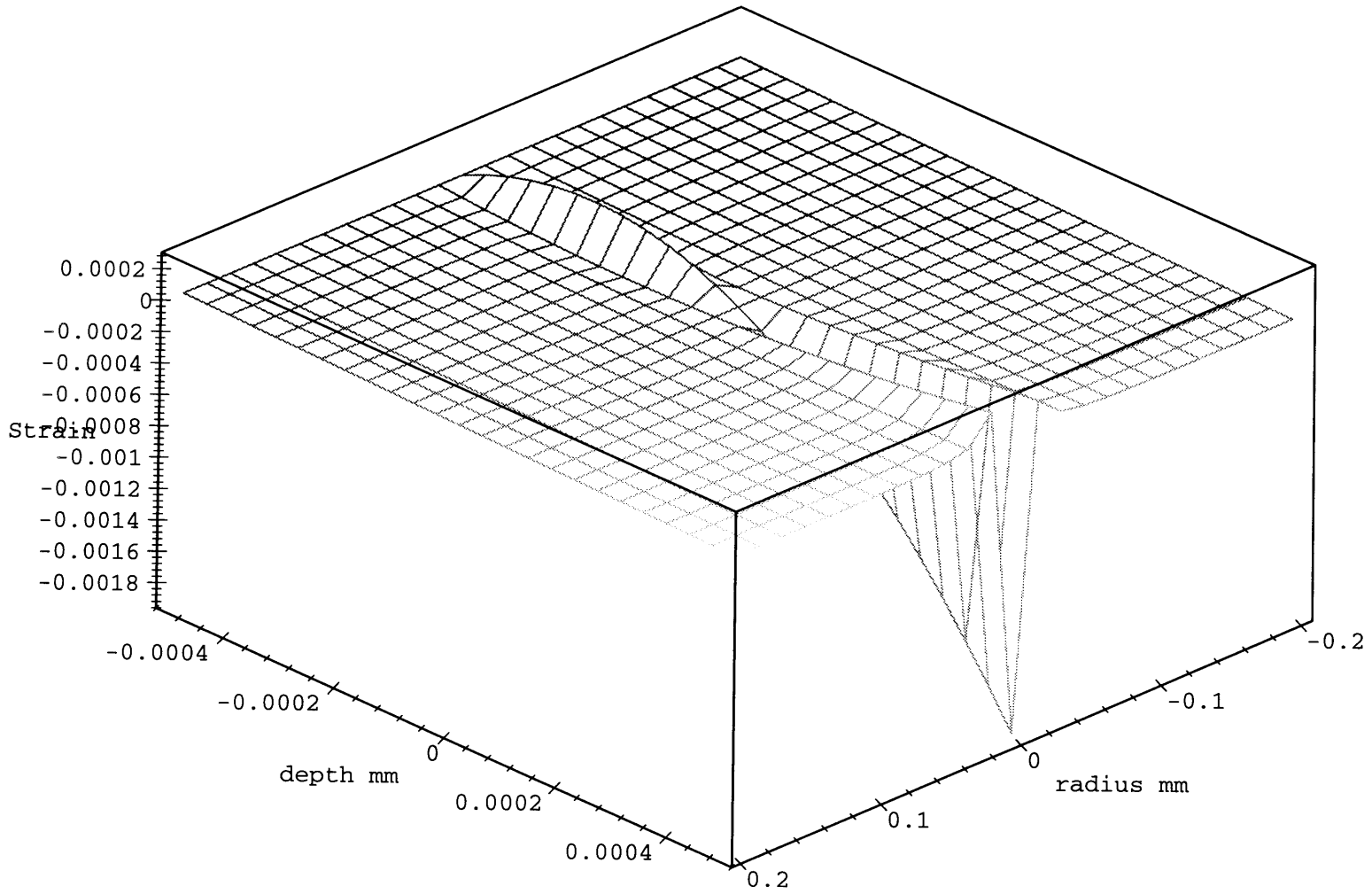

Fig.4.12:NonLinear strains when classical theory valid-base case

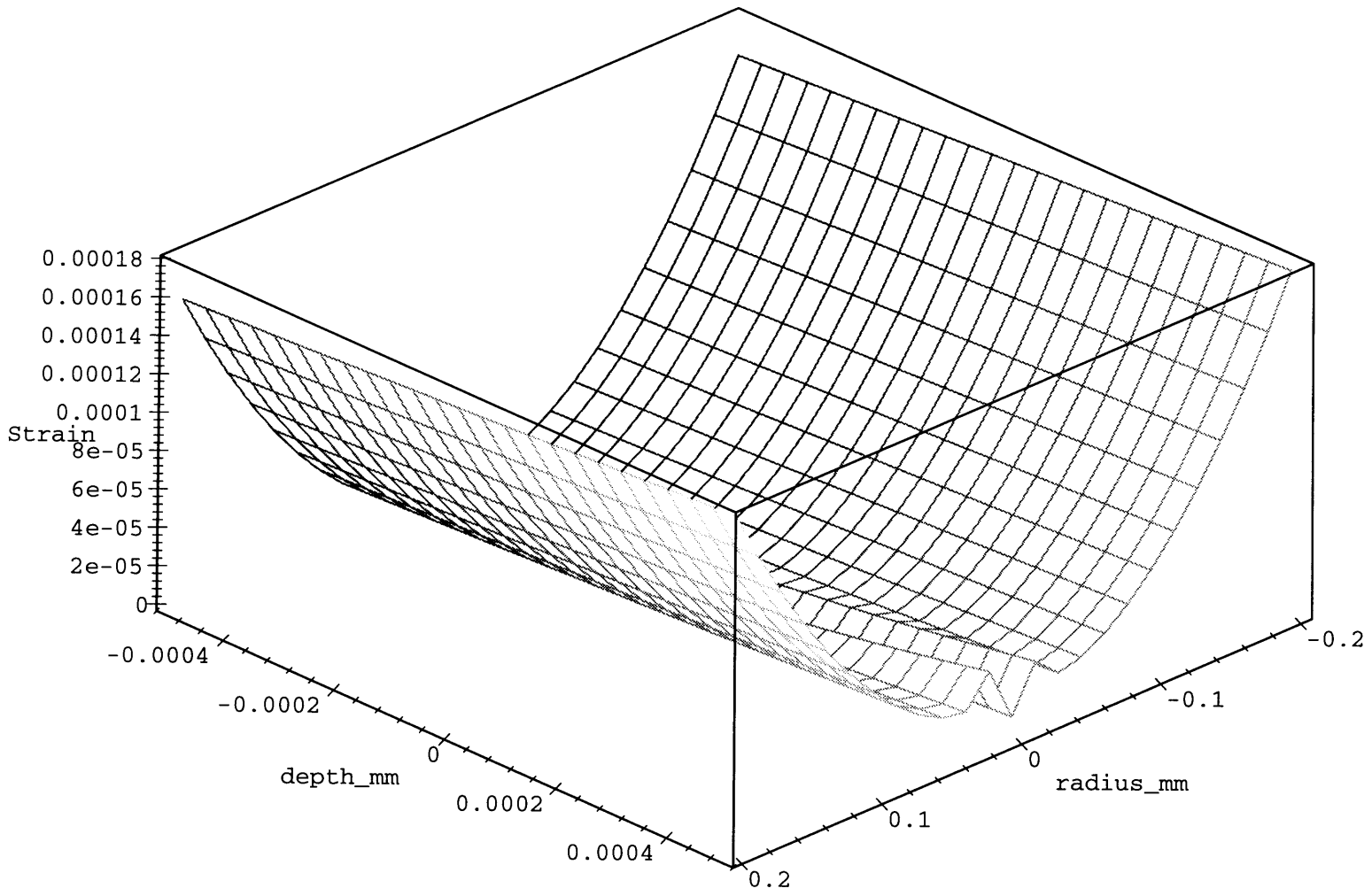

Fig.4.13:Linear minus non-linear strains when classical theory valid-base case.

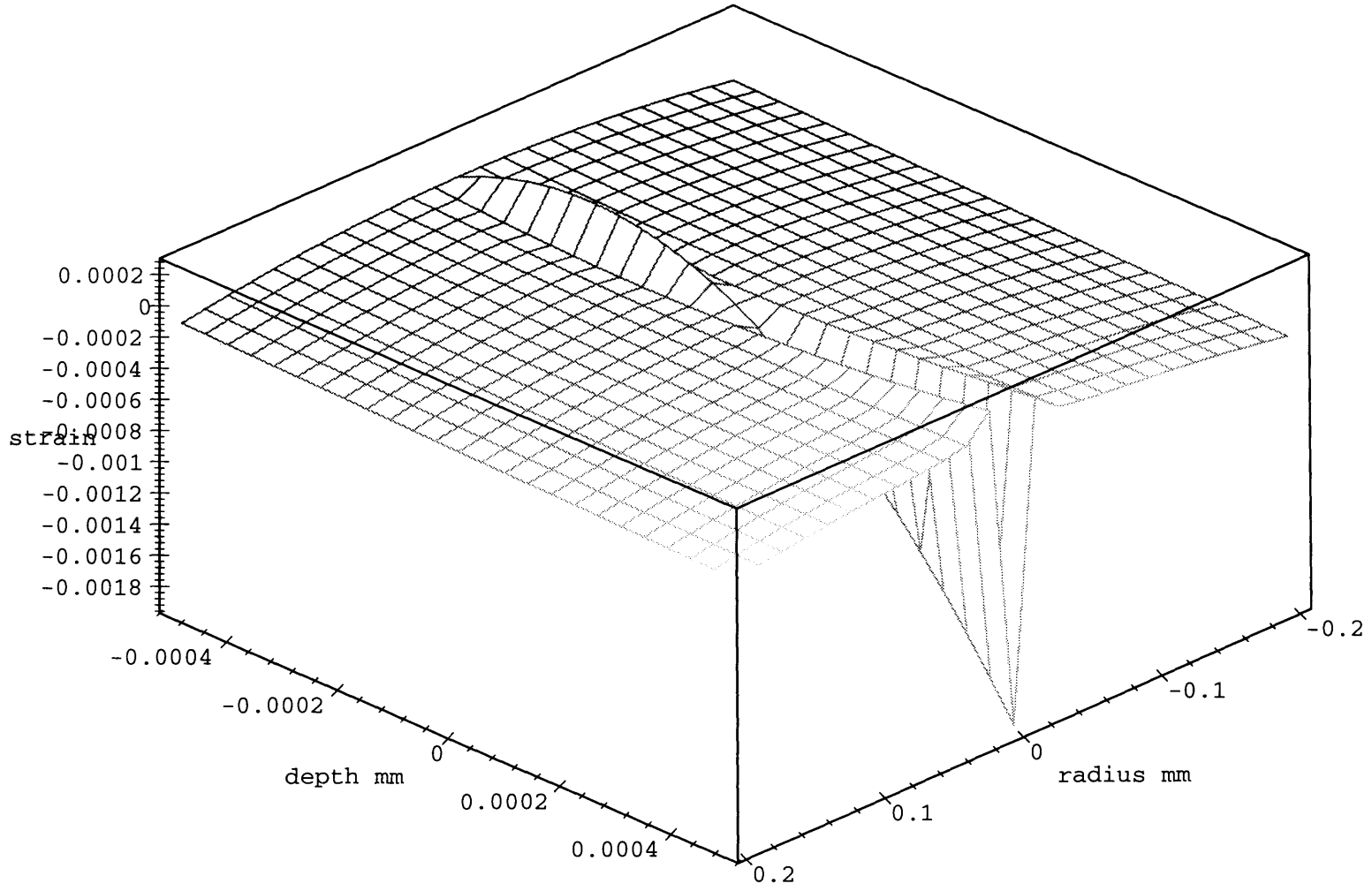

Fig.4.14:Linear strains when classical theory invalid-base case with 40% surface heating.

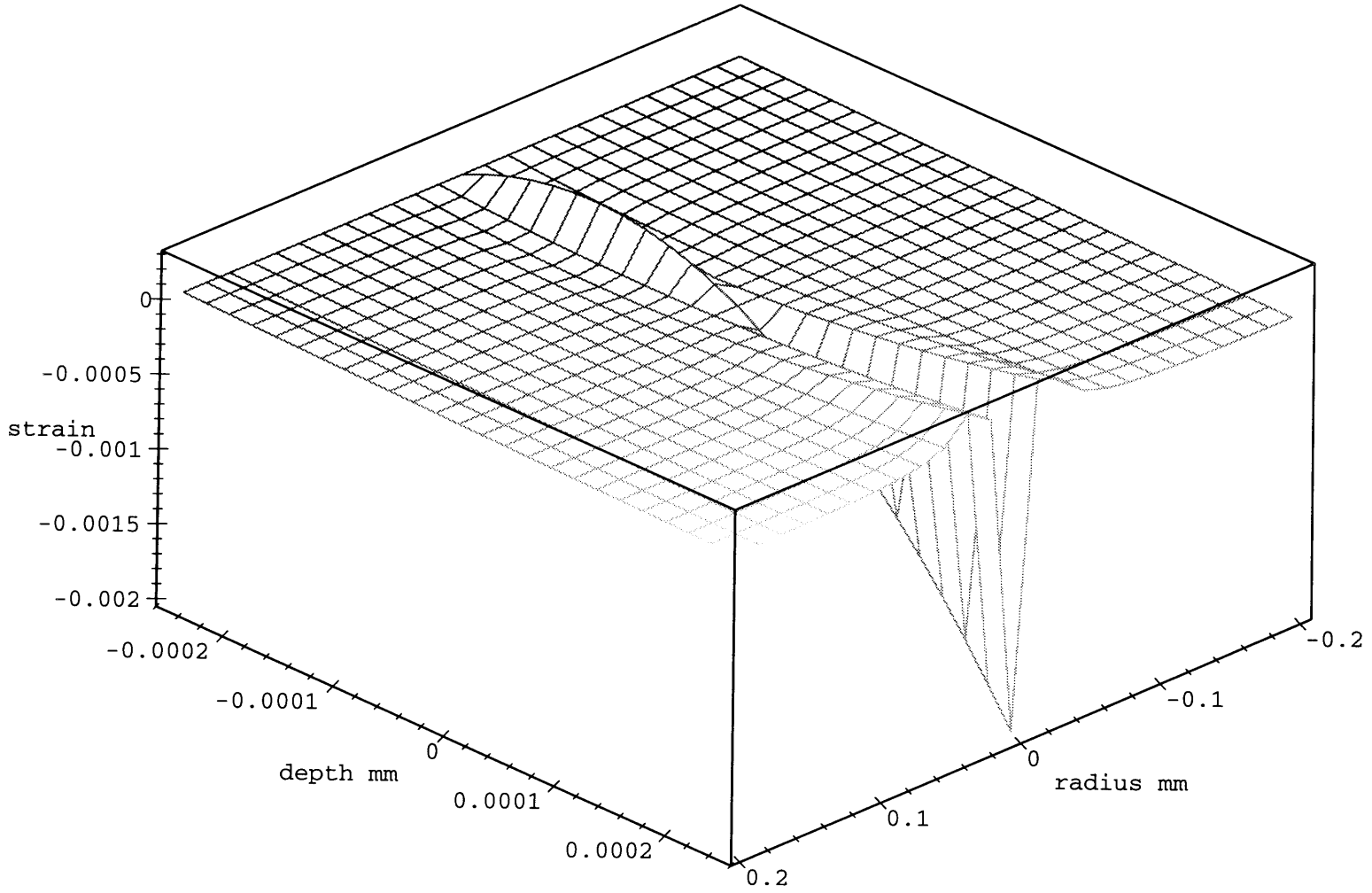

Fig.4.15:Non-linear strains when classical theory invalid-base case with 40% surface heating.

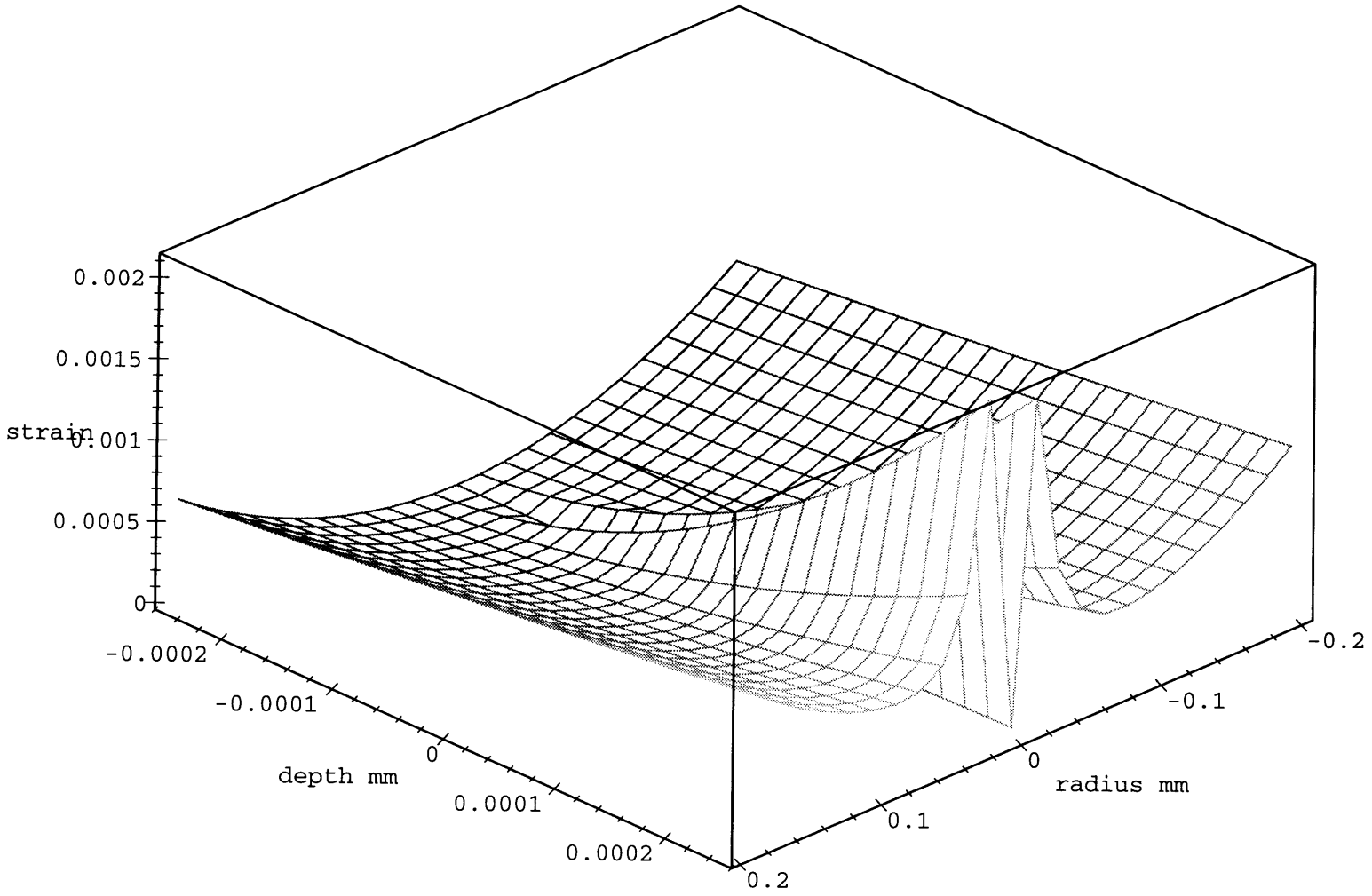

Fig.4.16:Linear minus non-linear strains when classical theory invalid-base case with 40% surface heating.

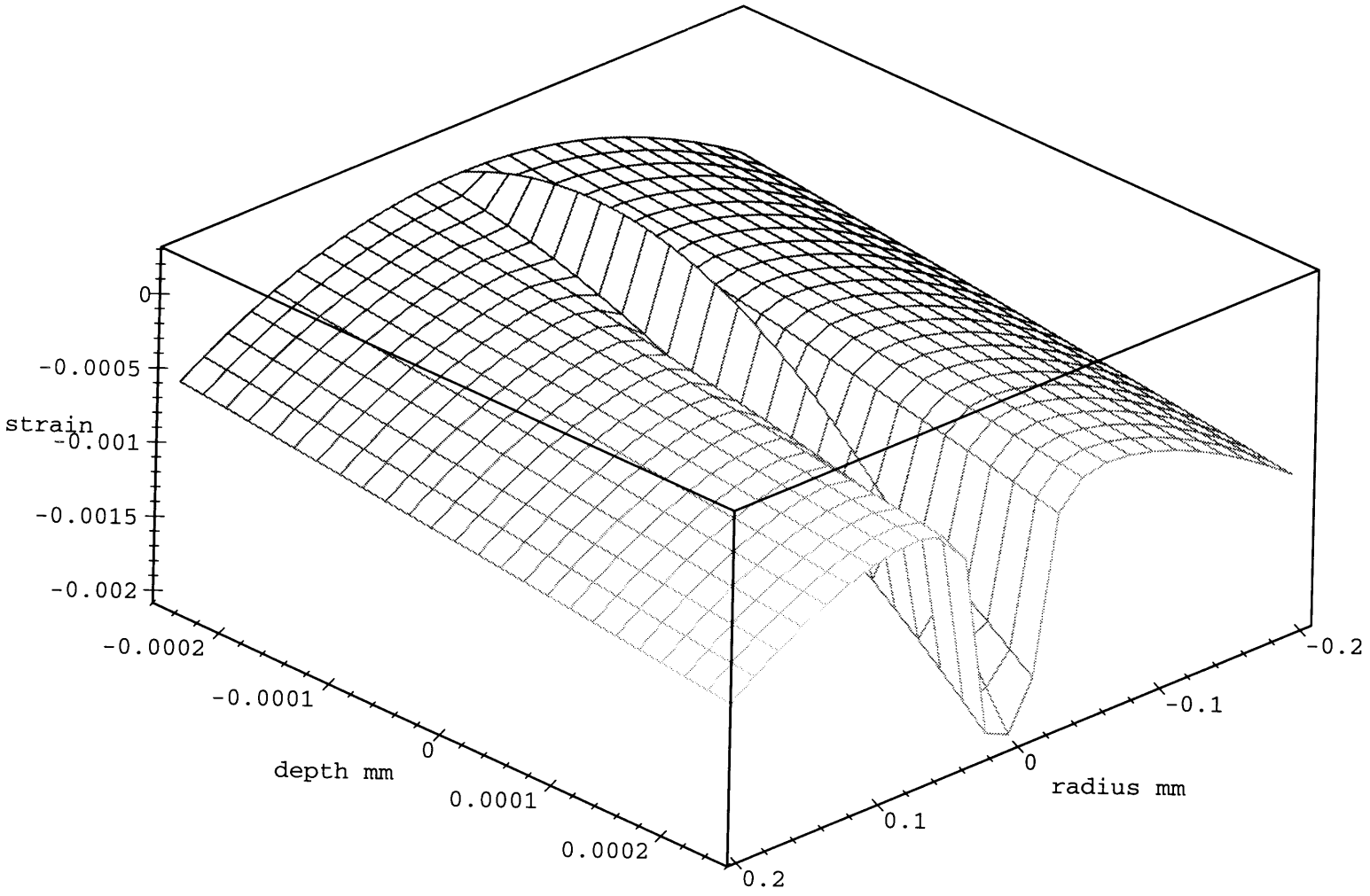

4.3.3.5 Elastic Limits

Based on the solutions to equations 4.19 and 4.29, the temperature at which some materials yield can be found. These results are complied assuming that material properties can be approximated at the average temperature, the plate geometry conforms to the base case, and the jet has a diameter of 2 mm, with a maximum pressure of 5 MPa. The yield strength and ultimate strengths are functions of temperature for this calculation.

To determine elastic failure, the distortion energy theory has been used as recommend by Ugural[38]. This theory says that yielding occurs when,

$$\sigma_1^2 - \sigma_1\sigma_2 + \sigma_2^2 = \sigma_y^2 \tag{4.39}$$

where the principal stresses σ_1 and σ_2 are given by:

$$\sigma_{1,2} = \frac{\sigma_{rr} + \sigma_{\theta\theta}}{2} \pm \sqrt{\left(\frac{\sigma_{rr} + \sigma_{\theta\theta}}{2}\right)^2 + \tau_{r\theta}} \tag{4.40}$$

The results are given in table 4.11.

Material	Maximum Temperature (K)	% of Melting Temperature (K)	Flux (MW)
Molybdenum	788	27.2	63.9
Tungsten*	828	22.6	72.6
Aluminum 6061	568	57.2	62.4
Stainless Steel 304 L	653	39.1	6.05

Table 4.11: This shows temperatures for which the plate reaches yielding somewhere in the body. The minimum temperature is 20C.* Tungsten is a brittle material. See relevant discussion in sections 4.3.3.5 and 5.2.

Tungsten is the best material from the standpoint of the heat flux and temperature. Stainless steel performs the worst of the materials examined. These results suggest that plastic and viscoelastic behavior are primary concerns for materials subjected to their

[38]Ibid.

melting temperatures. In the elastic regime considered here, yielding occurs in a small region inside the hot spot. The exact location depends not only upon the location of maximum stress but on the rate at which the yield strength decreases with temperature. For example, yielding occurs for molybdenum mid-way through the plate thickness, whereas it occurs for aluminum at the plate surface. Note that tungsten behaves as both a brittle and ductile material in this heating configuration. Thus, its failure point is determined by comparing its stress field to both the ultimate and yield strengths.

These results show that materials best suited to high flux applications have a high melting point, a large ratio of yield strength to Young's modulus and expansion coefficient, and a large thermal conductivity. In particular, the large flux gap between stainless steel and aluminum suggests that thermal conductivity has a greater impact on allowable flux than does material strength for elastic behavior.

These rankings which result from this model are an improvement over the results that would be predicted by using the figure of merit system developed by U.C.L.A. researchers.[39] They suggested using the following equation as an estimate for the maximum flux in a material:

$$Q = \frac{2(1-\nu)k\sigma_y}{E\alpha} \tag{4.41}$$

This is simply derived from the stress equation for a uniformly heated fixed plate. The properties in this equation are all evaluated at the same temperature. This equation does not account for yield strength variations through the plate nor does it account for the brittle-ductile behavior of materials such as tungsten. Consequently, it can give specious results when a large temperature gradient exists across the plate thickness. A similar argument applies to the UCLA transient heating figure of merit. Section 8.2 discusses an improved ranking system for elastic and plastic materials.

The results given in section 4.1 do agree with the results of the UCLA study. This is expected since section 4.1 does not account for the temperature gradient across the plate thickness.

---

[39]Abou, et. al., *Magnetic Fusion Energy Plasma Interactive and High Heat Flux Components, Vol. 2,* UCLA/PPG-815, DOE Office of Fusion Energy, June 1984.

It is not immediately obvious if the elastic results given for tungsten can actually be achieved. Liu and Lienhard reported that tungsten failed by brittle fracture immediately after heating commenced[40]. This suggests that transient heating by flux exposure may be important for materials whose properties are very sensitive to temperature. The results in table 4.11 assume that the temperature distribution is present before a stress field exists. Section 5.2 presents a detailed argument on this subject.

4.4 Fixed Plate Results

4.4.1 Solution of Equations

This section examines the effect of fully restraining the base case circular plate described in section 4.3.4. The equations for thermal and mechanical stress need to be re-solved with new boundary conditions. The thermal stress equations include both membrane and bending stresses as explained in section 4.3.3. The edge boundary conditions for the bending equation (4.12b) are:

$$w = \frac{dw}{dr} = 0 \tag{4.42}$$

Hetnarksi [41] has solved this problem in a general form. The solution is:

$$w = \frac{-1}{2D}\int_0^b M_T r dr + \frac{r^2}{b^2}\int_0^b M_T r dr + \int_r^b \frac{1}{r}\int_0^r \frac{M_T}{D} r dr dr \tag{4.43}$$

The membrane stresses can be solved for by using equation 4.14 with the boundary conditions:

$$\begin{aligned} u(r=b) &= 0 \\ N_r &= 0, r \to 0 \end{aligned} \tag{4.44}$$

Johns[42] gives the solution before the application of boundary conditions:

---

[40]Liu, Xin and Lienhard V, J.H., *Extremely High Heat Flux Removal by Subcooled Liquid Jet Impingement*, HTD-Vol.217, ASME, 1992.

[41]Hetnarski, R.B., *Thermal Stresses, Vol. I.*, Elsevier Science Publishers B.V., 1986.

$$u = \frac{\alpha(1+\nu)}{r}\int_0^r T_n r dr + C_1 r + \frac{C_2}{r}$$

$$N_r = \frac{-E\alpha}{r^2}\int_0^r T_n r dr + \frac{EC_1}{1-\nu} - \frac{EC_2}{r^2(1+\nu)} \qquad (4.45)$$

$$N_\theta = \frac{E\alpha}{r^2}\int_0^r T_n r dr + \frac{EC_1}{1-\nu} + \frac{EC_2}{r^2(1+\nu)} - E\alpha T_n$$

Application of the boundary conditions yields (see appendix):

$$N_r = \frac{E\alpha}{r^2}\int_0^r T_n r dr + \frac{E\alpha}{1-\nu}\frac{1+\nu}{b^2}\int_0^b T_n r dr$$

$$N_\theta = \frac{E\alpha}{r^2}\int_0^r T_n r dr - E\alpha T_n + \frac{E\alpha}{1-\nu}\frac{1+\nu}{b^2}\int_0^b T_n r dr \qquad (4.46)$$

where:

$$T_n = \int_{H/2}^{H/2} T dz$$

4.4.2 Thermal Stress Correlations

For a fixed plate, variation of important parameters yields correlations for stress as was done in section 4.3.4. Changes in the mechanical properties of the material result in the same correlations as before. However, a change in geometry produces differences. Tables 4.12-4.13 summarizes the change in the principal stresses.

In the base case, as described in section 4.3.1, the maximum and minimum principal stresses are:

$$\sigma_1 = 1589.1 MPa$$
$$\sigma_2 = 550.5 MPa$$

---

[42]Johns, D.J., *Thermal Stress Analyses*, Pergamon Press Ltd, 1960.

Radius (m)	σ_1 (MPa)	σ_2 (MPa)
.1	1644.4	555.4
.15	1621.4	552.2
.2	1589.7	550.5
.25	1549.7	548.4
.3	1502	545.7

Table 4.12: Results for fixed plate; variation in radius

% of Radius Heated	a (m^{-2})	σ_1 (MPa)	σ_2 (MPa)
3.5	.003	1247.9	529.9
6	.005	1502	545.7
9	.0075	1589.7	550.5
12	.01	1621.4	552.2
18	.015	1644.4	553.4

Table 4.13: Results for fixed plate; variation in heating radius

Based on the results the following correlations can be made,

$$\sigma_1 \propto \frac{1589}{4.3E15}\frac{E\alpha\Delta T}{1-\nu}\left[-1686b^2-36b+1664\right]\left[1E8\left(3.47a^3-.145a^2\right)+1.95E5a+804\right]$$
$$\sigma_2 \propto \frac{550.5}{1.5E15}\frac{E\alpha\Delta T}{1-\nu}\left[-114b^2-9.7b+553.2\right]\left[-5.45E10a^4+2.82E9a^3-5.2E7a^2+4.15E5a+401\right] \quad (4.47)$$

error: $<\pm 1\%$

These are valid when:

$$\sigma_{1,2} \le \sigma_y$$

$$3\% << \frac{\%b_{heated}}{d} << 18\%$$

$$d > .5mm$$

4.4.3 Applicability of Classical Theory

The same procedure described in section 4.3.3.4 is used here to determine the parameter limits for which classical theory is valid.

In the fixed plate case, membrane strains are generally larger than bending strains. Referring to equation 4.11, this increases the importance of the liner strain term relative to the non-linear strain term. Additionally, since membrane stresses dominate the thermal stress problem, mechanical strains caused by jet induced deflection are not important for small jets ($\leq$ 2 mm diameter).

Thus, it is expected that the validity of the fixed plate case is less sensitive to parameters variation compared to the simple supported case. Table 4.14 shows the limiting parameters.

Parameter	Limiting Value
Plate Radius (m)	> 75
Hot Spot Radius (% of Plate Radius)	> 18 %
Linear Expansion Coefficient	>> 200
Temperature Gradient	>> 9000
Plate Thickness (mm)	< .5

Table 4.14: Limiting parameters for validity of classical theory to fixed plate. ">>" refers to cases where no limit was found. The value given in these cases is the last one for which the strains were evaluated.

These results show that the clamped beam is less sensitive to most parameter variations than the simply supported case.

4.4.4 Elastic Limits

Elastic limits have been complied in Table 4.15. The calculations assume that material properties can be approximated at the average temperature, the plate geometry conforms to the base case, and the jet has a diameter of 2 mm with a maximum pressure of 5 MPa. The yield strength - and ultimate strength for tungsten - is a function of the temperature for this calculation.

Material	Maximum Temperature (K)	% of Melting Temperature	Flux (MW)
Molybdenum	400	14.6	14
Tungsten*	463	12.2	27.93
Aluminum	438	42.1	33.6
Stainless Steel 304 L	378	22.3	1.36

Table 4.15: This shows temperatures for which the fixed plate reaches yielding somewhere in the body. Minimum temperature is 20 C. * Tungsten is a brittle material. See discussion in sections 4.3.3.5 and 5.2.

For clamped plates, aluminum yields the highest flux level. When the fixed plate is kept within elastic limits, the allowable temperatures do not vary greatly between the different materials. Under these conditions, thermal conductivity is the determining factor.

Table 4.15 shows that there is a significant change in allowable temperatures from the simply supported to the fixed case. This is a consequence of increased membrane stresses. In the simply supported case, higher allowable temperatures make material strength as important an issue to heat flux as conductivity. For example, aluminum does not perform as well relative to the other materials in the simply supported case since its yield strength decreases much more quickly with temperature.

4.5 Conclusions

A number of important conclusions can be drawn from free beam problem. It was noted that when the area of localized heating is much larger than the thickness of the heated beam, the temperature distribution can be assumed to be linear through the thickness. Additionally, considering the surface of the beam, when the temperature variation of the hot spot in one direction is much more gradual than in other direction, it is reasonable to assume that the temperature distribution will be two dimensional. These two approximations do not significantly alter the temperature distribution for the cases considered in section 4.2, but allow simpler solutions for the thermal stress problem.

The free beam also illustrated an important difference with the results of section 4.1. The results of that section showed that large membrane stresses will exist in a small region when a beam is essentially heated at a point. This section showed that as the area of the

hot spot increases, the thermal stresses decrease. However, stresses are still centered near the point of maximum temperature.

When plates are restrained, thermal stresses increase significantly. If a plate is to remain elastic, the maximum temperature it supports will be substantially lower than its melting temperature. The less expansion is allowed in a plate, the lower the temperature gradient that it can support. As the gradient decreases the mechanical strength becomes less important than the thermal conductivity for determining maximum heat flux.

This chapter has identified correlations that can be used, within the applicable ranges of classical theory, to predict the maximum thermal and mechanical stresses in both the fixed and simply supported cases. The correlations can help predict when thermal or mechanical stresses dominate the problem. They can also be used to find a preliminary estimate of the allowable temperature.

The user of the correlations should be aware, that finding the maximum stress is not a substitute for finding the stress field. Yielding can occur at low stress levels due to the yield strength's dependence on temperature. The stress field can be found using the equations provided in this chapter or with the computer programs given in the appendix.

Chapter 5

Localized Heating Numerical Models - Plastic Behavior

5.1 Finite Element Model Description

This chapter incorporates the important aspects identified in chapter 3 which could not be examined analytically. These include: temperature dependent properties, transients, and plasticity. Finite element models have been constructed using ANSYS[43]. The ANSYS programs are located in appendix C.

Figure 5.1 shows the basic finite element model used. Axisymmetric two dimensional elements are used to create a half beam with its origin at zero and its edge at a radius of 200 mm. One hundred elements make up the radius of the beam. The element width increases with the radius. An ANSYS spacing factor of 20 (see appendix C, matlab program listing for definition) is used to increase the element size. However, the first millimeter of the plate consists of 10, .1 mm wide elements. This fine mesh is used to model the cooling jet boundary condition. All elements are *1/s* mm high. The variable *s* is the number of elements which comprise the thickness of the plate. Good resolution is achieved for values of *s* greater than or equal to three.

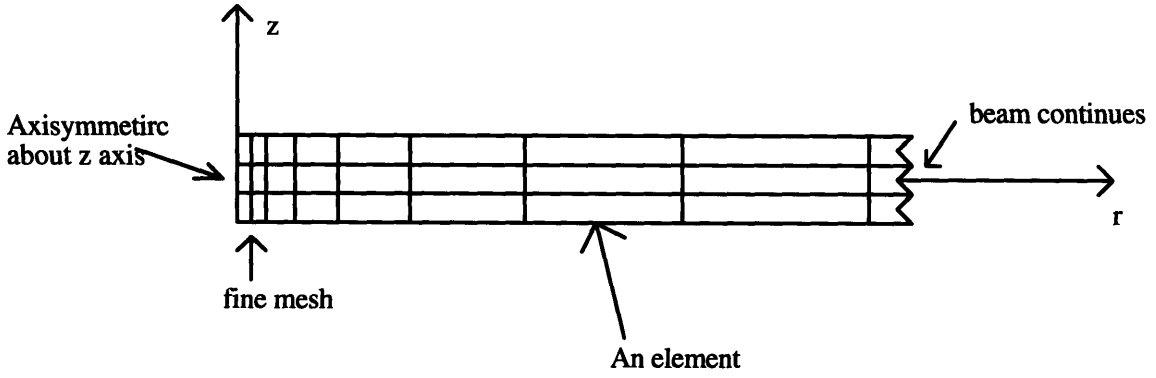

Figure 5.1: The basic finite element model

Figure 5.2 shows the finite element model with thermal boundary conditions. The top surface is exposed to a flux which is maximum at the center of the plate and decreases in a

[43]ANSYS Version 4.4a, Swanson Analysis Systems Inc., Houston Pennsylvania.

gaussian manner with the radius. At 9 % of the total radius, the incident heat flux is zero. Referring to equation 4.1a, this is the value of a for which $T_0 = T_{hot} e^{\frac{-2(.09b)^2}{a^2}}$, where b is the radius of the plate. The base of the plate undergoes convective cooling due to the jet. The maximum value of the heat transfer coefficient occurs in the stagnation zone. Here a value of 500 kW/m^{2}K is used.[44] The rate of convection decreases with the square of the radius- $h(r) \propto 1 - \frac{1}{20 r_j} \frac{r^2}{d}$.[45]

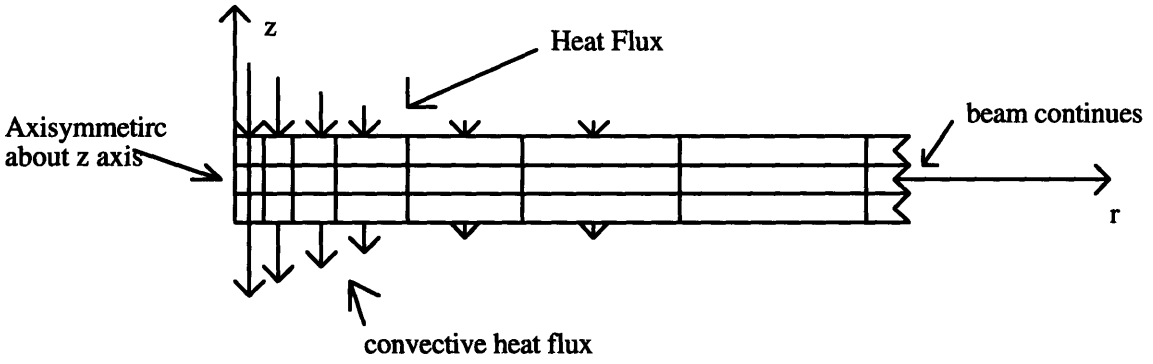

Figure 5.2: Thermal boundary conditions for finite element model.

The thermal boundary conditions are applied to each element face rather than to each node. Since each element has a different width, the location of each node must be determined before the boundary conditions are applied. A program has been written in Matlab[46] for this purpose (see appendix C). The plate is considered adiabatic on element faces free of either flux loads or convection.

Figure 5.3 shows the finite element model with mechanical boundary conditions. There are two conditions. The edge is fixed, and the first millimeter of the plate is subjected to jet pressure. Only the fixed beam is considered in this chapter. Its results are more conservative than the simply supported case.

---

[44]Liu, Xin, *Liquid Jet Impingement Heat Transfer and its Potential Applications at Extremely High Heat Fluxes,* Ph.D Thesis, M.I.T., Cambridge, MA, 1992.
[45]Liu, Xin, *Liquid Jet Impingement Heat Transfer and its Potential Applications at Extremely High Heat Fluxes,* Ph.D Thesis, M.I.T., Cambridge, MA, 1992.
[46]Matlab 4.0c, MathWorks Inc., Natick, MA.

Since the elements in the first millimeter are evenly spaced, the Matlab program is not needed to find the location of each pressure boundary condition. The pressure across each element face is given by the following formula,

$$P = P_o e^{-ar^2} \tag{5.1}$$

where P is the pressure at radius r, P_o is pressure at the origin, and a is defined such that: $\lim_{r \to 1mm} e^{-ar^2} << \frac{P}{P_0}$.

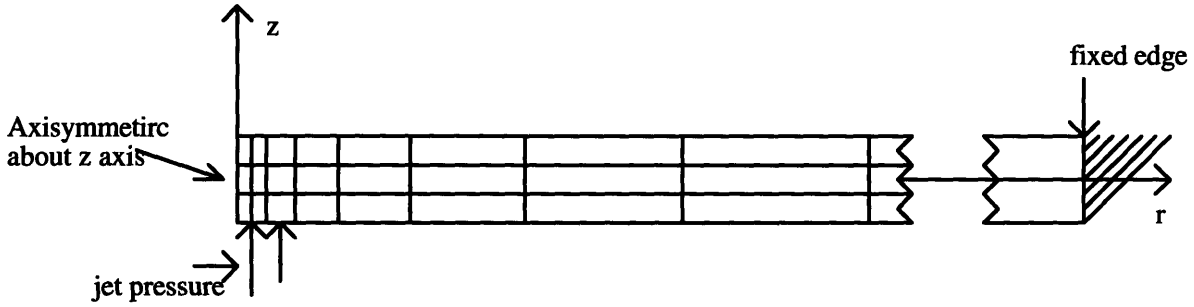

Figure 5.3: Mechanical boundary conditions for finite element model.

The material properties in the model are temperature dependent (see appendix B for formulas).

To model plastic behavior, a bi-linear stress-strain curve (see figure 5.4), which is temperature dependent, is used. This type of curve is suggested for metals by the ANSYS modeling manual.[47]

[47]ANSYS Version 4.4a, Swanson Analysis Systems Inc., Houston Pennsylvania.

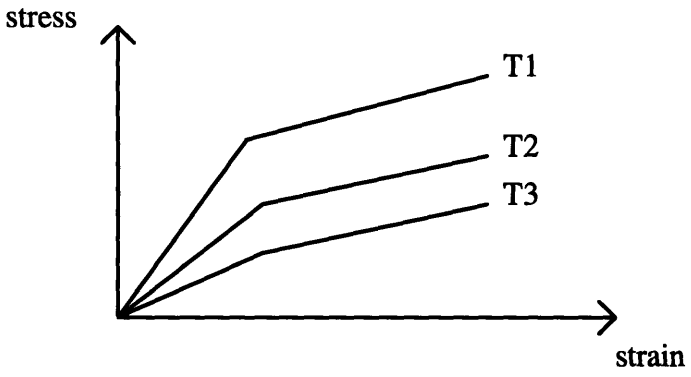

Figure 5.4: Form of a bi-linear stress strain curve at various temperatures.

Transient analysis is limited by a lower bound on the time step. ANSYS manuals recommend that the time step equal:

$$ITS = \frac{\delta^2}{4\alpha_t} \tag{5.2}$$

where, δ is the height of the conducting element, and α is the thermal diffusivity. A time step of .0005 sec is used for molybdenum, tungsten, and aluminum. A time step of .01 sec is used for steel.

To calculate thermal stresses in ANSYS, a thermal analysis is used to find the temperature distribution at each time step. The calculated nodal temperatures are "load steps" which are input into a structural analysis program. Plasticity calculations are performed for each input load step.

5.2 Behavior of Brittle Materials

As mentioned in section 4.3.35, Liu and Lienhard observed that tungsten failed by brittle fracture before it melt. Before presenting specific results, the behavior of tungsten should be examined. This discussion provides insight on how materials fail at extreme heat fluxes.

This section discusses the behavior of tungsten under transient thermal stresses. To apply the argument given here to other brittle materials, these metals must have large Young's moduli, similar to tungsten's, in the elastic range.

Figures 5.5-5.7 (a-c) show the temperature distributions and thermal stresses in three candidate materials - tungsten, aluminum, and steel. The temperature distribution is shown in graph a; the graph of the maximum principal stress is shown in graph b, and the graph of the minimum principal stress is shown in graph c. The flux loading on each material is the flux which causes melting in the steady state case. All graphs are for the second time step.

Failure is determined by the maximum shear stress theory[48]. This theory is applicable to inelastic failure. It states that material failure occurs when

$$|\sigma_1 - \sigma_3| > \sigma_u(T) \qquad (5.3)$$

where, σ_u is the ultimate strength, a function of temperature.

Using equation 5.3 with the ANSYS results, shows that neither steel nor aluminum, both ductile materials, fail at the beginning of the transient (see section 3.3 for discussion of transients caused by temperature and flux boundary conditions). However, tungsten fails at its top surface. The graph shows that while the bottom half of the tungsten plate is brittle, the top half is ductile. The behavior of the bottom half of the plate is based on the elastic region of the bi-linear stress-strain curve. The ductile region of the plate can behave either as an elastic or a plastic material depending on the stress level.

Steel and aluminum behave in a similar manner to tungsten. However, tungsten, is distinguished from the other metals by its large Young's modulus, and its higher ratio of material strength to Young's modulus in the brittle region. The attributes of the brittle material allow it to achieve higher stress levels in the brittle region than could be achieved if it were ductile. However, the stresses in the top and bottom of the plate are coupled. As the stress level in the bottom increases, stresses in the top half also increase.

---

[48]Ugural, A.C. and Fenster, S.K., *Advanced Strength and Applied Elasticity*, Elsevier North Holland, 1981.

Almost mid-way through the plate thickness a neutral axis develops. On either side of this axis, stress levels increase. This is best shown in the graph of the minimum principal stress (graph c). The classical neutral axis that develops in pure bending does not exist, because membrane stresses are also present. As the stresses in the brittle region increase with time its bending stresses are duplicated in the ductile region. The ductile region is also under the influence of greater membrane stresses, but its strength is lower than the brittle region's. At the top surface, the largest membrane and bending stresses occur. These two stresses combined surpass the ultimate strain (stress) that tungsten can accommodate. Fracture ensues at the surface of the hot spot.

Since the brittle region does not fracture, continued heating will rapidly increase the rate of crack propagation through the plate. Consequently, tungsten failures start early in the heating process and they will be a catastrophic failures.

This behavior is not necessarily limited to brittle materials. This can also occur in a material whose strength decreases rapidly with temperature, but whose Young's modulus decreases slowly with temperature. Such a material would mimic the behavior of tungsten.

The above discussion applies to thermal transients resulting from heat flux boundary conditions. If the transient had been caused by a temperature boundary condition, brittle materials are again expected to fail. Section 3.3 shows that in this case, thermal stresses are a maximum immediately after heating begins. Since a brittle material cannot plastically deform, section 3.2 suggests that a temperature gradient on the order of a material's melting temperature will result in fracture for most brittle metals.

Numerical analysis shows that between heat flux loads of 25-30 MW, transients in tungsten do not cause yielding before steady state. This means that the results given in chapter 4 for the locally heated fixed plate hold true. When plastic behavior is allowed, transients do not cause failure below 60 MW (see section 5.3).

In order to overcome the catastrophic failure that transients may induce in tungsten, a free tungsten plate can be uniformly heated above its transition temperature, then restrained, and then heated to the maximum temperature on its top surface and cooled to the transition temperature on the bottom surface. In this way, the tungsten plate will behave as a ductile material.

An alternative, and a more practical method of overcoming the problems of tungsten's brittleness is to slowly and uniformly heat the plate surface such that a large temperature gradient develops in the plate only after the entirety of the beam is above the transition temperature. The steady state plastic results given in chapters 6 and 7 assume this heating procedure. A more indirect version of the same idea which is still applicable to localized heating, is to uniformly heat the unrestrained metal above the transition point, and then plastically deform it. Once cooled, the metal will have a higher yield strength. This process can be repeated until the yield strength of ductile tungsten is approximately the same as the ultimate strength of tungsten. Consequently, the metal will act elastically for large stress levels.

Notes on figures:

Figures 5.5a-c

Figure 5.5a: Transient temperature distribution in tungsten plate. Left end is center of plate. Picture shows first tenth of radius. Incident flux is 290 MW, present time is 0.001 secs.

Figure 5.5b: Transient maximum principal stress distribution in tungsten plate. Left end is center of plate. Picture shows first tenth of radius. Incident flux is 290 MW, present time is 0.001 secs.

Figure 5.5c: Transient minimum principal stress distribution in tungsten plate. Left end is center of plate. Picture shows first tenth of radius. Incident flux is 290 MW, present time is 0.001 secs.

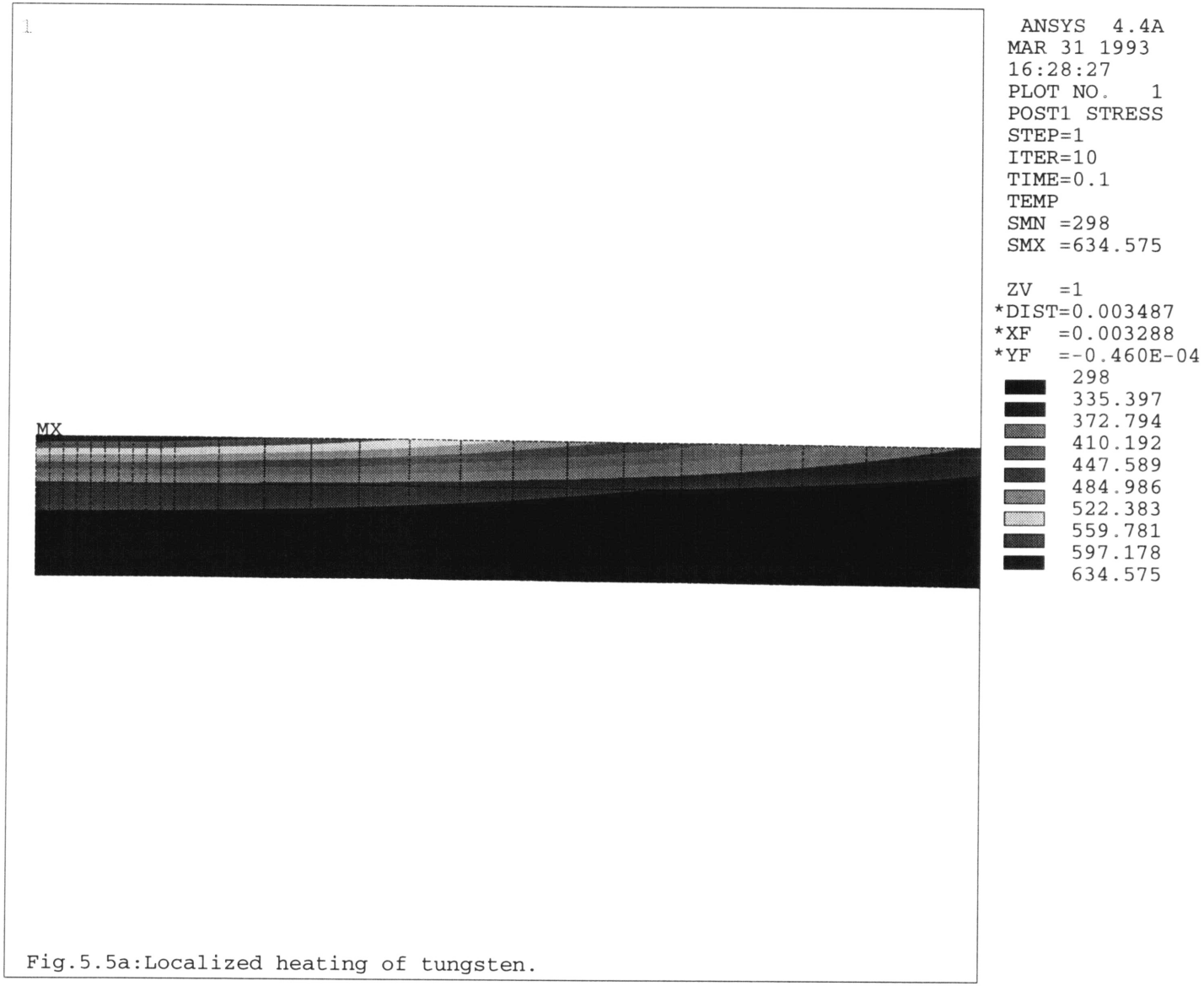

Fig.5.5a:Localized heating of tungsten.

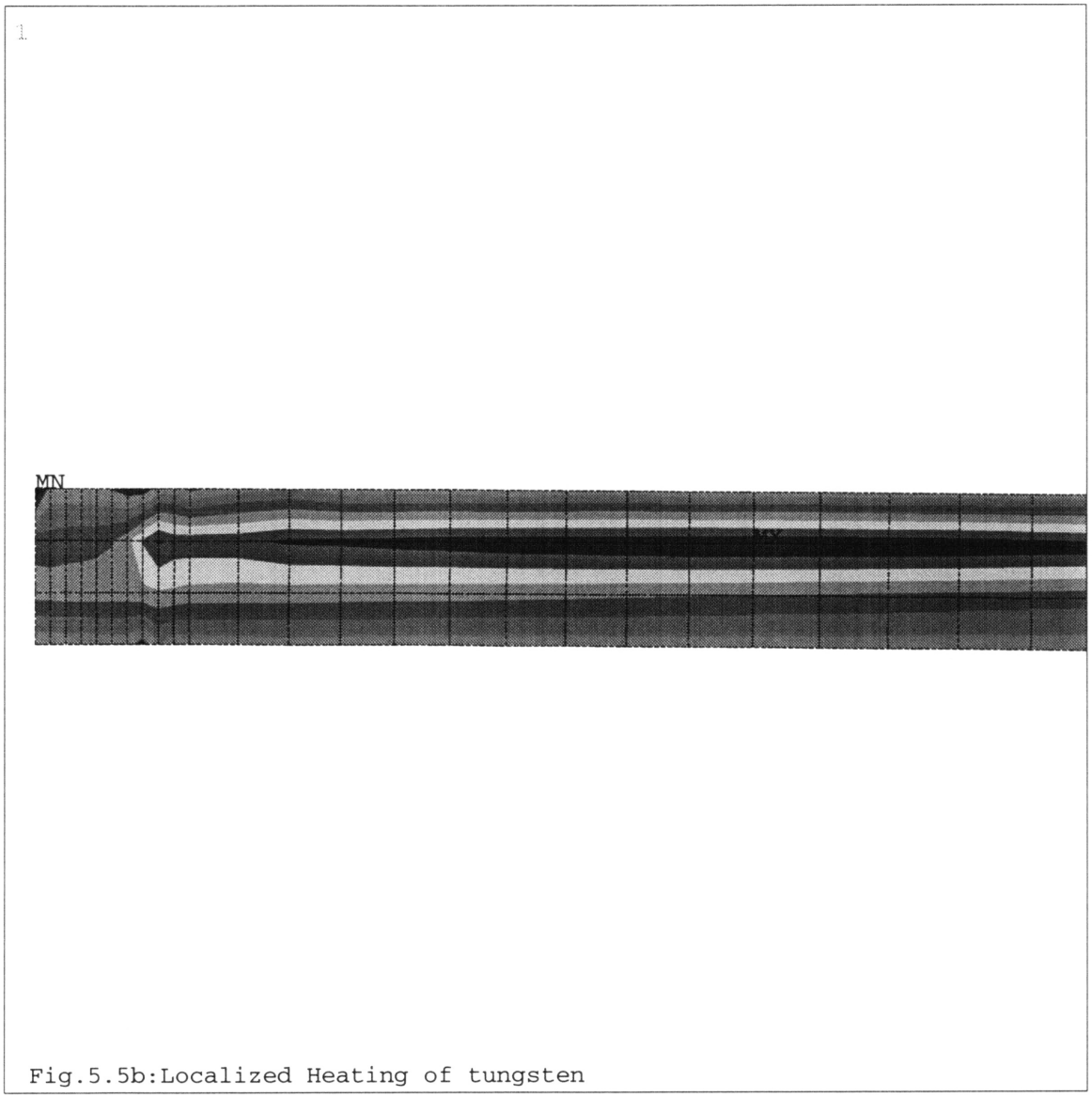

Fig.5.5b:Localized Heating of tungsten

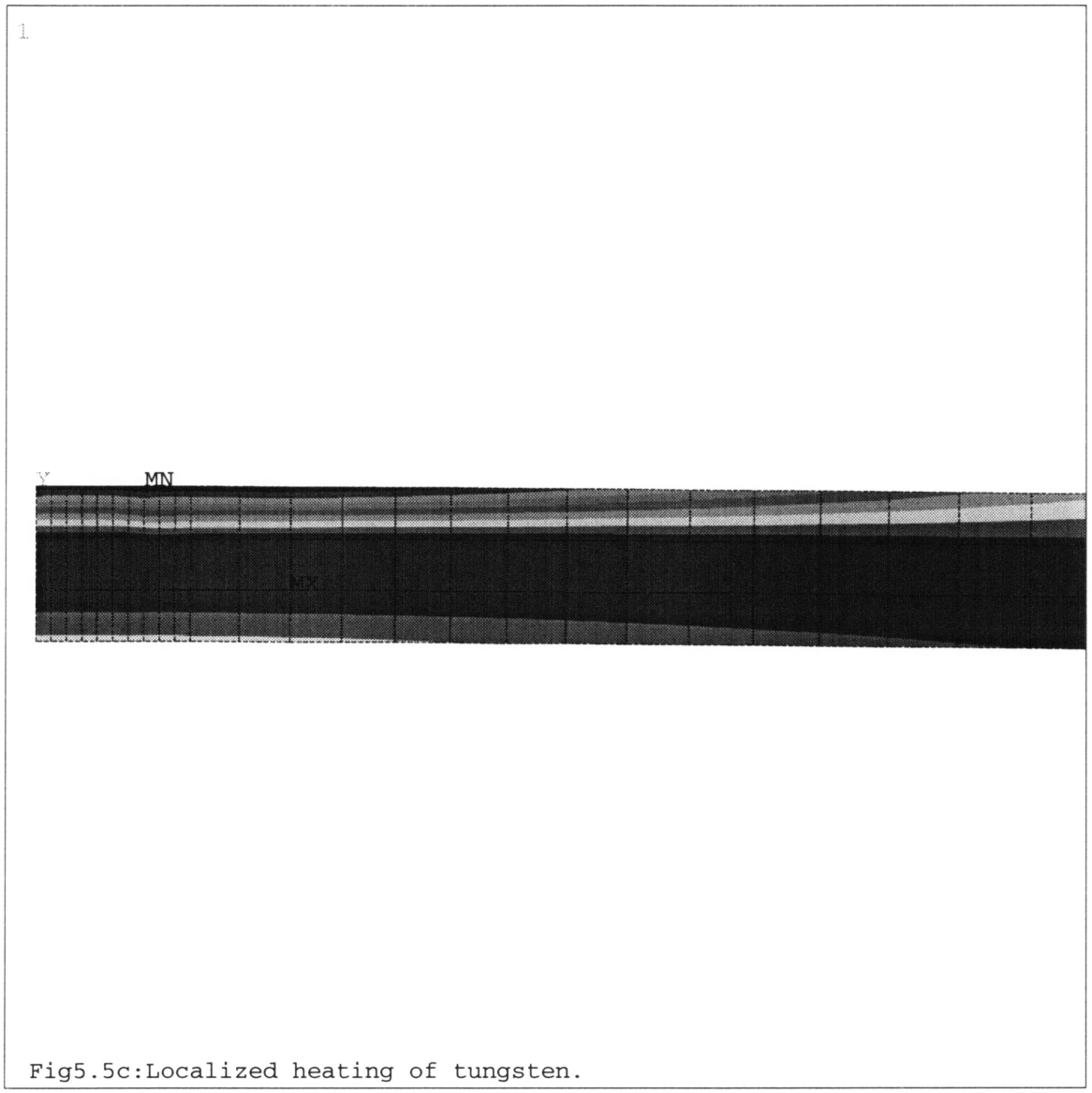

Fig5.5c:Localized heating of tungsten.

Notes on figures:

Figures 5.6a-c

Figure 5.6a: Transient temperature distribution in steel plate. Left end is center of plate. Picture shows first tenth of radius. Incident flux is 35 MW, present time is 0.01 secs.

Figure 5.6b: Transient maximum principal stress distribution in steel plate. Left end is center of plate. Picture shows first tenth of radius. Incident flux is 35 MW, present time is 0.01 secs.

Figure 5.6c: Transient minimum principal stress distribution in steel plate. Left end is center of plate. Picture shows first tenth of radius. Incident flux is 35 MW, present time is 0.01 secs.

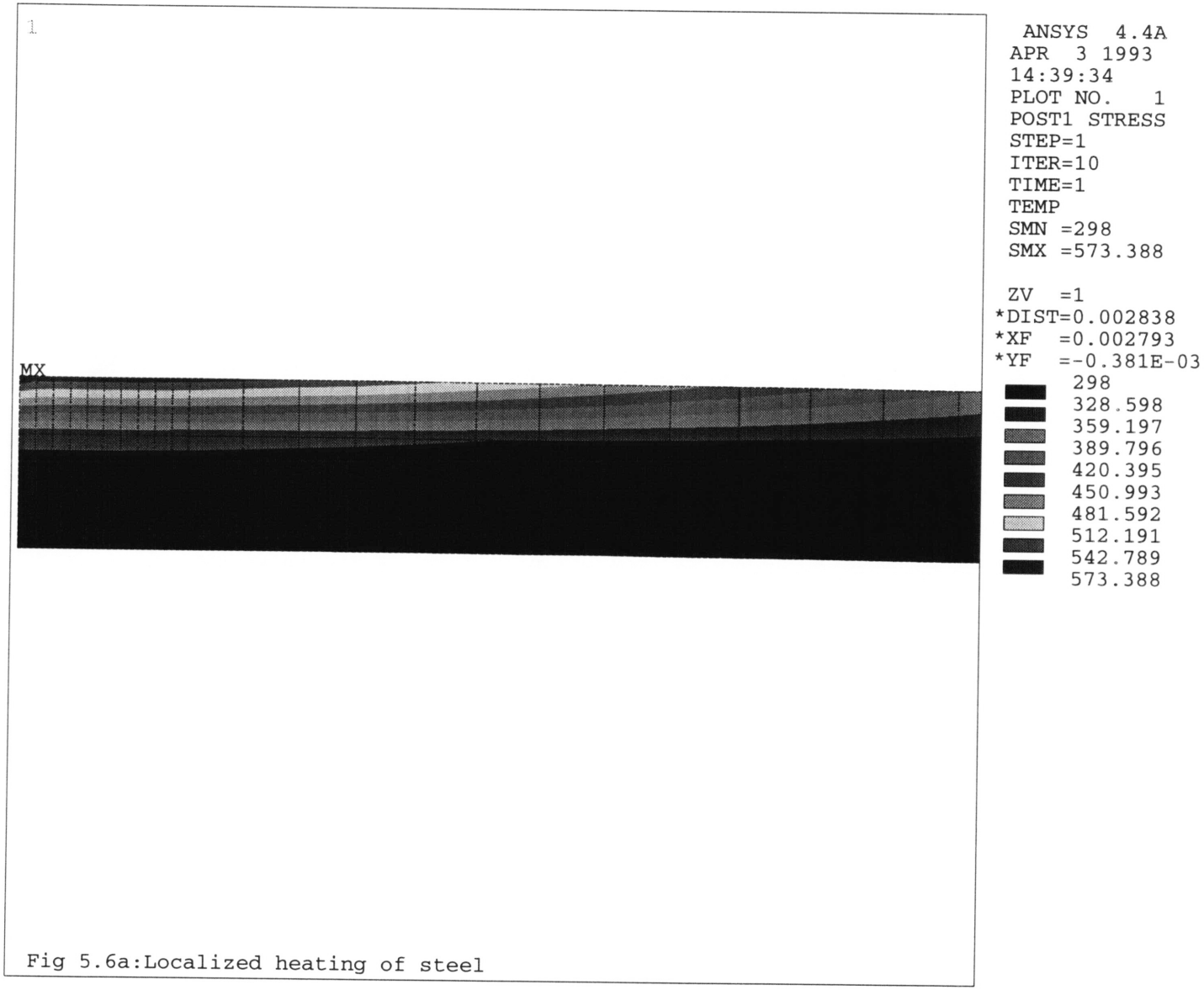

Fig 5.6a:Localized heating of steel

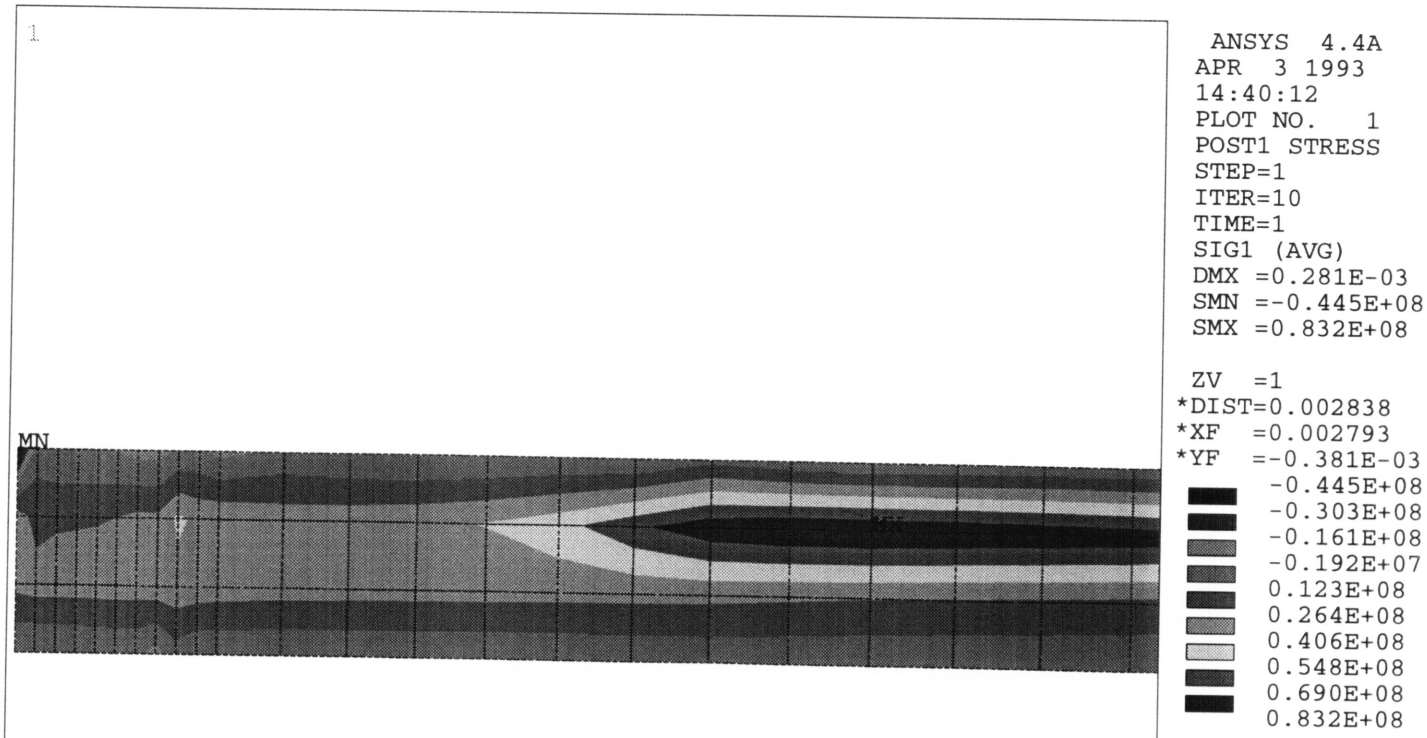

Fig.5.6b:Localized heating of steel

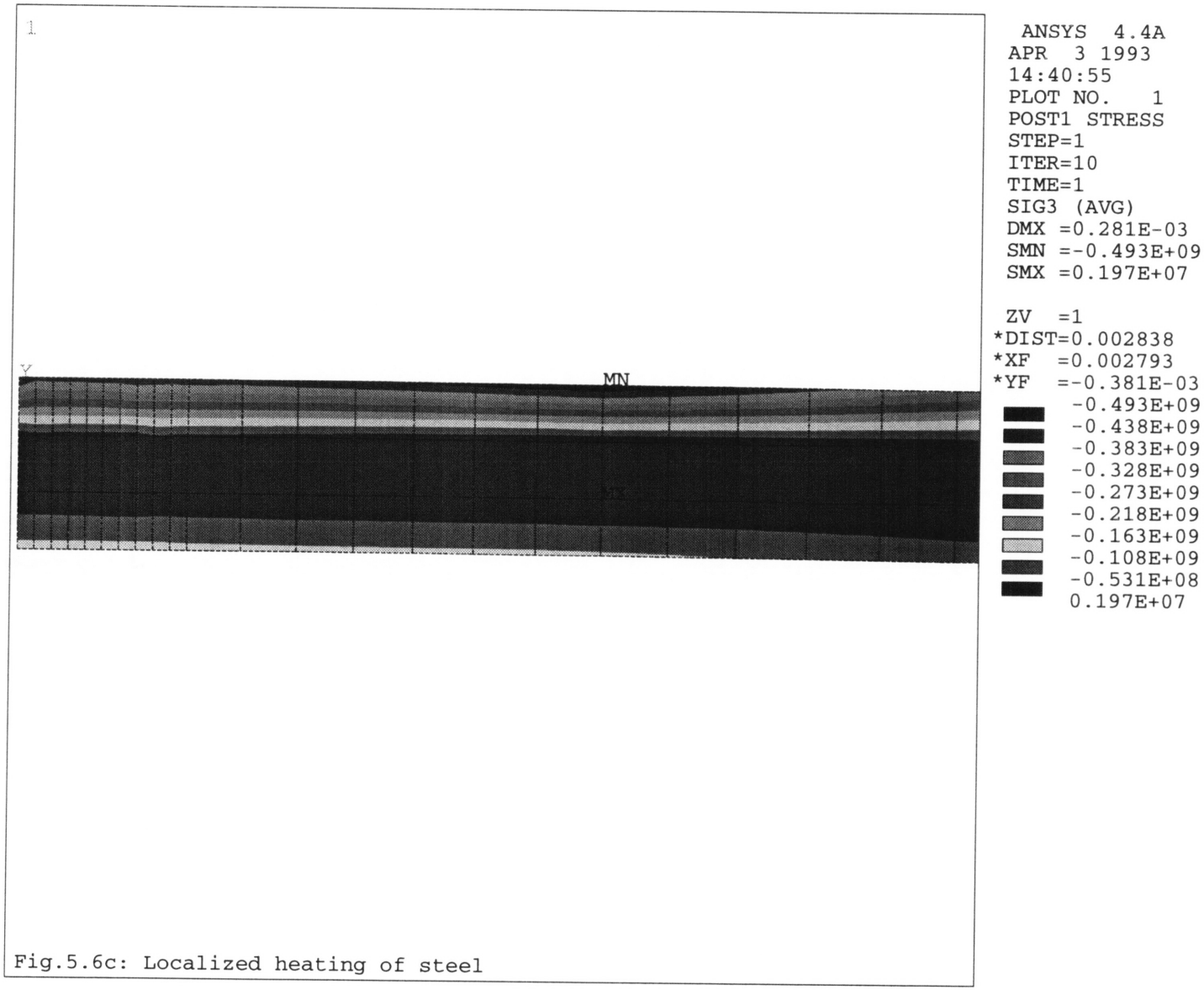

Fig.5.6c: Localized heating of steel

Notes on figures:

Figures 5.7a-c

Figure 5.7a: Transient temperature distribution in aluminum plate. Left end is center of plate. Picture shows one third of radius. Incident flux is 110 MW, present time is 0.001 secs.

Figure 5.7b: Transient maximum principal stress distribution in aluminum plate. Left end is center of plate. Picture shows one third of radius. Incident flux is 110 MW, present time is 0.001 secs.

Figure 5.7c: Transient minimum principal stress distribution in aluminum plate. Left end is center of plate. Picture shows one third of radius. Incident flux is 110 MW, present time is 0.001 secs.

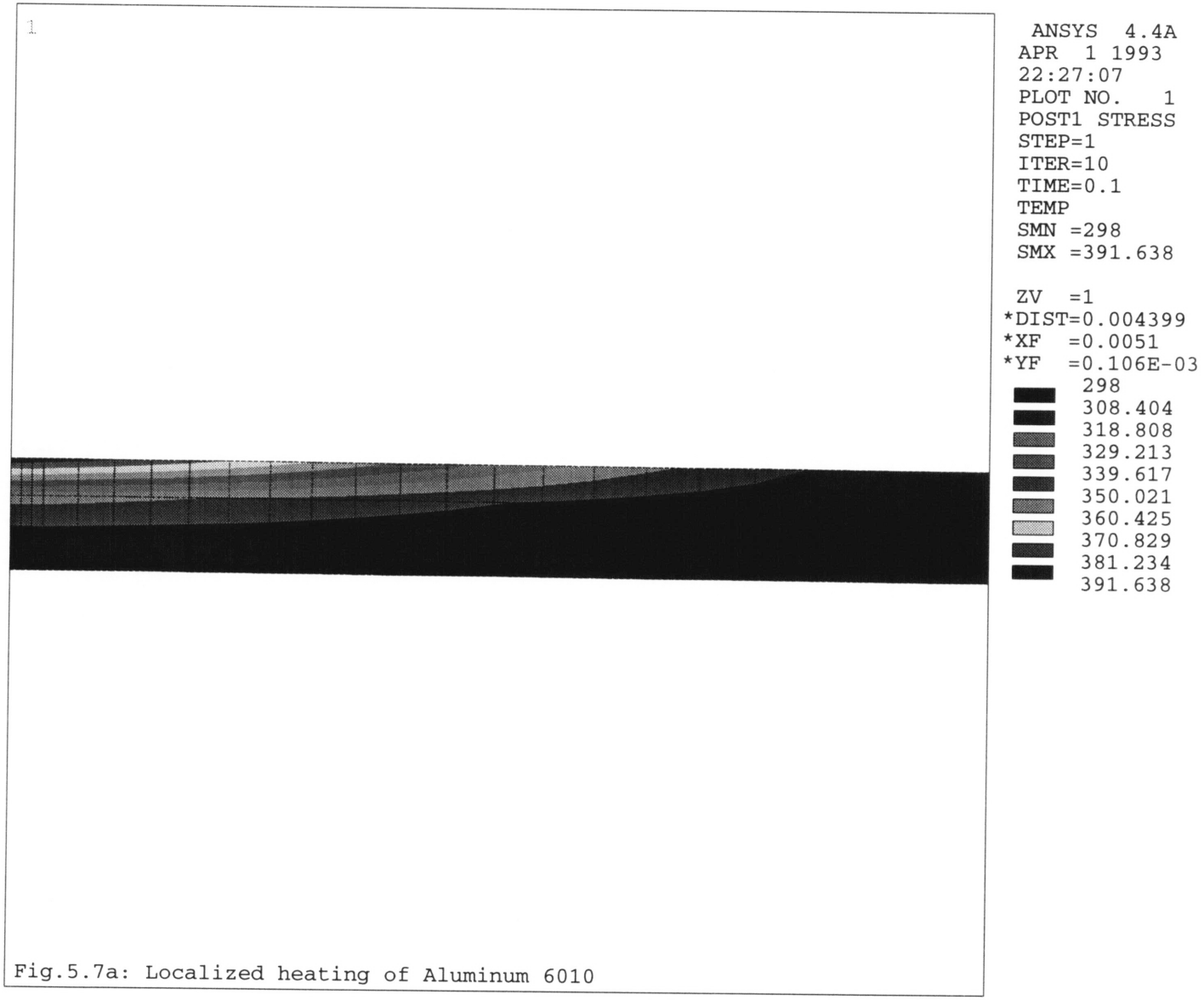

Fig.5.7a: Localized heating of Aluminum 6010

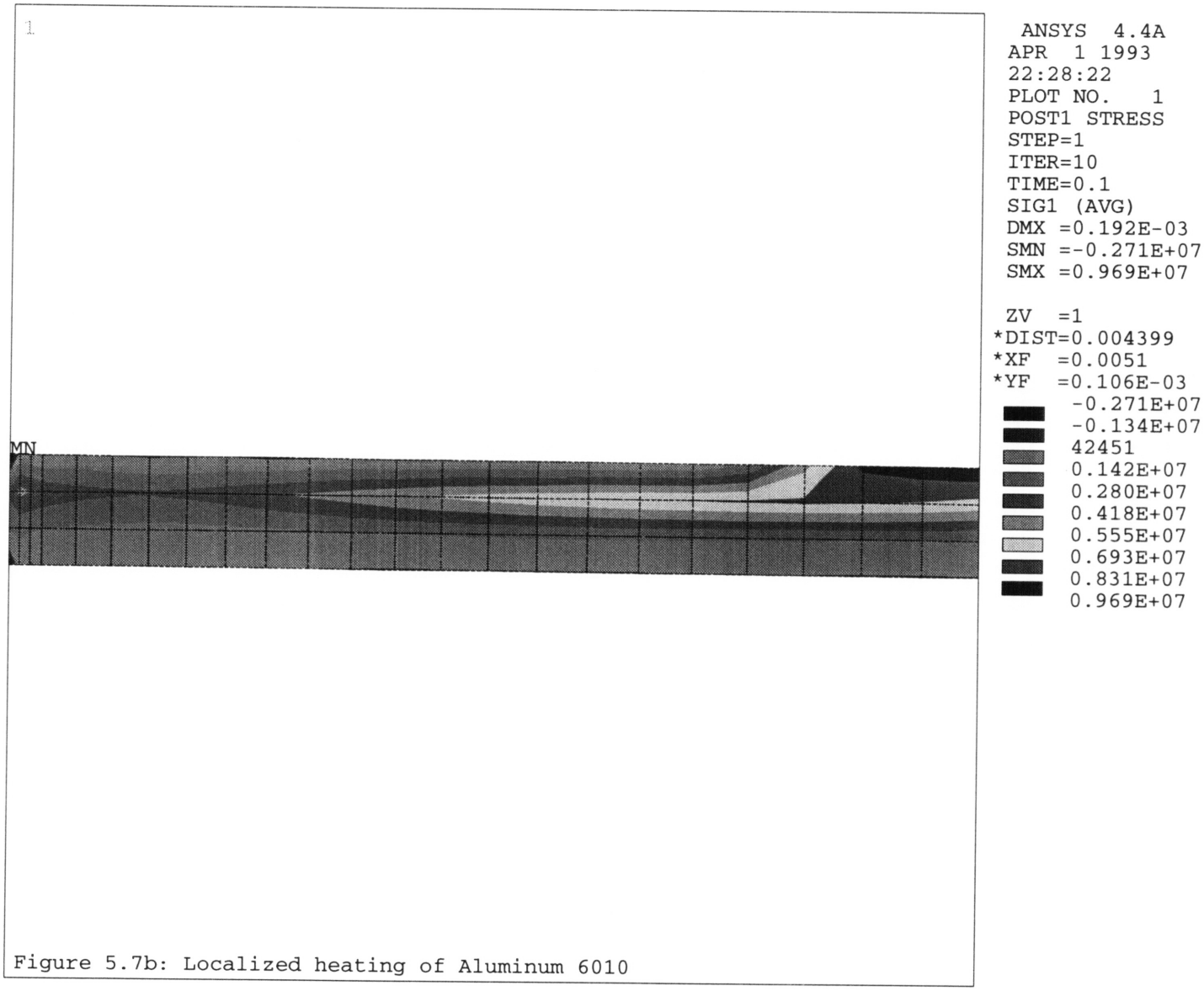

Figure 5.7b: Localized heating of Aluminum 6010

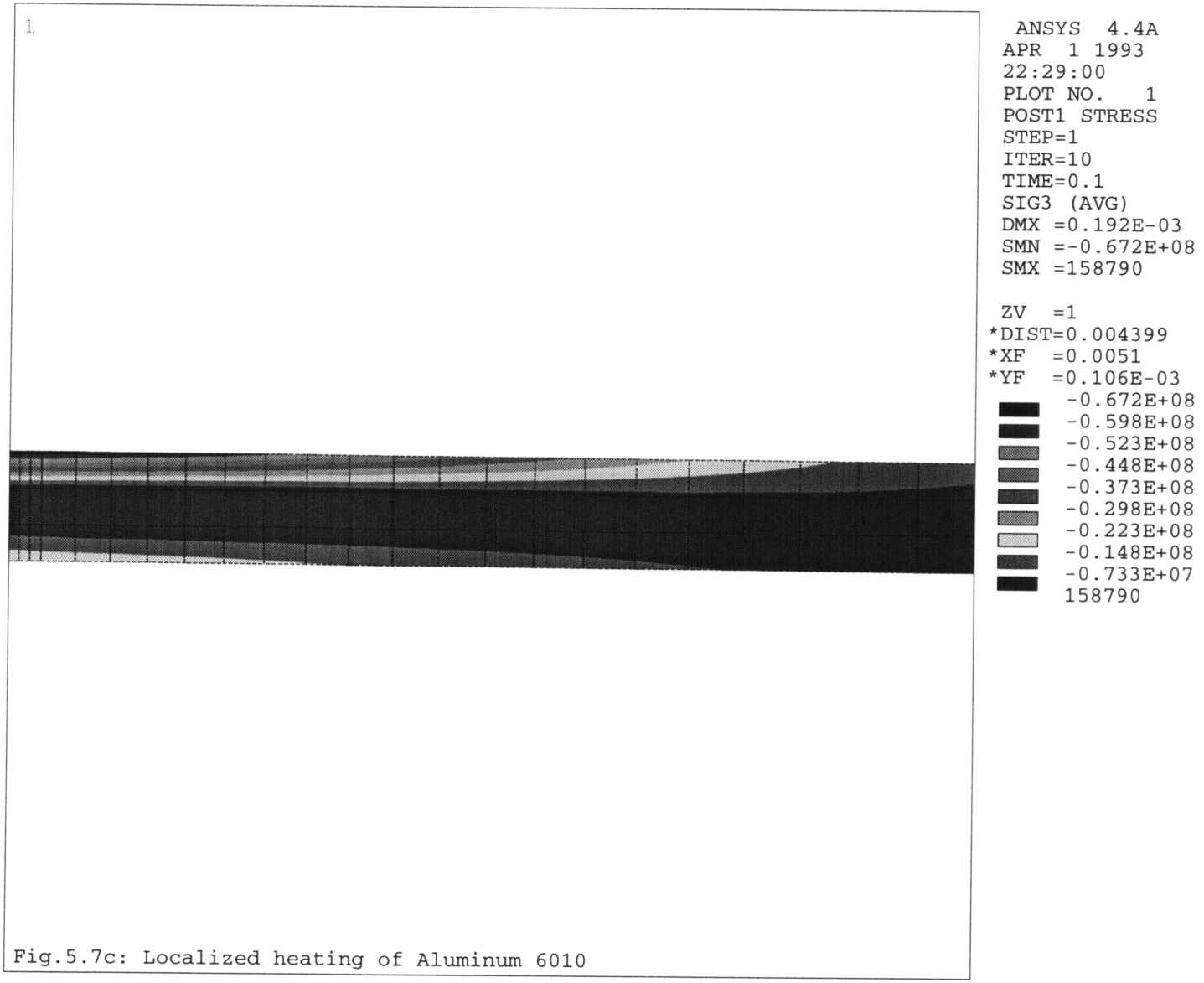

Fig.5.7c: Localized heating of Aluminum 6010

5.3 Plastic Limits

Table 5.1 shows the heat fluxes which cause the ultimate strength to be surpassed somewhere in the plate. These results are for the localized heating base case. Failure is determined as described in section 5.2.

Material	Flux at Elastic Limit (MW)	Flux at Plastic Limit (MW)	Flux at Melting Point (MW)	Percentage Increase
Molybdenum	14	55	200	293 %
Tungsten	27.9	60	290	115 %
Steel	1.36	5	35	268 %
Aluminum	33.6	45	110	34 %

Table 5.1: Achievable fluxes for a clamped circular plate of 200 mm radius and 1 mm thickness. Percentage increase refers to the increase in flux level when allowing for plastic deformation. Results are for steady state heating. * See section 5.2.

Table 5.1 shows that the achievable flux levels increase substantially if plastic deformation is allowed. Note, these results do not suggest fluxes near the melting point cannot be achieved. They do suggest that such fluxes cannot be achieved for the chosen plate geometry. Results in chapter 7 show that flux levels greater than 400 MW are achievable.

If plastic deformation is considered, tungsten appears to be the best metal of the four. At low temperatures aluminum performs well since its high conductivity compensates for its low strength. At high temperatures, the mechanical strength dominates the results. Tungsten and molybdenum outpace aluminum. These results are for the steady state case.

Additionally, at high temperatures creep becomes important. As pointed out in section 3.4, molybdenum performs much better from a creep standpoint than does tungsten.

5.4 Conclusions

If plastic deformation is allowed, significant thermal stress relief occurs and high temperature gradients can be supported by materials. Thus, mechanical strength at elevated temperatures becomes the dominant factor in determining which material can transmit the largest heat flux.

The maximum heat flux limits in the current configuration are substantially lower than the flux which induces melting. This does not mean melting fluxes cannot be achieved in other configurations. Chapter 6-8 discuss this point further.

This chapter showed that transients are important for determining failure in certain high strength materials, particularly brittle ones. As heating progresses in a brittle metal, two regions are established. The properties and strengths of each region vary significantly. The property differences create high stress levels in the weaker region and cause catastrophic failure soon after heating starts.

The results in this chapter are not limited to cases where the beam length is much larger than the thickness. For a given plate thickness, increasing the radius augments stress levels. Therefore, the results given in this chapter are conservative relative to designs with smaller radii. The radius used in this chapter is employed in order to compare results with chapter 4. The finite element models given in the appendix can be easily modified to consider different plate dimensions.

Chapter 6

Uniform Surface Heating Analytical Models - Elastic Regime

The previous two chapters considered the case when only a small portion of a circular plate is heated. This chapter investigates what happens when the entire top plate surface is heated uniformly.

The same equations used in chapter 4 can be re-used here if the variable a is large enough so that the exponential term in equation 4.1a is essentially zero. However, for completeness, the stress-strain equations will be re-solved without using the gaussian decay term. Both approaches give the same results.

This chapter only considers the case of a fixed plate. There are two reasons for this. First, the fixed case is the most conservative. Second, a simply supported plate uniformly heated on its surface will not be thermally stressed. No bending stresses are present since the temperature distribution is linear. There are no membrane stresses since the plate is free to expand axially. The stresses in the simply supported case are from the jet only.

6.1 Solution of the Equations

Equations 4.12a-b must be re-solved but under different thermal boundary conditions. Figure 6.1 shows the heating configuration and equation 6.1 gives the new thermal boundary conditions.

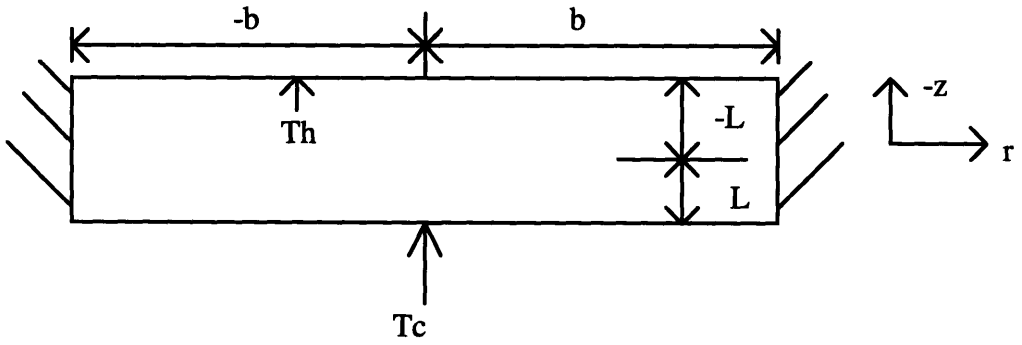

Figure 6.1: Clamped plate uniformly heated on top surface.

boundary conditions:

$$\begin{aligned} z &= -L, & T &= T_h \\ z &= L, & T &= T_c \\ \frac{\partial T}{\partial r} &= 0, & r &= -b, b \end{aligned} \qquad (6.1)$$

Figure 6.1 suggests that the one-dimensional models given in chapter 3 are applicable to this case. Classical plate theory will be used instead of the simpler one-dimensional models. This is done because the mechanical stress solution (see section 4.3.5) is a classical plate solution. Since the thermal and mechanical solutions are superimposed, consistency is desirable.

In the uniform heating of a fixed plate's surface, the deflection equation (4.43) evaluates to zero. However, membrane stresses (equation. 4.45) are present. The previous solution for membrane stresses (equation. 4.46) can be used here with an appropriate temperature field substitution. The mechanical stress solution (equation. 4.31) can be applied as before.

These equations are used with material properties evaluated at the average plate temperature to develop stress correlations (section 6.2) and determine elastic limits (section 6.3).

6.2 Thermal Stress Correlations

This is a membrane stress problem. Therefore, it is expected that the thermal stresses will be independent of geometry. Tables 6.1 and 6.2 shows the maximum (σ_1) and minimum (σ_2) principal stress values for various values of plate diameter and plate thickness. These stress values are based on the plate parameters considered in section 4.3.4.

Plate Radius (m)	σ_1 (MPa)	σ_2 (MPa)
.05	1348	494.4
.1	1348	494.4
.2	1348	494.4
.3	1348	494.4

Table 6.1: Effect of change in radius on thermal stress levels. Parameters based from base case of section 4.3.4.

Plate thickness (mm)	σ1 (MPa)	σ2 (MPa)
1	1348	494.4
2	1348	494.4
3	1348	494.4
4	1348	494.4

Table 6.2: Effect of change in thickness on thermal stress levels. Parameters based from base case of section 4.3.4.

Therefore, the following correlations can be established for uniform heating:

$$\sigma_1 = 7.95\times10^{-7}\frac{E\alpha\Delta T}{1-\upsilon} \qquad \sigma_2 = 2.92\times10^{-7}\frac{E\alpha\Delta T}{1-\upsilon} \qquad (6.2)$$

The correlations for the maximum values of the principal stresses are valid if the stress level is below the yield stress and if buckling does not occur.

6.3 Elastic Limits and Buckling

Although the geometry does not affect the thermal stress level, it does influence the possibility of buckling. Therefore, to define elastic limits, elastic stability must first be established. Depending of the material and on the geometry, buckling may set a more conservative elastic limit than yielding. Note that buckling is generally not important for small hot spots; localized heating tends to induce elastic/plastic material behavior. Consequently, buckling was not considered in chapter 4.

Boley present the following buckling criteria for bodies with an arbitrary temperature distribution in z only[49]:

$$N_{Tcr} = (1-\upsilon)\left(1+\frac{a^2}{b^2}\right)\left(\frac{\pi^2 D}{a^2}\right) \tag{6.3}$$

where a is the plate radius, b is the thickness, and D is the bending rigidity as defined above. Equation 4.12c describes the thermal force term N_T. Buckling does not occur if $N_T << N_{Tcr}$.

Table 6.3 shows the buckling criteria for the candidate materials with two different radii.

Material	N_{Tcr} if a = 200 mm	N_{Tcr} if a = 5 mm
Molybdenum	1.95E8	2.04E8
Tungsten	2.5E8	2.64E8
Steel	1.17E8	1.22E8
Aluminum	3.87E7	4.05E7

Table 6.3: Buckling criteria for a 1 mm thick plate. Properties are evaluated at 500 K, except for tungsten which is evaluated at 650 K (See elastic limits below). Plate thickness is the dominate parameter affecting buckling criteria.

Notice that radius variations do not have significant impacts on buckling criteria. Actually, thickness variations dominate changes in buckling criteria. However, for purely thermal considerations, plate radii of both 5 and 200 mm will be examined below.

When a plate is uniformly heated on its top surface, the entire base of the plate needs to be cooled. For a 200 mm radius plate, one jet cannot provide sufficient cooling. If the plate is only 5 mm, the heat transfer coefficient will still be large at the edge.[50] Thus, a 5 mm long plate can be effectively cooled by a single jet. The 200 mm plate is examined for academic reasons - to compare results of uniform and localized heating.

Tables 6.4-6.5 shows the elastic limits for the heating configuration shown in figure 6.1. There is a single cooling jet, with a 1 mm radius and a maximum pressure of 5 MPa.

---

[49]Boley, B.A., *Theory of Thermal Stress*, John Wiley and Sons, Inc., 1960.
[50]Liu, Xin, *Liquid Jet Impingement Heat Transfer and its Potential Applications at Extremely High Heat Fluxes*, Ph.D Thesis, M.I.T., Cambridge, MA, 1992.

Material	Maximum Temperature (K)	Maximum Flux (MW)
Molybdenum	445	19.8
Tungsten*	600	44.4
Stainless Steel	425	1.95
Aluminum	485	44.9

Table 6.4: Limiting heat fluxes for elastic behavior. Plate radius equals 200 mm. *Tungsten is a brittle material. See section 5.2.

Material	Maximum Temperature (K)	Maximum Flux (MW)
Molybdenum	450	20
Tungsten*	605	44.7
Stainless Steel	430	1.97
Aluminum	490	45.4

Table 6.5: Limiting heat fluxes for elastic behavior. Plate radius equals 5 mm. *Tungsten is a brittle material. See section 5.2

Comparing tables 6.4 and 4.15 shows that the maximum flux increases when the plate is uniformly heated on its surface instead of locally heated. This occurs because there are no bending stresses present in the uniform heating case.

The results also show that as the allowable temperatures increases from the localized to the uniform case, the gap between material rankings change. At higher temperatures, thermal conductivity is no longer the dominant factor in determining heat flux. Mechanical strength has a strong influence as well.

These elastic limits can be checked for elastic stability by using equation 4.12 c and comparing the results to the buckling criterion given in table 6.3. The values of N_T / N_{Tcr} are shown in table 6.6 for each material. The largest plate is used for comparison since buckling is most likely to occur in this case.

Material	N_T/N_{Tcr}
Molybdenum	.001
Tungsten	.0011
Aluminum	.0014
Steel	.002

Table 6.6: Ratio of thermal force to thermal buckling criteria for a 200 mm radius plate. Note that buckling does not occur for any material within the chosen elastic limits.

Table 6.6 shows that buckling is unlikely in the elastic range. However, buckling may occur if plastic deformation is allowed.

Tables 6.4 and 6.5 indicate another important point. The elastic limits are essentially independent of plate length. This is expected since elastic membrane stress problems are independent of geometry and since jet induced mechanical stresses are a weak function of the plate diameter. Additionally, buckling criteria is a weak function of plate diameter. Therefore, for elastic design, the plate size should be chosen based on the heat transfer effectiveness of the jet.

Due to the decrease in convection heat transfer along the plate, shorter plates have more uniform temperature distributions. Long plates can have highly non-linear temperature distributions. These non-linearities will introduce bending stresses and thus decrease the elastic limits given in tables 6.3-6.4.

6.4 Limits of Classical Theory

Since there are no transverse strains due to temperature, the strain relations (4.11) are always linear in the absence of mechanical loads, i.e. the classical plate theory is always valid for the thermal problem alone.

Mechanical strains can still invalidate the linear strain equations. Using the base case parameters described in section 4.3.4, non-linear strains are important when either the beam thickness is $<<$ .5 mm, the stagnation pressure $>$ 35 MPa, or when the jet diameter is $>$ 7 mm. Since none of these cases are considered here, classical plate theory is valid for the models described in this chapter.

6.5 Conclusions

Uniformly heating the surface of a plate reduces bending stress levels and thus increases the flux limits for elastic behavior compared to localized heating.

Additionally, the reduction in stress levels increases the temperature gradient that can be supported. Therefore, thermal conductivity does not dominate material performance. Instead both conductivity and strength are important for the temperature levels considered in this chapter.

Elastically stability is not an issue for a plate uniformly heated on its surface and cooled on its base. Consequently, in elastic design the plate length needs to be chosen based on thermal considerations.

Chapter 7

Uniform Surface Heating Numerical Models - Plastic Regime

7.1 Model Description

As discussed in chapter 6, the geometry for the uniform surface heating case must be changed from that used in the localized heating case. The radius must be decreased to account for the decrease in convective cooling along the radius. Figure 7.1 shows the new geometry.

Since the plate radius has been decreased, a fine mesh is no longer needed to model the jet pressure boundary condition. The finite element model (see program in appendix C) consists of 50 elements evenly spaced along the radius of the beam. The remainder of the modeling efforts and assumptions described in section 5.1 are applicable here.

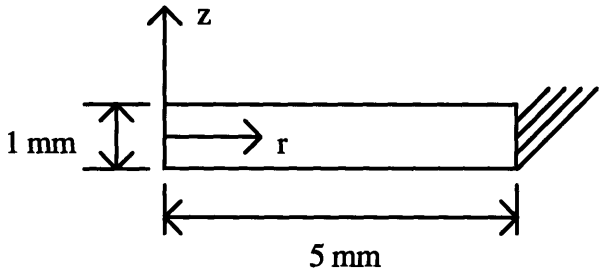

Figure 7.1: Uniform surface heating base case. Plate radius decreased to account for jet convection.

7.2 Plastic Limits

Table 7.1 shows the limiting heat fluxes for the elastic and plastic cases. Failure is determined by the maximum shear stress theory (see section 5.2).

Material	Flux at Elastic Limit (MW)	Flux at Plastic Limit (MW)	Flux at Melting Point (MW)	Percentage Increase
Molybdenum	19.8	190	190	860 %
Tungsten*	44.4	200	275	350 %
Steel	1.95	15	35	669 %
Aluminum	44.9	100	100	123 %

Table 7.1: Results for uniform heating. Plate radius of 5 mm; Plate thickness of 1 mm. Results are for steady state case. The elastic values are taken from the table 6.4, elastic limits for a short uniformly heated plate. The percentage increase refers to the difference between the elastic and plastic values. * See section 5.2 for discussion on heating brittle materials.

Table 7.1 shows that plastic deformation substantially increases the achievable fluxes over cases where the material behaves elastically. This increase is due to the stress-relief offered by plastic deformation.

Chapter 5 considered the increase in heat flux limits for plastic behavior when the material is locally heated. Comparing tables 5.1 and 7.1 shows that the percentage increase in flux level is much greater in the uniform case than in the localized case. There are two reasons for this. First, the uniform case has lower stress levels in the elastic regime since bending stresses are smaller (bending stresses develop if the plate's base is cooled by a non-uniform convective process). It is logical to assume that the absence of bending stresses will continue in the plastic regime if excessive deformation does not occur.

The second reason for lower stress levels is the shorter plate length of the uniformly heated beam. This significantly lowers plastic stresses. Section 6.4 stated that plate length is not important for materials behaving elastically. When a material behaves plastically, plates with large radii develop a buckled kink. Significant bending stress can develop in this kink for both the localized and uniform cases. Since the uniformly heated plates are very short, these kinks do not develop, and thus they experience lesser bending stresses.

Along the same lines, shorter plates do not experience large deflections. This is a consequence of their large moments of inertia. Table 7.2 shows the values of deflection for the limiting heat fluxes in the plastic regime.

Material	Deflection (mm)
Molybdenum	.022
Tungsten	.015
Aluminum	.0128
Stainless Steel	.0121

Table 7.2: Deflection for plastic plates subjected to maximum fluxes given in table 7.1.

Table 7.2 shows that at the maximum flux, deflections are two orders of magnitude less than the thickness. This is good from a design standpoint, since small deflections are needed to maintain serviceability.

Table 7.1 also points out that for extreme heat fluxes, molybdenum performs significantly better than aluminum, whereas aluminum performed better in the elastic case. There are two reasons for this behavior. The first and more simplistic explanation is that at high strength materials can support large temperature gradients if allowed to plastically deform. Materials with larger thermal conductivities but lower strengths will support smaller temperature gradients. In the case of aluminum and molybdenum, the high conductivity of the former is not sufficient to compensate for the lower temperature gradient that it supports.

The slope of the material's plastic stress-strain curve is also important. This slope is called the secant modulus, E_T. According to equations 3.6, the plastic stress, σ_p, is proportional to,

$$\sigma_p \propto E_T \alpha \Delta T \tag{7.2}$$

The plastic stress-strain curve is a function of the strain and the yield point and can often be described by[51],

$$\sigma_p = \sigma_y + p\varepsilon^n \tag{7.3}$$

Therefore,

$$E_T = \frac{\partial \sigma_p}{\partial \varepsilon} = pn\varepsilon^{n-1} \tag{7.4}$$

So,

$$Q \propto k\Delta T = \frac{k\sigma_u}{\alpha pn\varepsilon^{n-1}} \tag{7.5}$$

This equation suggest that given two materials with equivalent ultimate strengths, the material whose plastic stress-strain curve has a steeper slope will plastically deform less readily and thus achieve a lower heat flux. Molybdenum and steel have higher strength to slope ratios than do tungsten and aluminum. Additionally, as the temperature level increases, this ratio increases for first set of metals and decreases for the second set. This helps explain why steel and molybdenum achieve a large percentage increase in heat flux between the elastic and plastic cases. Section 8.2 incorporates the idea behind equation 7.5 to aid material selection.

---

[51]Ugural, A.C. and Fenster, S.K., *Advanced Strength and Applied Elasticity*, Elsevier North Holland, 1981.

7.3 Effect of Geometry Variations on Plastic Limits

Uniformly surface heated molybdenum has been chosen to examine the impact of geometry changes. Molybdenum has been chosen since it appears to be the most widely applicable metal in the plastic regime (see chapter 8). Both the radius and thickness are varied to determine the maximum achievable flux.

The tractions introduced by a small jet, 2 mm diameter and 5 MPa maximum pressure, are used in all calculations.

Thickness (mm)	Flux at Plastic Limit (MW)	Flux at Melting Point (MW)
3	75	75
2	105	105
1	190	190
0.75	235	235
0.5	315	315
0.25	425	485

Table 7.3: Effect of thickness change on uniformly surface heated molybdenum. Plate radius is 5 mm used.

Radius (mm)	Flux at Plastic Limit (MW)	Flux at Melting Point (MW)
5	190	190
10	187	187
15	184	184
20	180	175
40	127	100

Table 7.4: Effect of length change on uniformly surface heated molybdenum. Decrease in melting flux due to the decrease in convective cooling efficiency as radius increases. Plate is 1 mm thick.

These tables suggest a number of interesting results. First, for very thin plates, fluxes over 400 MW are achievable. This has been borne out by experiments where molybdenum was

allowed to melt to very thin levels[52]. Table 7.3 shows that for radius/thickness ratios less than 20, molybdenum can accommodate the melting flux.

Radius change has a profound impact on allowable fluxes. As the radius increases, plastic deformations result in increased bending near the plate center. At the base of the resulting kink, high stress levels develop. As the radius increases, allowable flux decreases. Table 7.4 shows that for radius/thickness ratios less than 20, molybdenum can accommodate the melting flux.

Both geometry cases suggest that when molybdenum designs keep radius/thickness ratios below 20, the melting flux can be achieved. This ratio is only for the case of uniformly surface heated molybdenum with clamped edges.

7.4 Discussion of Liu and Lienhard Experiment

The key difference between the Liu and Lienhard experiments and this work is that the experiments allowed melting to occur whereas this study does not. Melting resulted in a solid curved boundary to develop beneath a liquid pool. The point of interest for these cases is the thinnest portion of the beam. This region can be viewed (conservatively) as a clamped beam of a smaller thickness and diameter than the entirety of the plate. See figure 7.2.

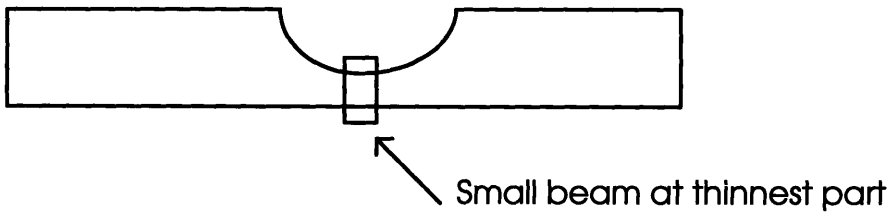

Figure 7.2: Concept of considering thinnest portion of a beam as a clamped sub-beam.

In view of the results presented in section 7.3, it is reasonably to expect molybdenum to survive melting point flux levels across very thin beams. As the beam thickness decreases,

[52]Liu, Xin and Lienhard V, J.H., *Extremely High Heat Flux Removal by Subcooled Liquid Jet Impingement*, HTD-Vol.217, ASME, 1992.

the effective radius of the sub-beam also decreases. Thus, even at melting point fluxes a radius/thickness ratio less than 20 can be maintained in the sub-region. If this is the case, failure would not be expected.

A numerical simulation of this case has been considered for the geometry shown in figure 7.3. Figures 7.4-7.6 illustrate the results in molybdenum for the temperature distribution, σ_1, and σ_3, respectively. Failure depends on the radius of curvature. As the radius increases, stresses increase. Radii greater than that shown in figure 7.3 were considered first. The radius was reduced until stress levels decreased to the strength of the material.

As heating begins, plastic deformation occurs in the top portion of the plate, but this region melts away as heating progresses. As the plate melts, the plate undergoes stress relief. This stress and stress-relief cycle continues until steady state is reached. At this point the remaining unmelted region (see figure 7.2) undergoes plastic deformation. Consequently, a temperature boundary condition has been applied to the arc shown in figure 7.3. The heat flux across the thinnest portion of the plate is approximately 380 MW.

The results show that the maximum stresses are near the ultimate strength of the material. They are located in a small region away from the center of the plate. This suggests that plates in the Liu and Lienhard experiment can survive melting point temperatures across small regions. Second, if failure occurs it will be a small localized crack located within the plate thickness but off center. Such a failure is not easily detectable, but it will eventually result in catastrophic failure if the plate is subjected to more heating cycles.

In the case of tungsten, melting does not occur under the Liu and Lienhard experimental conditions (table 7.1 shows that tungsten can not support melting heat fluxes even in the uniform surface heating case). Without melting, internal stress relief results only from plastic deformations. However, section 5.2 pointed out that at extreme heat flux levels plastic deformation in tungsten induces rapid fracture due to the influence of the material's high strength brittle region.

7.5 Conclusions

A plate uniformly heated on its surface and undergoing plastic deformation can achieve melting fluxes for some materials.

Under this heating configuration the most important determinants of heat flux are the mechanical strength and the slope of the plastic stress-strain curve.

Finally, in the plastic regime, the length to thickness ratio is very important. In the case of molybdenum, when the ratio is less than 20, melting fluxes can be achieved.

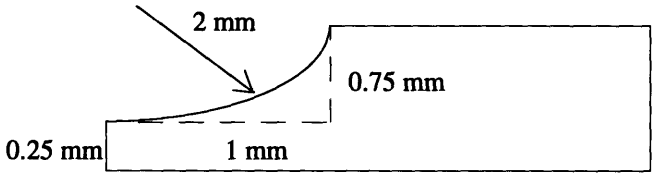

Figure 7.3: Geometry for numerical model of experiment.

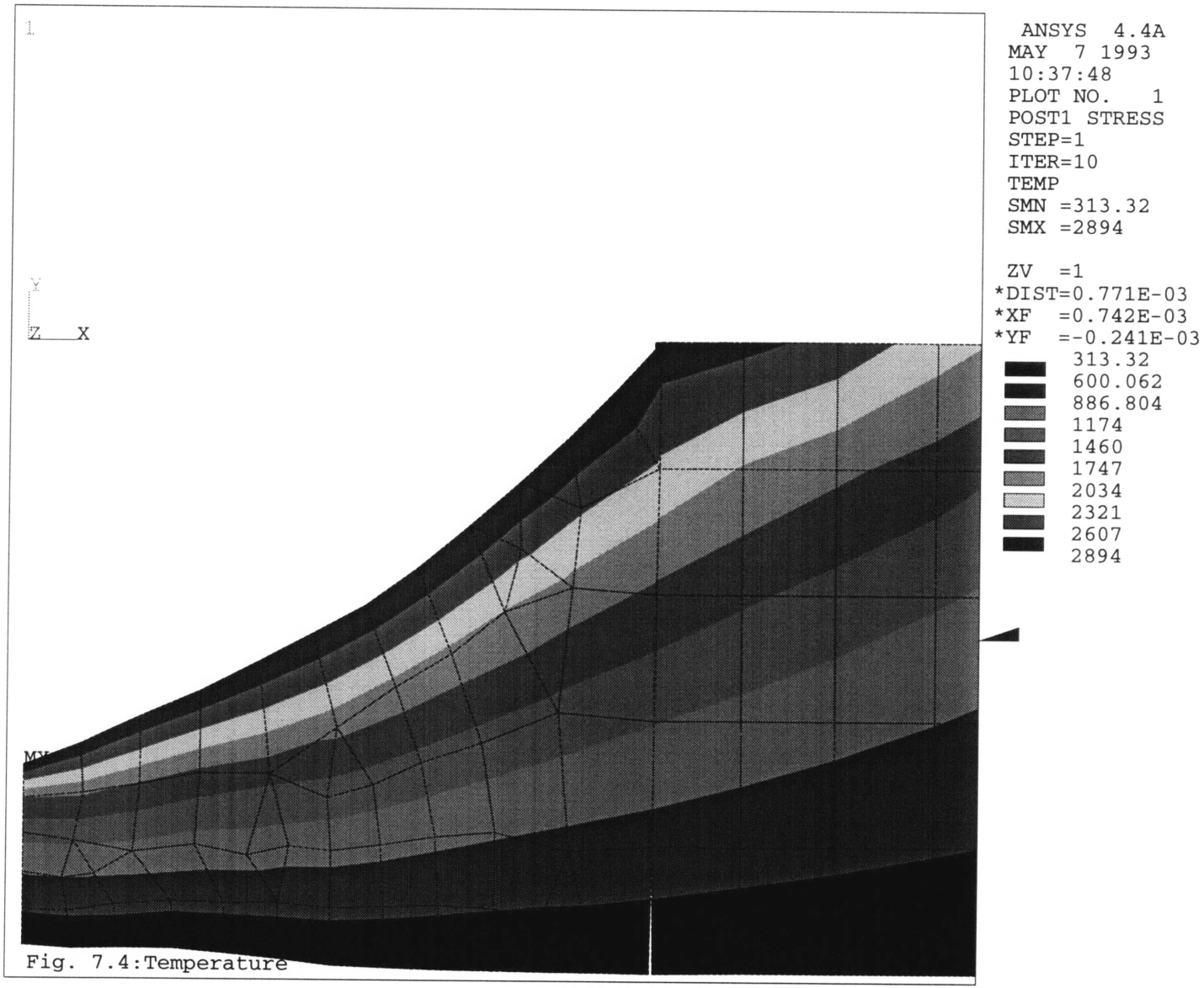

Fig. 7.4:Temperature

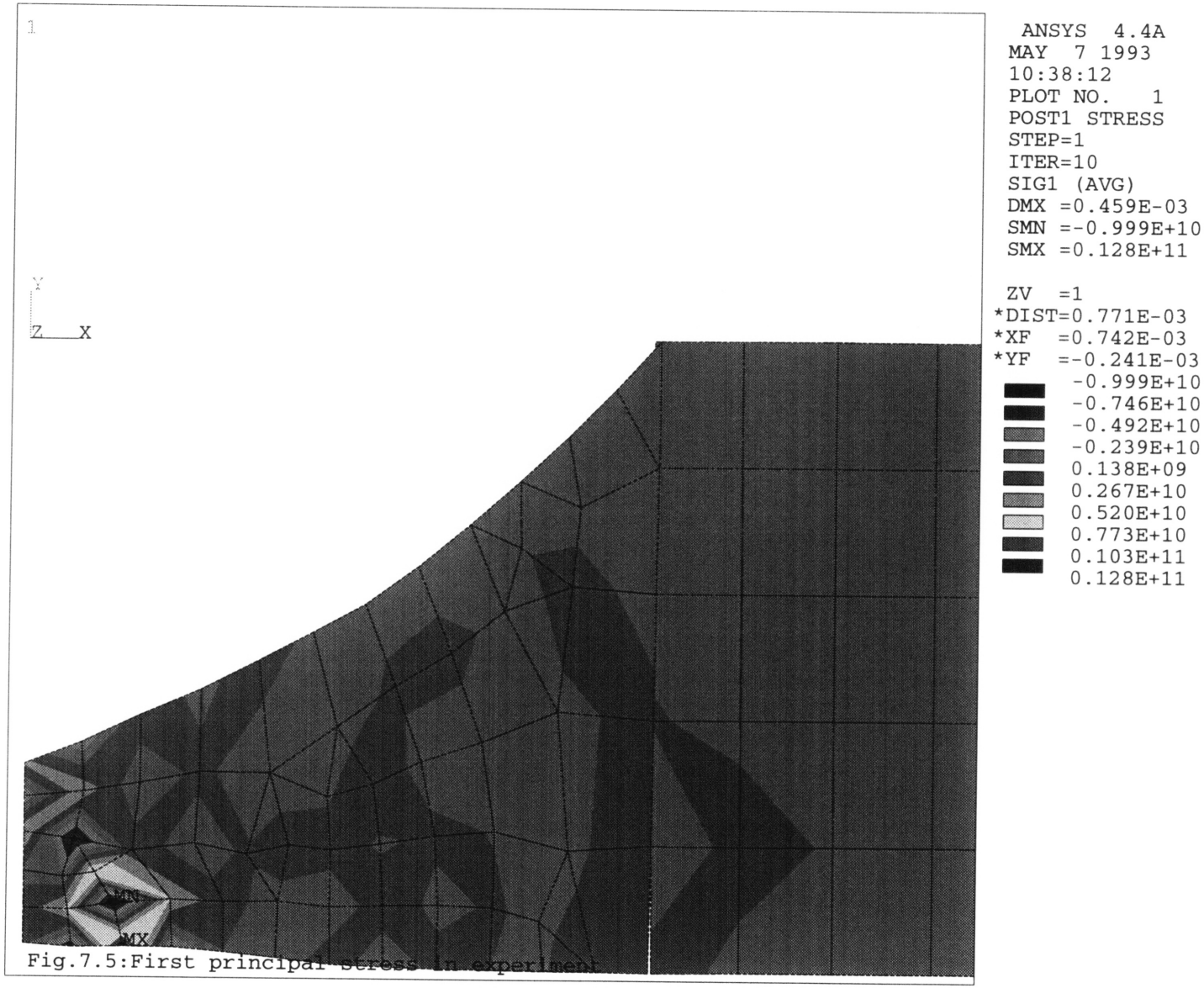

Fig.7.5:First principal stress in experiment

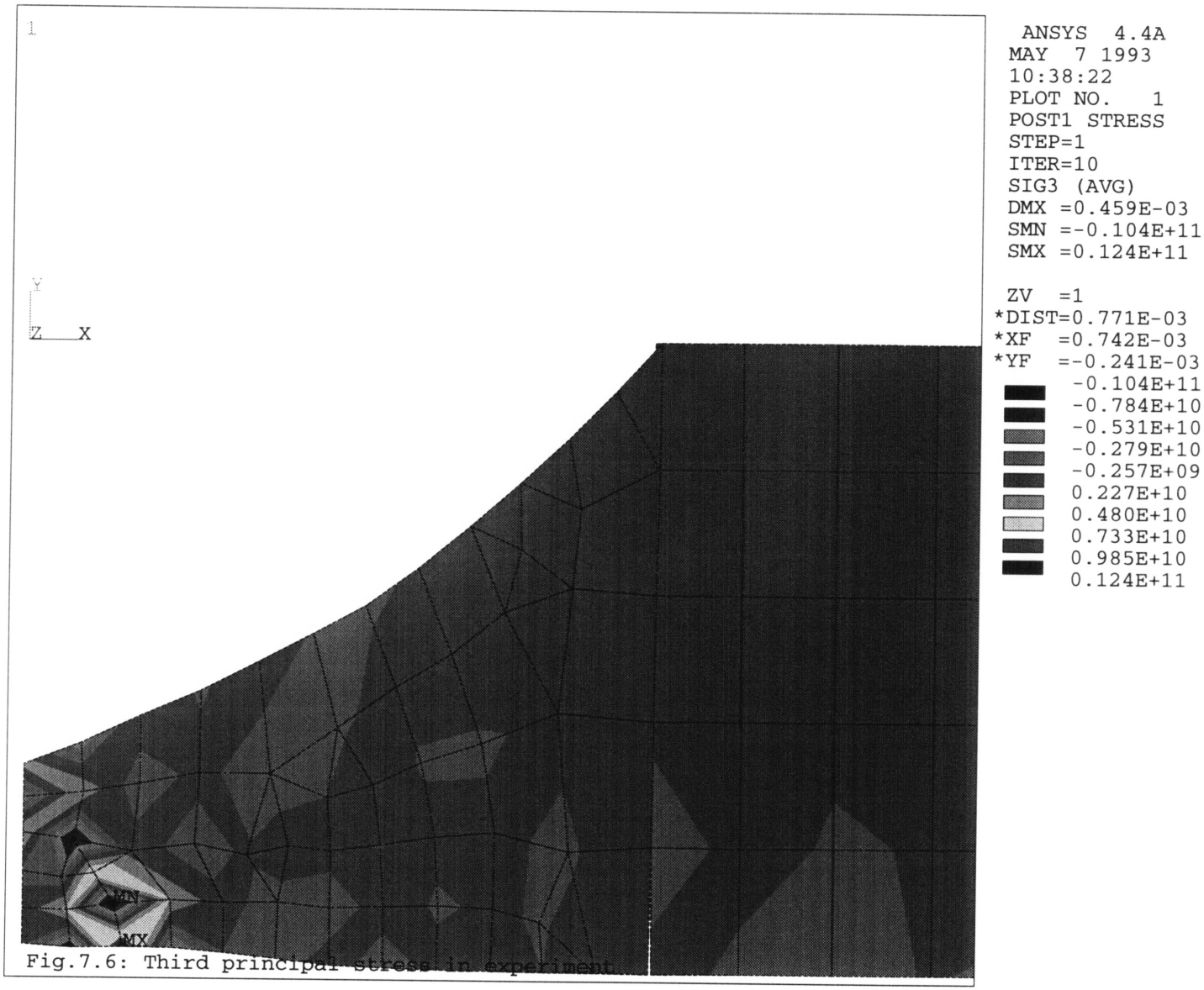

Fig.7.6: Third principal stress in experiment

Chapter 8

Conclusions and Design Tips

8.1 Design Methodology

Figure 8.1 describes how to use the models developed in this thesis for design. The first step in the process is to make a quick estimate of whether or not elasticity holds. The designer must determine if the material surface is localized or uniformly heated. Additionally, a mechanical end condition must be chosen. The designer is then directed to the appropriate model. Note that for the uniform surface heating of a simply supported plate, there are only jet induced stresses.

Once a model is selected, the designer should use the correlation developed in each section to determine the maximum stress level. This value must be compared to the yield strength at the maximum temperature in the body. If the stress is below the yield, elasticity is assumed. This assumption is checked again after the final solution.

If the analytical models are used, a steady state temperature distribution is required. There are three cases where the transient behavior limits heat flux, and thus numerical models must be used. If the material is brittle, sharp strength variations may facilitate failure at elevated temperatures (section 5.2). A free beam will only be thermally stressed when non-linearities are present. Thus, the transients can have higher thermal stresses than the steady state case (note that if the material's properties are a strong function of temperature, steady state can be more conservative). Similarly, a stepped temperature boundary condition for a restrained beam induces greater thermal stresses during transients (see section 3.3).

The analytical models for localized heating require that a linear temperature variation through the thickness be allowed. This can be assumed when the heating radius is much larger than the thickness of the plate. Restrained cases require that classical theory be satisfied. This includes requirements from small deflections and linear strain approximations (see sections 4.3.2 and 4.3.3.4). If all of these restrictions are met, a valid solution can be given.

This resultant stress field must then be compared to the yield strength of the material as a function of temperature throughout the body. If at all points in the body, equation 4.40 holds, the elasticity assumption is valid. If any of these requirements are not met, the numerical models should be used.

The numerical models given in the appendix can be used for those cases where the analytical models fail. The designer needs to change the body's geometry, material properties, end restraint conditions (a list of which is provided in each program), and if necessary, cooling jet properties, to accurately model the design at hand. Generally, these changes can be easily made by changing the values of the appropriate parameters. Instructions on how to use the numerical codes are included in the appendix. The numerical models should be used with care. The solutions are sensitive to the number of iterations and convergence criteria applied. It is recommended that the designer compare the numerical results with a similar limiting analytical result, if possible.

The design can be tentatively chosen via modeling, but it will require creep and/or fatigue testing. These experiments will place limits on the service life of the design.

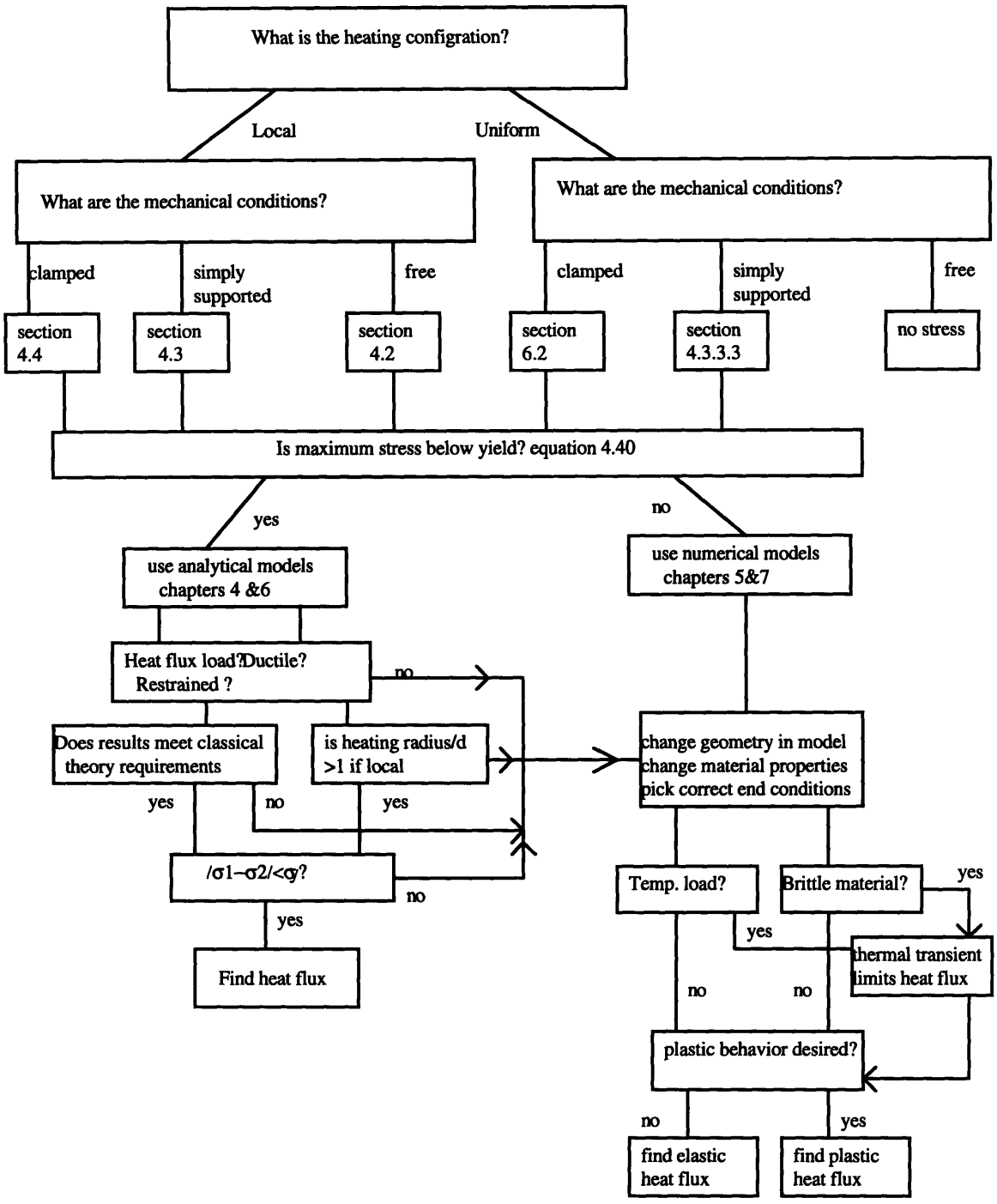

Figure 8.1: Design methodology flow chart. See description in section 8.1.

8.2 Material Selection

Sections 4.3.3.5 and 7.2 discuss systems to rank material performance at high heat fluxes. In the elastic range, equation 3.6 is the simplest equation which can be used. For a fixed plate with a linear temperature gradient through the thickness (y-direction), this equation becomes:

$$\sigma(T_t) = E(T_t)\alpha(T_t)(T_t - T_o) \tag{8.1}$$

Equation 8.1 must result in stress values below the yield strength, $\sigma_y(T_t)$, throughout the body. That is, $\sigma \leq \sigma_y$. If this inequality is true, the material does not yield under the imposed temperature gradient. The heat flux is then given by

$$Q = -k\frac{dT}{dy} \tag{8.2}$$

The results are shown in table 8.1 for the candidate materials. These results are not the same as would be predicted by the UCLA system described in section 4.3.3.5. The UCLA system does not account for material property variations with temperature.

Material	Flux (MW)	Relative Performance Value
Aluminum 6061	65.7	1
Tungsten	34.6	.52
Molybdenum	19.2	.29
Stainless Steel 304L	1.8	.027

Table 8.1: Relative ranking of candidate materials if fixed and elastic.

The results show that in the elastic range, Aluminum is the best choice for a fixed plate. In the elastic range thermal conductivity is the dominant parameter affecting attainable heat flux. Notice that these rankings are the same as found in chapters 4 and 6 for fixed plates. However, the gap between materials has increased. This occurs because the simpler one dimensional model used to develop this ranking system accounts for temperature

dependent properties. In the analytical models of chapters 4 and 6, properties were evaluated at the average temperature.

Section 7.2 suggests that a new ranking system is needed if plates are allowed to plastically deform. The simplest system is based on equation 3.9. Equation 7.5 cannot be used as written because the ultimate strength varies throughout the body. Instead the same procedure described for elastic materials is adopted here. The stress for the fixed plate is:

$$\sigma(T_t) = E_T(T_t,\varepsilon)\alpha(T_t)(T_t - T_o)$$
$$\textit{where:} \qquad (8.3)$$
$$E_T = pn\varepsilon^{n-1} \text{ (see section 7.2)}$$

If equation 8.2 results in stresses below the ultimate strength, σ_u, at every point in the body, the material does not fail. In this case, the heat flux is given by equation 8.2. Note that if the material is modeled with a bi-linear stress strain curve, the secant modulus, E_T, is not a function of strain. Instead it depends only on temperature. The modulus can be chosen conservatively to yield meaningful results. Results based on the bi-linear assumption are shown in table 8.2. The secant modulus is assumed to be the initial slope of the stress-strain curve.

Material	Flux (MW)	Relative Performance Value
Tungsten	272.9	1
Molybdenum	229.5	.84
Aluminum 6061	141.8	.52
Stainless Steel 304L	15.5	.057

Table 8.2: Relative ranking of candidate materials if fixed and allowed to behave plastically.

When extremal heat fluxes are experienced, high material strength in the plastic regime is necessary. Tungsten appears to be the obvious choice. However, if the heating process continues for long time periods (in tungsten's case on the order of minutes), tungsten is a bad choice. It is poor in creep at temperatures near its melting point. Molybdenum is a better material since its heat flux at the plastic limit is similar to tungsten's, but it has superior creep properties. However, molybdenum is vulnerable to rapid oxidization at

temperatures exceeding 775 K. Methods are available to mitigate molybdenum's oxidation problems including coating the metal and working in an inert atmosphere.

8.3 Design Tips and New Design Ideas

Once a material has been chosen design can commence. This section summarizes the issues concerning heating configuration raised throughout the thesis.

a) Localized versus uniform surface heating - Uniform surface heating substantially increases the heat flux level at which failure occurs. However, it also decreases the flux level at which melting occurs as a result of smaller fin effects. When a system operates at an extremal heat flux, the ratio of allowable to melting heat flux is important since heating perturbations may occur. If a perturbation causes the allowable flux to be exceeded, local cracking occurs. If a perturbation causes melting, a portion of the material is completely destroyed from a structural viewpoint. Thus, it is generally desirable to have a sizable difference between the melting and allowable fluxes. This can be accomplished by incorporating a factor of safety into the design, or by providing thermal fin effects.

Fin effects can be realized by localizing the heating. A large heating radius which encompasses the whole plate surface but creates smaller temperatures at the edges of the hot spot, can accomplish this. If the radius is large enough, bending stresses will be small, but fin effects will be present.

An alternative method for providing fin effects, but perhaps more costly, is to build end restraints out of a highly conductive metal, e.g. copper. This would effectively raise the melting flux of the plate metal.

b) Plate dimensions - The thinner the better, but keep the length to thickness ratio less than 20 (the ratio will change if molybdenum is not used; materials with greater secant modulii than molybdenum will have larger ratios, those with lesser modulii will have smaller ratios.). This suggests creating a series of mini-plates which are very short and thin instead of one large thick plate.

The plates cannot be infinitesimally thin. They are also loaded mechanically by a cooling jet. The jet stress increases as the inverse of the square of the plate thickness (equation

4.33). Thus, very thin plates may undergo large deflections and possibly rupture due to the cooling jet. A good estimate of the limiting thickness can be obtained by using equation 4.36 which tells when thermal stresses dominate the problem. If the inequality in equation 4.36 holds, mechanical stresses should not cause rupture.

Even if plate thickness is decreased, a small jet stress level can be maintained by modifying the jet radius and pressure in accordance with equation 4.33. The limit to decreasing these values is primarily a heat transfer problem.

c) Restraints - The more expansion allowed the better. Elastic restraints or designs which pin either the top or bottom surface of the plate, are preferable to clamping the plate's ends. Thus, if the system consists of a series of plates, as recommended in the part b, the plates need not have their edges joined. This reduces membrane stresses.

d) Stress relief - The greatest advantage the designer has when dealing with high heat flux systems, is that materials relieve thermal stresses by plastically deforming. Plastic deformation should be designed for.

Chapters 5 and 7 showed that plastic deformation significantly increases the heat flux which causes material failure. Additionally, when the beam length is similar to the thickness, deflections are small. Thus, it is possible to allow plastic deformation without corrupting the system.

e) Increase strength - If elastic behavior is desired, pre-stressing the material to a point near its ultimate strength is an option. Once a plastically deformed material is unloaded, it will behave elastically when re-loaded if the stress level is less than the stress it was deformed to. If the stress level the material is deformed to approximates the ultimate strength, the material essentially becomes brittle when re-loaded. The same caveats that accompany tungsten apply to these materials.

f)Transient based system - At very high flux levels, ductile materials behave essentially elastically in the first few milliseconds after heating (see figures 5.6-5.7). If a metal behaves elastically, it can undergo a number of heating cycles before fatigue failure occurs. Additionally, since within the first few milliseconds the temperature gradient is still small relative to the steady state, the incident flux can be increased over the limits given in chapters 4 and 6. The percentage increase depends not only on the material and heating

configuration, but the time during which the flux is incident upon a module. The longer the time period, the smaller the percentage increase. The finite element models given in the appendix can be used to calculate the maximum flux for a given time period, material, and heating configuration.

Estimates can be made of the residence heating time for molybdenum when subjected to a given heat flux. Table 6.4 states that molybdenum can hold a 19.8 MW steady state heat flux without yielding. This flux can be increased if the plate is heated for less time than needed to achieve steady state. Equations 3.6 and 3.8 give the thermal stress field for the one-dimensional case. The maximum stress occurs at the top surface of the beam. The lowest yield strength also occurs at the top surface. Therefore, the stress can be compared to the yield strength at the top surface to find the time at which elastic failure occurs. Results have been complied in table 8.3 for a 1 mm thick, fixed, molybdenum plate.

Material	Incident Heat Flux (MW)	time to yield (milliseconds)
Molybdenum	50	0.9
	100	0.23
	150	0.1
	200	0.08

Table 8.3: Time to yielding in a fixed, 1 mm thick, molybdenum plate, if the incident heat flux is greater than the steady state limiting value (table 6.4). The velocity of the plate equals diameter/ time to yield. For small plates, say 10 mm (see b), the velocity is on the order of 5 m/s for 50 MW.

Table 8.3 shows that the flux can be increased over the steady state limit. However, the residence times are very small - approximately 500 times less than the heating duration needed to achieve steady state. If a mechanical system can be devised to realize these small residence times, it is possible to design very reliable and predictable heat exchanger modules. Either the position of the flux source or the heat exchanger itself can changed with time, e.g. a rotary regenerator. Two examples of such systems are sketched below. In figure 8.1, two attached heat exchanger modules are exposed to a heat source. The flux from the source is either incident upon module 1 or module 2 during a given period of time. While one module is heated the other is cooled.

Figure 8.2 shows a system were a number of attached plates move back and forth from right to left and then left to right. Above the plates is a flux source, and below each plate is a cooling jet. The plates need not be rigidly attached. They may be elastically attached, this would reduce stress levels considerably.

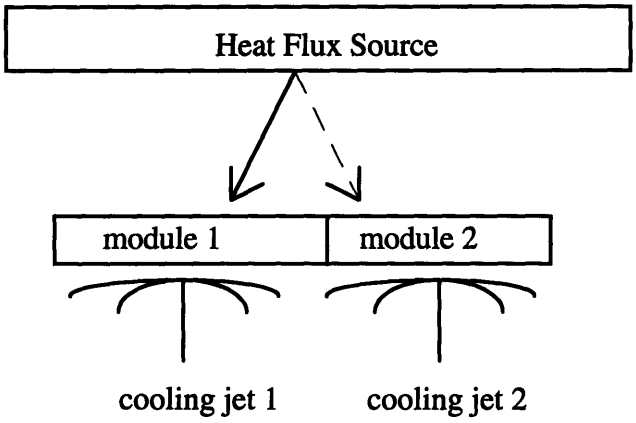

Figure 8.2: Transient based system with varying heat flux position.

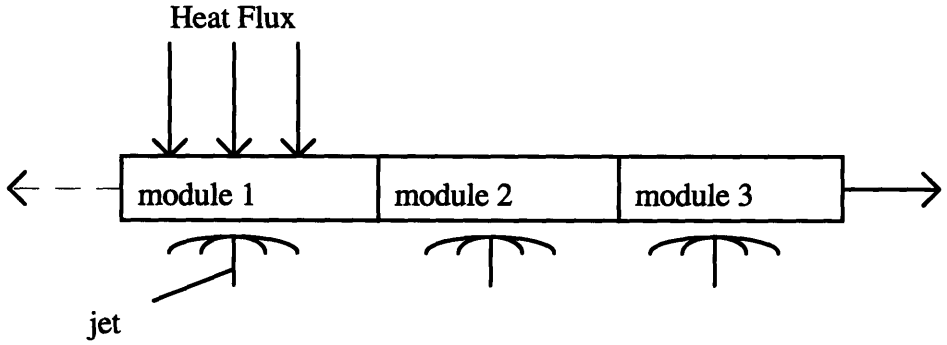

Figure 8.3: Transient design with varying module position.

Appendix

Appendix A: Solution of Equations
Appendix B: Material Properties of Candidate Materials
Appendix C: Program Listings

Appendix A: Solution of Equations

I. Rectangular beam with nonsymmetrical gaussian boundary conditions on its top and bottom surfaces

This section describes the solution procedure for equation 4.2. Refer to section 4.2 for the boundary conditions and a sketch of the problem.

The boundary conditions can be made homogeneous by introducing the function ϕ such that $\phi = T - T_O$. To simplify the solution the coordinate system is shifted such that its origin is at the middle of the plate's bottom surface. Thus, the boundary conditions become,

$$\begin{aligned} &y = 0, \phi = T_c e^{-bx} \\ &y = H, \phi = T_h e^{-ax} \\ &x = L/2, \phi = 0 \\ &x = -L/2, \phi = 0 \end{aligned} \tag{A.1}$$

The general solution to Laplace's equation is:

$$\phi = (A\cos\lambda x + B\sin\lambda x)\left(Ce^{\lambda y} + De^{-\lambda y}\right) \tag{A.2}$$

The solution is arrived at by using superposition. The first boundary condition is set to zero and a solution for ϕ is found. Then the boundary conditions given in A.1 are re-applied, but now the second boundary condition is set to zero. The two solutions for ϕ are added to get the final result.

Setting the second boundary condition to zero and applying the third and fourth boundary conditions yields:

$$\begin{aligned} &A = -B\tan\lambda L/2 \\ &\textit{and} \\ &\lambda = \frac{2n\pi}{L} \end{aligned} \tag{A.3}$$

Applying the first boundary condition (set to zero) yields C= -D. The final boundary condition necessitates a Fourier series solution:

$$\phi_1 = 2\sum_n E_n \sinh\frac{2n\pi x}{L}\sin\frac{2n\pi x}{L}$$

where,

$$E_n = \frac{2}{L\sinh(2n\pi H/L)}\int_0^{L/2} T_h e^{-ax}\sin 2n\pi\frac{x}{L}dx \tag{A.4}$$

Similarly, the solution when the second boundary condition is set to zero yields,

$$\phi_2 = 2\sum_n E_n \sinh\frac{2n\pi(H-y)}{L}\sin\frac{2n\pi x}{L}$$

where,

$$E_n = \frac{2}{L\sinh(2n\pi H/L)}\int_0^{L/2} T_c e^{-bx}\sin 2n\pi\frac{x}{L}dx \tag{A.5}$$

This can be found by simply switching the origin of the coordinate system to the top surface of the beam and re-solving as before. The solution for ϕ is thus,

$$\phi = \phi_1 + \phi_2 \tag{A.6}$$

II. Solution for thermal membrane stresses in a fixed plate

The general solution for the membrane stress terms is (see section 4.4.1):

$$u = \frac{\alpha(1+\nu)}{r}\int_a^r T_n r dr + C_1 r + \frac{C_2}{r}$$

$$N_r = \frac{-E\alpha}{r^2}\int_a^r T_n r dr + \frac{EC_1}{1-\nu} - \frac{EC_2}{r^2(1+\nu)} \tag{A.7}$$

$$N_\theta = \frac{E\alpha}{r^2}\int_a^r T_n r dr + \frac{EC_1}{1-\nu} + \frac{EC_2}{r^2(1+\nu)} - E\alpha T_n$$

The term a is the inner radius of the plate. The solution will first be given for a small radius a, and then the limit will be taken as a approaches zero so that the results are valid for the solid plate.

The boundary conditions are:

$$u(r=b)=0$$
$$N_r=0, r\to 0 \tag{A.8}$$

Applying the edge condition yields:

$$C_2=-(1+\nu)\int_a^b T_n r dr - C_1 b^2 \tag{A.9}$$

Applying the center condition and substituting A.9 gives:

$$C_1=\frac{\alpha\left(\int_a^a Trdr-\int_a^b Trdr\right)}{\frac{a^2}{1-\nu}+\frac{b^2}{1+\nu}} \tag{A.10}$$

As a approaches zero, C_1 and C_2 reduce to:

$$C_1=-\frac{(1+\nu)\alpha}{b^2}\int_0^b Trdr$$
$$C2=0 \tag{A.11}$$

Therefore, the membrane stress terms become:

$$N_r=\frac{E\alpha}{r^2}\int_0^r T_n r dr+\frac{E\alpha}{1-\nu}\frac{1+\nu}{b^2}\int_0^b T_n r dr$$
$$N_\theta=\frac{E\alpha}{r^2}\int_0^r T_n r dr-E\alpha T_n+\frac{E\alpha}{1-\nu}\frac{1+\nu}{b^2}\int_0^b T_n r dr \tag{A.12}$$

where:

$$T_n=\int_{H/2}^{H/2} T dz$$

III. Plate deflection due to cooling jet

The governing equation is,

$$D\nabla^4 w = q(r) = Pe^{-ror^2} \tag{A.13}$$

with the edge boundary conditions:

Simply supported case	Fixed case	
$w = Mr = \frac{\partial^2 w}{\partial r^2} + \frac{\nu}{r}\frac{\partial w}{\partial r} = 0$	$w = \frac{dw}{dr} = 0$	(A.14)

The left hand side of equation A.13 can be expanded into:

$$\nabla^4 w = \frac{1}{r}\frac{d}{dr}\{r\frac{d}{dr}[\frac{1}{r}\frac{d}{dr}(r\frac{dw}{dr})]\} \tag{A.15}$$

Thus, a particular solution of w can be found by repeated integration of the pressure distribution term, q(r). The general form of the solution with the particular and homogeneous parts is:

$$w = c_1 \ln(r) + c_2\frac{r^2}{4} + c_3 r^2 \ln(r) + c_4 + w_{particular}$$

where (A.16)

$$w_{particular} = \int_0^r \frac{1}{z}\int_0^z y\int_0^y \frac{1}{x}\int_0^x \frac{rq(r)}{D} drdxdydz$$

The particular solution for the gaussian function described in section 4.3.3.2 is:

$$w_{particular} = \frac{\Pr^2}{16Dr_o}\left[e^1 - 2 + 2\ln r + \gamma(1) + \ln r_o\right]$$

$$\gamma(n) = \lim_{m\to\infty}\sum_{k=1}^{n}\frac{(\ln k)^n}{k} - \frac{(\ln m)^{n+1}}{n+1} \tag{A.17}$$

Additionally, the requirements that the deflection and the slope of the deformed plate approach finite values at the center of the plate means that both C_1 and C_3 must be zero.

Imposing the boundary conditions given in A.14 yields the remaining constants:

fixed case	simply supported case
$C2 = \frac{-P}{4Dr_o}\left[e^1 - 1 + 2\ln b + \gamma(1) + \ln r_o\right]$	$C2 = \frac{-P}{4Dr_o}\left[\gamma(1) + 2\ln b + \ln r_o + e^1 + \frac{1-\nu}{1+\nu}\right]$
$C4 = \frac{Pb^2}{16Dr_o}$	$C4 = \frac{Pb^2}{16Dr_o}\frac{3+\nu}{1+\nu}$

(A.18)

Therefore, the deflections for both cases simplify to:

$$w_{simple} = \frac{\mathrm{Pr}^2}{16Dr_o}\left(-2 + 2\ln r - 2\ln b + \frac{1-\nu}{1+\nu}\right) + \frac{Pb^2}{16Dr_o}\frac{3+\nu}{1+\nu}$$
$$w_{fixed} = \frac{P}{16Dr_o}\left(-r^2 + 2r^2\ln r - 2r^2\ln b - b^2\right) \qquad \text{(A.19)}$$

Appendix B: Material Properties of Candidate Materials

Functional forms of the candidate materials' properties are given below. These functions are based on the data given in references 16-20. Polynomial fits have generally been used since the finite element code employed in this thesis, ANSYS, accepts material properties as polynomials.

The percentage error given is the most conservative error estimate for temperatures ranging from 273 K to melting. All temperatures in the equations below are the absolute temperature of the material and are measured on the Kelvin scale.

I. Molybdenum

$E = 367.76 - .12T$ {GPa} $\pm 13.5\%$ error

$\alpha = (5.05 + 0.00031T + 0.36\times10^{-6}T^2)\times10^{-6}$ $\pm 6.8\%$ error.

$\alpha_t = (-9.4\times10^{-12}T^3 + 9.5\times10^{-8}T^2 - 3.46\times10^{-4}T + .6329)\times10^{-4}$ {m^2 / sec} $\pm 11.1\%$ error

$k = 150.4 - 0.039T$ < 1500 K $\pm 7\%$; > 1500 K $\pm 20\%$ {W / mk}

$\sigma_y = 1.39\times10^{-9}T^3 + 3.7618\times10^{-5}T^2 - .2321T + 330.37$ {MPa} $\pm 13\%$ error

$\sigma_u = 6.83\times10^{-12}T^4 + 5.92\times10^{-10}T^3 - 6.32\times10^{-5}T^2 - .1356T + 460.5$ {MPa} $\pm 12.8\%$ error

II. Tungsten

$E = -2.8\times10^{-5}T^2 - .0111T + 478.76$ {GPa} T < 2500K $\pm 11\%$; T > 2500K $\pm 29\%$

$\alpha = (0.0012T + 3.53)\times10^{-6}$ $\pm 10\%$ error.

$\alpha_t = (-2.76\times10^{-11}T^3 + 2.13\times10^{-7}T^2 - 5.65\times10^{-4}T + .8003)\times10^{-4}$ {m^2 / sec} $\pm 6.4\%$ error

$k = -4.65\times10^{-9}T^3 + 3.44\times10^{-5}T^2 - 0.0911T + 178.54$ $\pm 2\%$; {W / mk}

$\sigma_y = 4370e^{-0.0055T} + 81.6$ {MPa} $\pm 20\%$ error

$\sigma_u = 0.10036\times10^{-10}T^4 - 0.1039\times10^{-6}T^3 + 0.000411T^2 - 0.7714T + 749$ {MPa} $\pm 12\%$ error

III. Aluminum 6061

$E = 100.4 - 0.065T \ \{GPa\} \ \pm 1.1\% \ error$

$\alpha = (11.18 + 0.0049T) \times 10^{-6} \ \pm 1.7\% \ error.$

$\alpha_t = (-4.4678 \times 10^{-4} T + 1.1147) \times 10^{-4} \ \{m^2 / \sec\} \ \pm 4.4\% \ error$

$k = 250.7 - 0.047T \ < 1500 \ K \ \pm 7\%; \ > 1500 \ K \ \pm 20\% \ \{W / mk\}$

$\sigma_y = -2.268 \times 10^{-8} T^4 + 6.1958 \times 10^{-5} T^3 - 0.0603T^2 + 24.1506T - 3127 \ \{MPa\} \ T < 750K \ \pm 16\% \ ; \ T > 750K \ \pm 60\%$

$\sigma_u = -2.1687 \times 10^{-8} T^4 + 5.9056 \times 10^{-5} T^3 - 0.0572T^2 + 22.66T - 2855 \ \{MPa\} \ \pm 1.3\% \ error$

IV. Stainless Steel 304L

$E = 231.3 - 0.094T \ \{\text{GPa}\} \ \pm 1.7\% \text{ error}$

$\alpha = (15.9 + 0.0033T) \times 10^{-6} \ \pm 6.8\% \text{ error.}$

$\alpha_t = (0.0017T + 3.01) \times 10^{-6} \ \{\text{m}^2 / \text{sec}\} \ \pm 1\% \text{ error}$

$\text{k} = 8.5 + 0.018\text{T} \ \pm .4\% \ \{\text{W / mk}\}$

$\sigma_y = \frac{450}{810}(-5.4608 \times 10^{-7} T^3 + 0.0018T^2 - 2.2T + 1334.4) \ \{\text{MPa}\} \ \pm 17\% \text{ error}$

$\sigma_u = -2.2485 \times 10^{-6} T^3 + 0.0044T^2 - 2.974T + 1093.8 \ \{\text{MPa}\} \ \pm 5.1\% \text{ error}$

Appendix C: Program Listings

Maple Program Listings

I. Steady state one-dimensional problem

```
> #One dimensional temperature and thermal stress distribtuion for isotropic and temperature
> #dependent property cases.
>
>
> Young:=(-.12*(T+To)+367.76)*10^3:     # Youngs modulus MPa
> alpha:=(.033*(T+To)+.7)*10^(-7):      # linear coefficient of thermal expansion
> H:=.5:                                # Height of beam
> Th:=2883:                             # Hot temperature , degress K
> Tc:=293:                              # Cold temperature, degress K
> To:=298:                              # Ambient temperature, degress K
> T:=(((Tc-Th)*(1/(2*H))*y)+(Th+Tc)/2)-To:
> cond:=100:                            # thermal conductivity W/mk
> flux:=eval(-1*cond*diff(T,y)*1000/(1*10^6)):  # heat flux  in Mw
> stressn:=-Young*alpha*T:              # thermal stress terms
> stresst:=(1/(2*H))*int(Young*alpha*T,y=-H..H):
> stressb:=((3*y)/(2*H^3))*int(Young*alpha*T*y,y=-H..H):
> stress:=stressn+stresst+stressb:
> plot(stress,y=-H..H);
>
> #Anistropic Problem with conductivity as a function of temperature
> #V is new temperature variable
> #centered in midplane
> #Temperatures must be in kelvin
> #To use this section, change Young and  alpha to functions of temperature., check end
> #input thermal conducivity,k not cond,  below as a function of temperature.
> #Check plot of V to ensure that its goves the correct temperatures at the ends.  If not
> #the wrong solution was picked (see below).
> k:=-.039*V+150:  #per mm
> one:=int(k,V):                        #Kirchoff transformation
> two:=one-subs(V=Th,one):
> km:=(1/(Tc-Th))*int(k,V=Th..Tc):      #Effective conductivity
> three:=km*(Tc-Th)*(y+H)/(2*H):
> V2:=[solve(two-three=0,V)]:           #Solve for temperature
> V3:=V2[1]-To:                         # Temperature rise, choose first solution from list
> plot(V3+To,y=-H..H);                  #Adding To give temp. dist. subtractin gives temp change
>
> stressnV:=-Young*alpha*V3:            # Stress components
> stresstV:=(1/(2*H))*int(Young*alpha*V3,y=-H..H):
> stressbV:=((3*y)/(2*H^3))*int(Young*alpha*V3*y,y=-H..H):
> stressV:=stressnV +stresstV +stressbV:
> fluxan:=km*(Th-Tc)/(2*H)/(1*10^6):    #Heat flux
```

II. Transient one-dimensional problem

```
> #This program calculates thermal stresses when flux or temperature transients exist
> #CAUTION for small times need to further expand fourier series always check the temperature plot
>
> Young:=150*10^9:              #Youngs modulus MPa
```

```
> alpha:=.53*10^(-4):          # linear coefficient of expansion
> alphas:=4*10^(-6):           # thermal diffusivity m^2/sec
> Q:=100*10^6:                  # heat flux boundary condition in MW\

> k:=154:
> Th:=2894:                     # temperature boundary condition in MW
> Tc:=298:                      # cold temperature
> To:=298:                      # ambient temperature
> l:=.01/2:                     #one half the thickness of the beam
>
> #If the temperature boundary condition is used, this is the temperature distribution
> T1:=(Th-Tc)/2*x/l+(Th+Tc)/2:
> An:=(1/(2*l))*int((To-T1)*cos((n+.5)*Pi*x/l),x=-l..l):
> T2:=sum(An*exp((-1)*(n+.5)^2*Pi^2*(alpha*t/l^2))*cos((n+.5)*Pi*x/l),n=0..40):
> T:=T1+T2:                          #Temperature
>
> #If the flux boundary condition is used, this is the temperature distribution
> an1:=(((-1)^n)/(2*n+1)^2):
> an2:=exp(-alpha*(2*n+1)^2*Pi^2*t/(16*l^2)):
> an3:=sin((2*n+1)*Pi*(x+l)/(4*l)):
> An:=sum(an1*an2*an3,n=0..10):
> T:=((Q*(x+l))/k)-((16*Q*l)/(k*Pi^2))*An:  # Temperature
> plot3d(stress/(1*10^6),x=-l..l, t=0.01..1,
title='Free_Molybdenum_Temperature_Loading',labels=['depth_mm','time_secs','MPa']);
>
> # Thermal stress distribution
> stressn:=-Young*alphas*T:
> stresst:=(1/(2*l))*int(Young*alphas*T,x=-l..l):
> stressb:=((3*x)/(2*l^3))*int(Young*alphas*T*x,x=-l..l):
> stress:=stressn+stresst+stressb:
```

III. Plastic limits for one dimensional heating

```
> #Plastic temperature limits in one-dimensional case
>
> #Procedure
> #It is know that strain=strainc+strainb*(y/c-1) and that max strain occurs at -H
> #sub y=-H, into equation above so that strain is the max strain experienced at this temperature.  Set this
> equation to the max strain found from the stress strain curve.
> #Find temperture to make the equation true. If temperature > Tmelt then material will not fracture.
> #This is iterative since strainmax must be estimated each time from the stress strain curve.
>
> #Molybdenum
> Tmelt:=2894:
> Tmax:=1800:
> sigmayp:=subs(Tp=Tmax,1.39*10^(-9)*Tp^3+3.76*10^(-5)*Tp^2-.2321*Tp+327.37):
> sigmau:=subs(Tp=Tmax,6.83*10^(-12)*Tp^4+5.92*10^(-10)*Tp^3-6.33201*10^(-5)*Tp^2-
.1356*Tp+465.5):
> alpha:=subs(Tp=Tmax,(10^(-6))*(5.05+.031*10^(-3)*(Tp-273)+.36*10^(-6)*(Tp-273)^2)):
> k:=120:
> Young:=subs(Tp=Tmax,(sigmayp+.59*(100*strain)^3-10.9*(100*strain)^2+57.6*100*strain)/strain):
> stresscurve:=strain*Young:
> with(plots):
> a:=plot(stresscurve,strain=0..0.1):
```

```
> b:=plot(sigmau,strain=0..0.1):
> display({a,b});
> strainmax1:=solve(stresscurve=sigmau,strain);
> strainmax:=strainmax1[1]:
>
>
> #Tungsten
> Tmelt:=3660:
> Tmax:=1000:
> sigmayp:=evalf(subs(Tp=Tmax,81.6+4379*exp(-.0055*Tp))):
> sigmau:=subs(Tp=Tmax,1.0036*10^(-11)*(Tp^4)-1.0392*10^(-7)*(Tp^3)+.00041104*Tp^2-
.7714*Tp+749):
> alpha:=subs(Tp=Tmax,(10^(-6))*(.0012*Tp+3.53)):
> k:=174:
> Young:=subs(Tp=T,(sigmayp+19614*(strain)^3-13442*(strain)^2+3442*strain)/strain):
> stresscurve:=strain*Young:
> with(plots):
> a:=plot(stresscurve,strain=0..0.3):
> b:=plot(sigmau,strain=0..0.3):
> display({a,b});
> strainmax1:=solve(stresscurve=sigmau,strain):
> strainmax:=strainmax1[1]:
>
> #Aluminium  {good up to about 900}
> Tmelt:=993:
> Tmax:=900:
> sigmayp:=subs(Tp=T,-2.268*10^(-8)*Tp^4+6.1958*10^(-5)*Tp^3-.0603*Tp^2+24.1506*Tp-3127):
> sigmau:=subs(Tp=Tmax,-2.1687*10^(-8)*Tp^4+5.91*10^(-5)*Tp^3-.0572*Tp^2+22.664*Tp-2855):
> alpha:=subs(Tp=T,(10^(-6))*(.0049*Tp+11.18)):
> k:=229:
> Young:=subs(Tp=T,(sigmayp+1000*(-5.6053*strain^3+1.9521*strain^2+.3361*strain))/strain):
> stresscurve:=strain*Young:
> with(plots):
> a:=plot(stresscurve,strain=0..0.3):
> b:=plot(sigmau,strain=0..0.3):
> display({a,b});
> strainmax1:=solve(stresscurve=sigmau,strain):
> strainmax:=strainmax1[1]:
>
>
> #Stainless Steel {good up to about 800, yield goes negative, so linearly interpolate after this }
> Tmelt:=1670:
> Tmax:=1200:
> sigmayp:=(250/871.2)*subs(Tp=T,-5.466*10^(-7)*Tp^3+.0018*Tp^2-2.1999*Tp+1334.4):
> sigmau:=subs(Tp=Tmax,-4.178*10^(-12)*Tp^5+2.041*10^(-8)*Tp^4-3.736*10^(-
5)*Tp^3+.0316*Tp^2-12.56*Tp+2321.1):
> alpha:=subs(Tp=T,(.0033*(T+298)+15.9)*10^(-6)):
> k:=19.3:
> Young:=(sigmayp+521*strain^3-1625*strain^2+1279*strain)/strain:
> stresscurve:=strain*Young:
> with(plots):
> a:=plot(stresscurve,strain=0..0.3):
> b:=plot(sigmau,strain=0..0.3):
> display({a,b});
```

```
> strainmax1:=solve(stresscurve=sigmau,strain):
> strainmax:=strainmax1[1]:
>
>
> #Temperature analysis (do not use Th, it will be solved for)
> H:=.005:              #mm Center is in mid-plane with sides at -h and h
> #Th:=1670:            #degress K
> Tc:=298:
> To:=298:
> T:=(((Tc-Th)*(1/(2*H))*y)+(Th+Tc)/2)-To:
> plot(T,y=-H..H);
>
> #Stress analysis
> c:=int(Young*y,y=-H..H)/(int(Young,y=-H..H)):
> strainc:=int(alpha*Young*T,y=-H..H)/(int(Young,y=-H..H)):
> strainb:=int(alpha*Young*T*(y/c-1),y=-H..H)/(int(Young*(y/c-1)^2,y=-H..H)):
>
> #Find Th which makes this true
> straintemp:=evalf(subs(y=-H,strain=-.018,Th=1200,-(alpha*T)+0*strainc+0*strainb*(y/c-1))):
> strainfinal:=solve(strain=subs(y=-H,Th=900,-alpha*T+strainc+0*strainb*(y/c-1)),strain):
> plot(straintemp,Th=1670);
```

IV. Hot spot on an infinite beam

```
> #Stresses in hot spot on infinite beam
> #Program solves for temperature at mechanical yield limit. Accounts only for membrane stresses
>
> a:=.06*.4:                    #radius of hotspot
> T:=(Tmax-298):                #Temperature rise
> Young:=(297.5-exp(.0035*Tmax))*10^9:          #Properties as a function of temperature
> alpha:=(.033*Tmax+.7)*10^(-7):
> sigmay:=114.7 +1781.5*exp(-.0052*Tmax):          #stress in hotspot
> stressrr:=-0.5*Young*alpha*T/(1*10^6):
> YieldTemp:=solve(stressrr=-(sigmay),Tmax);
> stressrrout:=(-.5*Young*alpha*T*(a/r)^2)/(1*10^6):
> plot(sigmay,Tmax=500..1500);\

>
> #Graphically solution        #solution above does not always work due to rounding
> F:=plot(-sigmay,Tmax=298..1273):
> G:=plot(stressrr,Tmax=298..1273):
> with(plots):
> display({F,G});
```

V. Two dimensional free beam problem

```
> #Free Beam Problem
>
>
> #Thermal stresses in free beam.  Temperature is a gaussian function of the radius
> #on the top and bottom surfaces.
> #Stresses are absent in the steady state isotropic case, but present for the anisotropic case.
```

```
> #As discussed in chapter 4, stresses result from the linear temperature variation approximation
> #these stresses are calculated here.
>
> L:=400:                          #Beam length in mm
> alphas:=18.5*10^(-6):          #linear coefficient of thermal expansion
> Young:=158*10^3:               #Young's modulus in GPa
> H:=1:                            #Height of beam in mm
> Tc:=293:                         #Cold temperature in K
> Th:=1104:                        #Hot temperature in K
> To:=298:                         #Average beam temperature
> k:=23/1000:                      #thermal conductivity in W/mmK
>
> #Temperature distribution
> a:=2*sin(n*Pi*x/L):
> fh:=Th*exp(-.1*(x-L/2)^2):
> B:=((1-(-1)^n)/2)*(2/L)*(1/sinh(n*Pi*H/L))*.5*int(fh*sin(n*Pi*x/L),x=0..L):
> c:=B*sinh(n*Pi*((y+H/2)/L)):
> fc:=-Tc*exp(-.1*(x-L/2)^2):
> d:=((1-(-1)^n)/2)*(2/L)*(1/sinh(n*Pi*H/L))*.5*int(fc*sin(n*Pi*x/L),x=0..L):
> f:=d*sinh(n*Pi*(H/2-y)/L):
> g:=a*(c+f):
> T:=sum(g,n=1..65)+To:
> plot3d(T,x=0..L,y=-
H/2..H/2,title='Figure_4_3_Hot_Spot_on_Top_Surface_of_Body',labels=['length_m','depth_m','temperatur
e_C']);
>
> #Linear Approximation of temperature
> Tap:=((fh+fc)*(y/H))+((fh-fc)/2)+To:
> fluxlinear:=evalf(subs(x=L/2,-k*diff(Tap,y))):
> plot3d(Tap,y=-
H/2..H/2,x=0..L,title='Figure_4_4_Hot_Spot_Linear_Approximation',labels=['length_m','depth_m','tempe
rature_C']);
>
> #Anisotropic temperature distribution- temperature dependent conductivity

> ko:=135:
> k:=-.039*V+150.4:
> zz:=int(k/ko,V):
> zz2:=subs(V=fh,zz)-subs(V=To,zz):
> yy2:=subs(V=fc,zz)-subs(V=To,zz):
> aa:=2*sin(n*Pi*x/L):
> BB:=((1-(-1)^n)/2)*(2/L)*(1/sinh(n*Pi*H/L))*.5*int(zz2*sin(n*Pi*x/L),x=0..L):
> cc:=BB*sinh(n*Pi*(y+H/2)/L):
> DD:=((1-(-1)^n)/2)*(2/L)*(1/sinh(n*Pi*H/L))*.5*int(yy2*sin(n*Pi*x/L),x=0..L):
> ff:=DD*sinh(n*Pi*(H/2-y)/L):
> gg:=a*(c+f):
> ee:=sum(gg,n=1..19):   #This is a T-To value instead of summing here sum after everything else
> V2:=subs(V=Tan,zz)-subs(V=To,zz):
> Tan1:=solve(ee=V2,Tan):
> Tan2:=Tan1[2]:
> T3:=(fh-Tc)*(y/(H))+(fh+Tc)/2:
> plot3d(T3,x=0..L,y=-
H/2..H/2,title='Figure_15_Linear_Approximation_for_Figure_14',labels=['length_m','depth_m','temperatu
re_C']);
```

```
>
>
> #Stresses if temperature linear in y
>
> functionx:=(Tap-((fh-fc)/2)-To)/y:
> potxy1:=((((H/2)^2-(y^2))*(((H/2)^2)-(5*y^2)))/120)*diff(diff(diff(functionx,x),x),x):
> potxy2:=-((((y^6)/360)-(((y^4)*((H/2)^2))/120)+(((9*y^2*(H/2)^4))/1400)-
((11*(H/2)^6)/12600)))*diff(diff(diff(diff(diff(functionx,x),x),x),x),x):
> shearxy:=(potxy1+potxy2)*(Young*alphas)*(1*10^(0)):
> potxx1:=((((3*(H/2)^2)-(5*y^2))*y)/30)*diff(diff(functionx,x),x):
> potxx2:=(((y^5)/60)-
(((y^3)*(H/2)^2)/30)+((9*y*(H/2)^4)/700))*(diff(diff(diff(diff(functionx,x),x),x),x),x)):
> stressxx:=(alphas*Young)*(potxx1+potxx2):
> potyy1:=-(((y*(y^2-(H/2)^2)^2))/120)*diff(diff(diff(diff(functionx,x),x),x),x):
> potyy2:=((y*(y^2-(H/2)^2)^2*(5*y^2-
11*(H/2)^2))/12600)*(diff(diff(diff(diff(diff(diff(functionx,x),x),x),x),x),x),x)):
> stressyy:=(alphas*Young)*(potyy1+potyy2):
> plot3d(stressyy,x=0..L,y=-H/2..H/2);
>
> #Stresses if temperature dependent conductivity
> Tf:=T3:          #new temperature variable, T can be assigned as well
>
> #stresses if can integrate, and not linear in y
> zero:=int(Tf,y):
> zeroa:=zero-subs(y=-H,zero):
> zerob:=subs(y=H,zero)-subs(y=-H,zero):
> one:=int(Tf*y,y):
> onea:=one-subs(y=-H,one):
> oneb:=subs(y=H,one)-subs(y=-H,one):
> two:=int(Tf*y^2,y):
> twoa:=two-subs(y=-H,two):
> twob:=subs(y=H,two)-subs(y=-H,two):
> three:=int(Tf*y^3,y):
> threea:=three-subs(y=-H,three):
> threeb:=subs(y=H,three)-subs(y=-H,three):
> four:=int(Tf*y^4,y):
> foura:=four-subs(y=-H,four):
> fourb:=subs(y=H,four)-subs(y=-H,four):
> five:=int(Tf*y^5,y):
> fivea:=five-subs(y=-H,five):
> fiveb:=subs(y=H,five)-subs(y=-H,five):
>
> #stresses if cannot integrate, and not linear in y
> with(student):
> zeroa:=simpson(Tf,y=-H..y,4):
> zerob:=simpson(Tf,y=-H..H,4):
> onea:=simpson(Tf,y=-H..y,4):
> oneb:=simpson(Tf,y=-H..H,4):
> twoa:=simpson(Tf,y=-H..y,4):
> twob:=simpson(Tf,y=-H..H,4):
> threea:=simpson(Tf,y=-H..y,4):
> threeb:=simpson(Tf,y=-H..H,4):
> foura:=simpson(Tf,y=-H..y,4):
> fourb:=simpson(Tf,y=-H..H,4):
```

```
> fivea:=simpson(Tf,y=-H..y,4):
> fiveb:=simpson(Tf,y=-H..H,4):
>
> #ratios for both cases
> r1:=y/H:
> r2:=(y/H)^2:
> r3:=(y/H)^3:
> r4:=(y/H)^4:
> r5:=(y/H)^5:
> r6:=(y/H)^6:
> r7:=(y/H)^7:
>
> part1:=-y*zeroa+onea+((H/4)*(1+2*r1+r2)*zerob)-(.25*(2+3*r1-r3)*oneb):
> part2:=((y^3)/6)*zeroa-((y^2)/2)*onea+(y/2)*twoa-.167*threea-
((H^3)/24)*(r2+2*r3+r4)*oneb+((H^2)/40)*(4*r1+10*r2+7*r3-r5)*oneb-
(H/8)*(1+2*r1+r2)*twob+(1/24)*(2+3*r1-r3)*threeb:
> part2d:=diff(diff(part2,x),x):
> part3:=((y^5)/120)*zeroa-((y^4)/24)*onea+((y^3)/12)*twoa-((y^2)/12)*threea+(y/24)*foura-
(1/120)*fivea+(H^5)*((1/180)-(1/90)*r1+(1/288)*r4-(1/240)*r5-(1/480)*r6)*zerob+(H^4)*((-
1/1050)*r1+(2/175)*r3+(1/48)*r4+(9/800)*r5-(1/1120)*r7)*oneb+(H^3)*((-1/48)*r2-(1/24)*r3-
(1/48)*r4)*twob+(H^2)*((1/60)*r1+(1/24)*r2+(7/240)*r3-(1/240)*r5)*threeb-
(H/96)*(1+2*r1+r2)*fourb+(1/480)*(2+3*r1-r3)*fiveb:
> part3d:=diff(diff(diff(diff(part3,x),x),x),x):
> last:=part1+part2d+part3d:
> last2:=Young*alphas*diff(diff(last,x),x):
> last3:=sum(last2,n=1..10):
> last3e:=evalf(subs(x=.5*L,y=H,last2)):
> plot3d(last2,x=0..L,y=-H/2..H/2);
> stress:=Young*alphas*last3/(1*10^6):
```

VI. Localized Heating of Simply Supported Plate

```
> #Simply supported circular disc with hot spot
>
> #Constants
> Young:=158*10^9:                    #Youngs Modulus
> alphas:=4.5*10^(-6):                #linear expansion coeffient
> poi:=.3:                            #poisson property
> a:=.02:                             #rate of gaussian decay
> d:=.001:                            #thickness of disc in meters
> b:=.2:                              #radius of disc in meters\
>
> #Temperature profile
> k:=124:                             #thermal conductivity in W/m-K

> To:=298:                            #ambient temperature of environment in Kelvin
> Tc:=298:                            #temperature of plate on jet side
> Thot:=1670-To:                      #maximium temperature of plate on heated side, add To
> Th:=To+Thot*(exp(-(2*r^2)/a^2)):    #equation for guassian hot spot on heated side
> T:=((Th-Tc)*(z/d)+(Th+Tc)/2)-To:    #Temperature distribution in plate
> flux:=evalf(subs(r=0,k*diff(T,z)))/(1*10^6):  #flux throught plate
> evalf(subs(z=d/2,r=.22*b,T)):       #tells the percentage of b for which the plate is heated
>
>
```

```
> #Membrane stresses
> Tn:=int(T,z=-d/2..d/2):
> Fm:=int(Tn*r,r=0..x):
> Fma:=subs(x=r,Fm):
> Fmb:=subs(r=b,Fma):
> u:=(alphas/r)*( (1+poi)*Fma + (1-poi)*((r/b)^2)*Fmb):              #displacement
> Nr:=((Young*alphas)/r^2) *(1/(1-poi))* ( ((r/b)^2)*Fmb - Fma):   #thermal force terms\
> Ntheta:=((Young*alphas)/r^2) * ( (r/b)^2*Fmb + Fma - Tn*r^2):
>
>
> #Bending stress
> F:=int(alphas*T*r,r=0..x):
> Fa:=subs(x=r,F):
> Fb:=subs(r=b,Fa):
> Faa:=int(Fa/r,r=0..x):
> Faaa:=subs(x=r,Faa):
> Faab:=subs(r=b,Faaa):
> Faaeq:=Faaa-subs(r=b,Faaa):
> w:=((1+poi)/d)*( Faaeq - ((1-poi)/(2*(1+poi)))*Fb*(1-(r/b)^2)):   #deflection (a negatie value)
> evalf(subs(r=b/200,z=d/2,w)):
> Mr:=((Young*d^2)/12)*((1/r^2)*Fa-(1/b^2)*Fb):                      #thermal moment terms
> Mtheta:=((Young*d^2)/12) *( (alphas*T) - (1/r^2)*Fa - (1/b^2)*Fb):
>
>
> #Total stresses
> Mt:=int(alphas*Young*(1/(1-poi))*T*z,z=-d/2..d/2):
> Nt:=int(alphas*Young*(1/(1-poi))*T,z=-d/2..d/2):
> stressr:=(1/d)*(Nr+Nt)+((12*z)/(d^3))*0*(Mr + Mt) -((Young*alphas)/(1-poi))*T:
> stresstheta:=(1/d)*(Ntheta+Nt)+((12*z)/(d^3))*0*(Mtheta + Mt)-((Young*alphas)/(1-poi))*T:
> stressrtheta:=0:
>
>
> #Jet stress
> BR:=Young*d^3/(12*(1-poi^2)):
> P:=5*10^6:
> tolerance:=10:
> ro:=.001:
> jetpro:=P*exp(-s*r^2):
> s2:=-evalf(ln(tolerance/P)/ro^2):
> jetpro2:=subs(s=s2,jetpro):
> wp:=(1/BR)*int(int(int(int(jetpro2*r,r=0..x)/x,x=0..y)*y,y=0..z)/z,z=0..r):
> wj:=wp+c2j*r^2/4+c4j:
> krj:=-diff(diff(wj,r),r):
> ktj:=-(1/r)*diff(wj,r):
> Mrj:=BR*(krj+poi*ktj):
> Mrjb:=subs(r=b,Mrj):
> c2js:=solve(Mrjb=0,c2j):
> wj1:=wp+c2js*r^2/4+c4j:
> wj1b:=subs(r=b,wj1):
> c4js:=solve(wj1b=0,c4j):
> wjs:=wp+c2js*r^2/4+c4js:
> krj2:=-diff(diff(wjs,r),r):
> ktj2:=-(1/r)*diff(wjs,r):
> Mrj2:=BR*(krj2+poi*ktj2):
```

```
> Mtj2:=BR*(poi*krj2+ktj2):
> stressrj:=6*Mrj2/d^2:
> stresstj:=6*Mtj2/d^2:
> stressrjd:=(2*z/d)*stressrj:
> stresstjd:=(2*z/d)*stresstj:
>
> #plot(wjs,r=b/200..b);
> evalf(subs(r=b/200,z=-d/2,stressrjd/10^6));
>
> #Prinicpal Stresses
> stressrtot:=(stressr-0*stressrjd)/(1*10^6):
> stressttot:=(stresstheta-0*stresstjd)/(1*10^6):
> shearrt:=0:
> sigma1:=((stressrtot+stressttot)/2)-sqrt(((stressrtot-stressttot)/2)^2+shearrt):
> sigma2:=((stressrtot+stressttot)/2)+sqrt(((stressrtot-stressttot)/2)^2+shearrt):
>
> factor(limit(subs(z=d/2,sigma1),r=0)):      #simplify stress terms
>
> #Failure Theories
> sigmay:=1.394*10^(-9)*(T+298)^3+3.7618*10^(-5)*(T+298)^2-.2321*(T+298)+330.37:
> sigmau:=500:
> test1:=sigmay^2:
> test2:=(sigma1^2)-(sigma1*sigma2)+sigma2^2:
> plot(subs(r=b/200,test1-test2),z=-d/2..d/2);
>
>
> #Check linear deflection assumption
> strainl:=subs(r=b/200,diff(u,r))-z*diff(diff(w,r),r)+z*diff(diff(wjs,r),r):
> strainn:=.5*(diff(w,r)-diff(wjs,r))^2:
> plot3d(strainl,r=b/100..b,z=-d/2..d/2);
> plot3d(strainn,r=b/100..b,z=-d/2..d/2);
> plot3d(strainl-strainn,r=b/100..b,z=-d/2..d/2);
>
>
> #Strain correlations
> TL:=((a^4)/(b^2))*(d-exp(-.00005*(b/a)^2)+(b/a)^2)+d*(2+exp(-.00005*(b/a)^2)-
((a/b)^2))+((z/d)^2)*(1-((a/r)^2)+(((a/r)^2)+1)*exp(-2*(r/a)^2))-(z/d)*(1+((a/r)^2)-((a/r)^2)*exp(-
2*(r/a)^2)):
> strainlcorr:=(-
.00014227/0.0034855)*evalf(subs(r=b/10,z=d/2,a=.01,poi=.3,b=.2,d=.001,Thot=1372,alphas=4.5*10^(-
6),(1+poi)*Thot*alphas*TL)):
> TN:=(1/d^2)*(((z/d)*((a^2)*((r/b^2)+(1/r)-exp(-2*(r/a)^2)/r)-(2*r))+(a^2)*((1/r)+(r/b^2)-exp(-
2*(r/a)^2)/r) +r)^2):
>
strainncorr:=(.000016096/0.001169579)*evalf(subs(r=b/10,z=d/2,a=.0075,poi=.3,b=.2,d=.001,Thot=1372
,alphas=4.5*10^(-6),(((1+poi)*alphas*Thot)^2)*TN)):
>
>
> #Quick Check for failure with stress correlations, Comparison at location of max stress
> thermalrcorr:=(215.5/787.09)*(1*10^(-6))*(Young*alphas*Thot*exp(-b^2))/(1-poi):
> thermaltancorr:=(156.02/787.09)*(1*10^(-6))*(Young*alphas*Thot*exp(-b^2))/(1-poi):
> jetcorr:=subs(z=-.25*d,stressjmax):
> stressrcorr:=thermalrcorr-jetcorr:
> stresstcorr:=thermaltancorr-jetcorr:
```

```
> sigma1corr:=((stressrcorr+stresstcorr)/2)+sqrt(((stressrcorr-stresstcorr)/2)^2):
> sigma2corr:=((stressrcorr+stresstcorr)/2)-sqrt(((stressrcorr-stresstcorr)/2)^2):
> test2corr:=(sigma1corr^2)-(sigma1corr*sigma2corr)+sigma2corr^2:
> test1corr:=(evalf(subs(r=0,z=-.25*d,sigmay)))^2:
> Fail:=test1corr-test2corr:      #positive means ok, negative means fail, not for jet dominated
```

VII. Localized Heating of Fixed Plate

```
> # Fixed plate with a guassian temperature distribution imposed top surface
>
> #Constants
> Young:=61.4*10^9:                #Youngs modulus
> alpha:=14.1*10^(-6):             #linear expansion coefficient
> poi:=.3:                         #poisson's ratio
> a:=.0075:                        #constant which expresses rate of gaussian decay
> d:=.001:                         #plate thickness in m
> b:=.2:                           #radius in m
>
>
> #Temperature characteristics
> k:=229:                          #thermal conductivity
> To:=298:                         #ambient temperature
> Tc:=298:                         #cold temperature
> Thot:=125:                       #hot temperature rise
> Th:=To+Thot*(exp(-(2*r^2)/a^2)): #maximum temperature function
> T:=((Th-Tc)*(z/d)+(Th+Tc)/2)-298: #temperature
> flux:=evalf(subs(r=0,k*diff(T,z)))/(1*10^6);
>
> #Membrane stresses
> Tn:=int(T,z=-d/2..d/2):
> Fm:=int(Tn*r,r):
> Fma:=Fm-subs(r=0,Fm):
> Fmb:=subs(r=b,Fm)-subs(r=0,Fm):
> C1:=((1+poi)*alpha/(b^2))*Fmb:
> C2:=0:
> u:=((((1+poi)*alpha)/r)*Fma) +C1*r:                    #displacement
> Nr:=(-Young*alpha/(r^2))*Fma +(Young*C1/(1-poi)):   #thermal force terms
> Ntheta:=(Young*alpha/(r^2))*Fma - Young*alpha*Tn + (Young*C1/(1-poi)):
>
>
> #Bending stresses
> BR:=(Young*d^3)/(12*(1-poi^2)):                        #Bending rigidity
> Nt:=((Young*alpha)/(1-poi))*int(T,z=-d/2..d/2):
> Mt:=((Young*alpha)/(1-poi))*int(T*z,z=-d/2..d/2):
> C3:=-(1/(2*BR))*int(Mt*r,r=0..b):
> C4:=-C3/(b^2):
> temp1:=int(Mt*r/BR,r):
> temp1a:=temp1-subs(r=0,temp1):
> temp2:=int(temp1a/r,r):
> temp2a:=subs(r=b,temp2)-temp2:
> w:=C3+C4*r^2+temp2a:                                   # deflection, a positive value
> kr:=-diff(diff(w,r),r):
> kth:=-diff(w,r)/r:
```

```
> Mr:=BR*(kr+poi*kth)-Mt:                                    # thermal moment terms
> Mth:=BR*(poi*kr+kth)-Mt:
>
> #Total stresses
> stressr:=(1/d)*(Nr+Nt)- ((12*z)/(d^3))*(Mr+Mt) - (Young*alpha/(1-poi))*T:
> stresstheta:=(1/d)*(Ntheta+Nt) -((12*z)/(d^3))*(Mth+Mt) -(Young*alpha/(1-poi))*T:
>
>
> #Jet Stresses
> P:=5*10^6:                          # program constants
> ro:=.001:
> tolerance:=10:
> jetpro:=P*exp(-s*r^2):
> s2:=-evalf(ln(tolerance/P)/ro^2):
> jetpro2:=subs(s=s2,jetpro):
> wp:=(1/BR)*int(int(int(int(jetpro2*r,r=0..x)/x,x=0..y)*y,y=0..z)/z,z=0..r):      #particular solution
> wj:=wp+c2j*r^2/4+c4j:                                                          #equation constants
> wjb:=subs(r=b,wj):
> diffwjb:=subs(r=b,diff(wj,r)):
> c2jf:=solve(diffwjb=0,c2j):
> wj1:=wp+c2jf*r^2/4+c4j:
> wj1b:=subs(r=b,wj1):
> c4jf:=solve(wj1b=0,c4j):
> wjf:=wp+c2jf*r^2/4+c4jf:
> krj:=-diff(diff(wjf,r),r):
> ktj:=-(1/r)*diff(wjf,r):
> Mrj:=BR*(krj+poi*ktj):
> Mtj:=BR*(poi*krj+ktj):
> stressrj:=6*Mrj/d^2:
> stresstj:=6*Mtj/d^2:
> stressrjd:=(2*z/d)*stressrj:
> stresstjd:=(2*z/d)*stresstj:
> evalf(subs(r=b/200,z=-d/2,stressrjd/10^0));
>
>
> #Prinicipal Stresses
> stressrtot:=(stressr-stressrjd)/(1*10^6):
> stressttot:=(stresstheta-stresstjd)/(1*10^6):
> shearrt:=0:
> sigma1:=((stressrtot+stressttot)/2)-sqrt(((stressrtot-stressttot/2)^2)+shearrt):
> sigma2:=((stressrtot+stressttot)/2)+sqrt(((stressrtot-stressttot/2)^2)+shearrt):
>
> #Failure Theories
> sigmay:=((2.61*10^(-5))*(T+298)^3)-(.0362*(T+298)^2)+(15.19*(T+298))-1720:
> sigmau:=500:
> #sigmay:=1.394*10^(-9)*(T+298)^3+3.7618*10^(-5)*(T+298)^2-.2321*(T+298)+330.37:
> #sigmay:=4370*exp(-.0055*(T+298))+81.6:
> #sigmay:=(450/810)*(-5.4608*10^(-7)*(T+298)^3+.0018*(T+298)^2-2.2*(T+298)+1334.4):
> test1:=sigmay^2:
> test2:=(sigma1^2)-(sigma1*sigma2)+sigma2^2:
> plot(subs(r=b/100,test1-test2),z=-d/2..d/2);
>
> #Check linear strain assumption
> strainl:=subs(r=b/200,diff(u,r)) -z*diff(diff(w,r),r)-z*diff(diff(wjf,r),r):
```

```
> strainn:=.5*(diff(w,r)+diff(wjf,r))^2:
> plot3d(strainl,r=b/200..b/1.01,z=-d/2..d/2);
> plot3d(strainn,r=b/200..b/1.01,z=-d/2..d/2);
> plot3d(strainl-strainn,r=b/200..b/1.01,z=-d/2..d/2);
```

VIII. Uniform Heating of Fixed Plate

```
> #Fixed plate, uniformly heated
>
> Young:=312*10^9:                  #Youngs modulus
> alpha:=4.2*10^(-6):               #linear coefficient of expansion
> poi:=.3:                          #poisson's ratio
> d:=.001:                          #plate thickness in m
> b:=.2:                            #plate radius in m
>
> #Temperature characteristics
> k:=147:                           #thermal conductivity
> To:=298:                          #ambient temperature
> Tc:=298:                          #cold temperature
> Thot:=595:                        #hot temperature
> T:=((Thot-Tc)*(z/d)+(Thot+Tc)/2)-298:  #temperature
> flux:=evalf(subs(r=0,k*diff(T,z)))/(1*10^6):
>
>
> #Membrane stresses
> Tn:=int(T,z=-d/2..d/2):
> Fm:=int(Tn*r,r):
> Fma:=Fm-subs(r=0,Fm):
> Fmb:=subs(r=b,Fm)-subs(r=0,Fm):
> C1:=((1+poi)*alpha/(b^2))*Fmb:
> C2:=0:
> u:=((((1+poi)*alpha)/r)*Fma) +C1*r:
> Nr:=(-Young*alpha/(r^2))*Fma +(Young*C1/(1-poi)):
> Ntheta:=(Young*alpha/(r^2))*Fma - Young*alpha*Tn + (Young*C1/(1-poi)):
>
>
> #Bending stresses
> BR:=(Young*d^3)/(12*(1-poi^2)):
> Nt:=((Young*alpha)/(1-poi))*int(T,z=-d/2..d/2):
> Mt:=((Young*alpha)/(1-poi))*int(T*z,z=-d/2..d/2):
> C3:=-(1/(2*BR))*int(Mt*r,r=0..b):
> C4:=-C3/(b^2):
> temp1:=int(Mt*r/BR,r):
> temp1a:=temp1-subs(r=0,temp1):
> temp2:=int(temp1a/r,r):
> temp2a:=subs(r=b,temp2)-temp2:
> w:=C3+C4*r^2+temp2a:
> kr:=-diff(diff(w,r),r):
> kth:=-diff(w,r)/r:
> Mr:=BR*(kr+poi*kth)-Mt:
> Mth:=BR*(poi*kr+kth)-Mt:
>
> #Total Stresses
> stressr:=(1/d)*(Nr+Nt)- ((12*z)/(d^3))*(Mr+Mt) - (Young*alpha/(1-poi))*T:
```

```
> stresstheta:=(1/d)*(Ntheta+Nt) -((12*z)/(d^3))*(Mth+Mt) -(Young*alpha/(1-poi))*T:
>
>
> #Jet solution
> P:=5*10^6:                              # program constants
> ro:=.001:
> tolerance:=10:
>  jetpro:=P*exp(-s*r^2):
> s2:=-evalf(ln(tolerance/P)/ro^2):
> jetpro2:=subs(s=s2,jetpro):
> wp:=(1/BR)*int(int(int(int(jetpro2*r,r=0..x)/x,x=0..y)*y,y=0..z)/z,z=0..r):      #particular solution
> wj:=wp+c2j*r^2/4+c4j:                                                            #equation constants
> wjb:=subs(r=b,wj):
> diffwjb:=subs(r=b,diff(wj,r)):
> c2jf:=solve(diffwjb=0,c2j):
> wj1:=wp+c2jf*r^2/4+c4j:
> wj1b:=subs(r=b,wj1):
> c4jf:=solve(wj1b=0,c4j):
>  wjf:=wp+c2jf*r^2/4+c4jf:
> krj:=-diff(diff(wjf,r),r):
> ktj:=-(1/r)*diff(wjf,r):
> Mrj:=BR*(krj+poi*ktj):
> Mtj:=BR*(poi*krj+ktj):
> stressrj:=6*Mrj/d^2:
> stresstj:=6*Mtj/d^2:
> stressrjd:=(2*z/d)*stressrj:
> stresstjd:=(2*z/d)*stresstj:
>
> #Prinicipal Stresses
> stressrtot:=(stressr-0*stressrjd)/(1*10^6):
> stressttot:=(stresstheta-0*stresstjd)/(1*10^6):
> shearrt:=0:
> sigma2:=((stressrtot+stressttot)/2)-sqrt(((stressrtot-stressttot/2)^2)+shearrt):
> sigma1:=((stressrtot+stressttot)/2)+sqrt(((stressrtot-stressttot/2)^2)+shearrt):
>
> #Failure Theories
> #sigmay:=(450/810)*(-5.4608*10^(-7)*(T+298)^3+.0018*(T+298)^2-2.2*(T+298)+1334.4):
> #sigmay:=2.61*10^(-5)*(T+298)^3-.0362*(T+298)^2+15.19*(T+298)-1720:
> sigmay:=4370*exp(-.0055*(T+298))+81.6:
> #sigmay:=1.394*10^(-9)*(T+298)^3+3.7618*10^(-5)*(T+298)^2-.2321*(T+298)+330.7:
> test1:=sigmay^2:
> test2:=(sigma1^2)-(sigma1*sigma2)+sigma2^2:
> plot(subs(r=b/200,test1-test2),z=-d/2..d/2);
>
>
> #check linear delfection assumption
> strainl:=subs(r=b/200,diff(u,r)) -z*diff(diff(w,r),r)-z*diff(diff(wjf,r),r):
> strainn:=.5*(diff(w,r)+diff(wjf,r))^2:
> plot3d(strainl,r=b/100..b/1.01,z=-d/2..d/2);
> plot3d(strainn,r=b/100..b/1.01,z=-d/2..d/2):
> plot3d(strainl-strainn,r=b/100..b/1.01,z=-d/2..d/2);
```

Matlab Program Listing

```
%This program determines where boundary conditions should be placed
%for a ANSYS model with a spacing factor.
%The user needs to input the RAD, SP, LNO terms used in the ANSYS code.
%Also input is needed on the diameter of the jet and heating radius desired.
%Three matrices are ouput. The matrix "loc" is the location of the elements
%in the ANSYS model in terms of meters. The matrix "Q" is the fraction
%of the maximium heat flux which acts at location on the beam. The maxtrix
%"H" is the fraction of the maximium heat transfer coeffieicent that acts
%on a location outside the stagnation zone of the jet. Note that the indicies
%for all three matricies are the same. Thus, if for example Q[8]=.4
%and loc[8]=.12, then at a radius of .12 m, 40% of the maximum heat flux acts
%on the beam.


RAD=.2;                          % radius of beam in m
sp=20;                           % spacing factor
Lno=100;                         % maximium node number
a=2/(.0075^2);                   % constant in expression exp(-2*r^2/a^2)
d=.002;                          % diameter of cooling jet
K=1;

inc=exp(log(sp)/Lno);            % increment on ANSYS element widith
x=.31/1000;                      % size of first element
                                 % x is found by summing "inc" over the RAD
                                 % and solving for x

loc(1)=.001;                     %start at primary portion of beam (1mm)
index=2;

for i=1:Lno                      % determine locations of elements
loc(index)=(inc^i)*x+loc(index-1);
index=index+1;
end

index=1;                         % reset index


for i=1:Lno                      % determine fractions
Q(index)=exp(-a*(loc(i))^2);
if (loc(i))^2 < d
H(index)=1-K*(((loc(i))^2)/d);
end
index=index+1;
end
```

ANSYS Numerical Code Listings

Instructions and advice on the use of ANSYS programs

The programs given below are for aluminum. If other materials need to be considered, the material properties in the code must be changed. See appendix B for properties of candidate materials.

The code assumes that the plate is three elements thick. If it is necessary to change this value, the user needs to generate more nodes by following the same pattern as used for the first three thickness. When changing the number of elements in the thickness, a greater or lesser number of elements results. This affects the creation of the secondary portion of the beam for the hot spot case. The user needs to change all references to the third thickness in the terms MAXN, CEN, etc., to the new thickness value.

If the radius of the plate is varied, significant changes in the model may be needed. First pick, a new radius by changing the term RAD. Load the program. If errors or warnings on meshing occur, the spacing factor (SP) needs to be changed. For larger radii, increase SP, for smaller radii reduce SP.

If either SP or RAD is changed, the placement of the boundary conditions will also change. To find the new placement, run the matlab program shown above with the new values of RAD and SP. Then re-write the boundary conditions in the ANSYS code.

A) Localized Heating Models for Aluminum 6010

There are two parts to this model. The first, determines the temperature distribution in an aluminum plate subjected to a small hot spot. The second program uses the temperature distribution to determine the stresses in the plate. Chapter 5 elaborates on the details.

The commands "C***" and "* " signify comments. Geometry and boundary condition variables which can be changed by the user are **bolded**. Read ANSYS instructions in Appendix C if geometry changes are necessary.

Only the models for aluminum are shown here. To consider other materials, the material properties need to be changed.

A.1) Thermal Model

```
/CORE,,,200000 * This line tells ANSYS how much memory it can use
/PREP7         * Commands that follow are from the PREP7 module
/TITLE, Localized heating of Aluminum 6010; Thermal
KAN,-1         * Thermal analysis follows
ET,1,55,,,1            * Use thermal axisymmetric element
R,1,1                  * Constants set to 1

MP,KXX,1,257.9,-.047           * Material properties (k,ρ,Cp)
MP,DENS,1,3010.6,-5.7879,.0033
MP,C,1,347.3,2.683,-.0039,2.25E-6

c*** MP,KXX,1,242              * Material properties that can be used for small transients
c*** MP,DENS,1,1578.859
c*** MP,C,1,860

RAD=.2                 * Radius of plate
D=.001/3                       *Thickness of element, assumes 3 elements thick
LNO=100                        * Number of nodes along radius in primary portion
INN=1                          * Increment nodes from 1 to LNO by INN
INL=LNO                        * Increment nodes in next thickness layer by INL
MAXN=4*LNO             * Last node in primary portion of plate
CEN=MAXN+1             * First node is secondary portion
CENL=CEN+9             * Last node on top surface of secondary portion
ECEN=3*(LNO-1)+1         * Last element on top surface of secondary portion
SP=20                          * Spacing factor between nodes of primary portion
                               * Allows finer meshing; matlab program determines
                               * boundary condition placement using this value.
C*** Primary portion of beam
C*** The primary portion of the beam consists of the all nodes elements after the first
C*** millimeter of the radius. Node 1 starts at the plate top and at a radius of 1 mm.
C*** The plate is three elements thick. This value should not be changed. If it is more
C*** nodes need to be generated and all references to maximum nodes need to be
C*** changed.

N,1,0.001                      * Location of first node
N,LNO,RAD                      * Node LNO located at distance RAD
FILL,1,LNO,,,,,SP              * Create nodes between 1 and LNO spaced by SP
NGEN,2,LNO,1,LNO,INN,,-D       * Generate nodes for 1st thickness
```

```
NGEN,2,2*LNO,1,LNO,INN,,-2*D        * Generate nodes for 2nd thickness
NGEN,2,3*LNO,1,LNO,INN,,-3*D        * Generate nodes for 3rd thickness


E,1,2,2+INL,1+INL                   * Create first element in 1st thickness
E,1+INL,2+INL,2+2*INL,1+2*INL       * Create first element in 2nd thickness
E,1+2*INL,2+2*INL,2+3*INL,1+3*INL * Create first element in 3rd thickness

EGEN,LNO-1,1,1                      * Create elements along 1st thickness
EGEN,LNO-1,1,2                      * Create elements along 2nd thickness
EGEN,LNO-1,1,3                      * Create elements along 3rd thickness

C*** Secondary portion of beam.
C*** The secondary portion of the beam consists of the first millimeter of the plate. Each
C*** element has a width of 0.1 mm. This allows a fine mesh to be generated. A fine
C*** mesh is needed to adequately model the effect of the cooling jet.

N,CEN                       * First node in secondary portion
N,CENL,0.0009               * Last node on top surface of secondary portion
FILL,CEN,CENL                       * Fill in nodes on top surface
NGEN,2,LNO,CEN,CENL,INN,,-D         * Nodes for 1st thickness
NGEN,2,2*LNO,CEN,CENL,INN,,-2*D     * Nodes for 2nd thickness
NGEN,2,3*LNO,CEN,CENL,INN,,-3*D     * Nodes for 3rd thickness

E,CEN,CEN+1,CEN+1+INL,CEN+INL       * 1st element in 1st thickness
E,CEN+INL,CEN+1+INL,CEN+1+2*INL,CEN+2*INL * 1st element in 2nd thicknes
E,CEN+2*INL,CEN+1+2*INL,CEN+1+3*INL,CEN+3*INL * 1st element in 3rd thick.
EGEN,9,1,ECEN                       * Generate elements along 1st thickness
EGEN,9,1,ECEN+1                             * Generate elements along 2nd thickness
EGEN,9,1,ECEN+2                             * Generate elements along 3rd thickness

E,CENL,1,1+INL,CENL+INL             * Generate last element in 1st thickness
E,CENL+INL,1+INL,1+2*INL,CENL+2*INL * Generate last element in 2nd thickness
E,CENL+2*INL,1+2*INL,1+3*INL,CENL+3*INL  * Generate last element in 3rd thick.

WSORT,X,0                                   * Resorts elements; reduces computing time
WSORT,Y,0

C*** Flux boundary conditions

FLU=110E6                   * Maximum heat flux incident on beam
EC,ECEN,1,1,FLU             * Convection term used to simulate flux (temp=flu, h=1,
                            * therefore q"=flu)
EC,ECEN+3,1,1,FLU,ECEN+10,1  * These lines consider secondary beam
EC,ECEN+27,1,1,FLU

EC,1,1,1,.97*FLU        * Flux over primary beam, generated by matlab program
EC,4,1,1,.94*FLU
EC,5,1,1,.91*FLU
EC,6,1,1,.87*FLU
EC,7,1,1,.82*FLU
EC,8,1,1,.77*FLU
EC,9,1,1,.72*FLU
```

```
EC,10,1,1,.65*FLU
EC,11,1,1,.59*FLU
EC,12,1,1,.53*FLU
EC,13,1,1,.46*FLU
EC,14,1,1,.4*FLU
EC,15,1,1,.34*FLU
EC,16,1,1,.28*FLU
EC,17,1,1,.23*FLU
EC,18,1,1,.18*FLU
EC,19,1,1,.14*FLU
EC,20,1,1,.08*FLU
EC,21,1,1,.05*FLU
EC,22,1,1,.04*FLU
EC,23,1,1,.02*FLU
EC,24,1,1,.015*FLU
EC,25,1,1,.01*FLU
EC,26,1,1,.005*FLU
EC,27,1,1,.003*FLU
EC,28,1,1,.002*FLU
EC,29,1,1,.0009*FLU
EC,30,1,1,.0004*FLU
EC,31,1,1,.0002*FLU
EC,32,1,1,.0001*FLU


C*** Jet convection boundary conditions

JET=5E5                         * Convection coefficient
EC,ECEN+2,3,JET,298    * Convection on secondary beam
EC,ECEN+19,3,JET,298,ECEN+26,1
EC,ECEN+29,3,JET,298

EC,3,3,.99*JET,298          * Convection on primary beam, values generated by matlab
                                * program
EC,2*(LNO-1)+2,3,.99*JET,298
EC,2*(LNO-1)+3,3,.99*JET,298
EC,2*(LNO-1)+4,3,.99*JET,298
EC,2*(LNO-1)+5,3,.99*JET,298
EC,2*(LNO-1)+6,3,.99*JET,298
EC,2*(LNO-1)+7,3,.99*JET,298
EC,2*(LNO-1)+8,3,.99*JET,298
EC,2*(LNO-1)+9,3,.99*JET,298
EC,2*(LNO-1)+10,3,.99*JET,298
EC,2*(LNO-1)+11,3,.99*JET,298
EC,2*(LNO-1)+12,3,.98*JET,298
EC,2*(LNO-1)+13,3,.98*JET,298
EC,2*(LNO-1)+14,3,.98*JET,298
EC,2*(LNO-1)+15,3,.98*JET,298
EC,2*(LNO-1)+16,3,.98*JET,298
EC,2*(LNO-1)+17,3,.97*JET,298
EC,2*(LNO-1)+18,3,.97*JET,298
EC,2*(LNO-1)+19,3,.96*JET,298
EC,2*(LNO-1)+20,3,.96*JET,298
EC,2*(LNO-1)+21,3,.95*JET,298
```

```
EC,2*(LNO-1)+22,3,.95*JET,298
EC,2*(LNO-1)+23,3,.94*JET,298
EC,2*(LNO-1)+24,3,.93*JET,298
EC,2*(LNO-1)+25,3,.927*JET,298
EC,2*(LNO-1)+26,3,.92*JET,298
EC,2*(LNO-1)+27,3,.91*JET,298
EC,2*(LNO-1)+28,3,.9*JET,298
EC,2*(LNO-1)+29,3,.89*JET,298
EC,2*(LNO-1)+30,3,.88*JET,298
EC,2*(LNO-1)+31,3,.87*JET,298
EC,2*(LNO-1)+32,3,.85*JET,298
EC,2*(LNO-1)+33,3,.84*JET,298
EC,2*(LNO-1)+34,3,.82*JET,298
EC,2*(LNO-1)+35,3,.81*JET,298
EC,2*(LNO-1)+36,3,.79*JET,298
EC,2*(LNO-1)+37,3,.77*JET,298
EC,2*(LNO-1)+38,3,.75*JET,298
EC,2*(LNO-1)+39,3,.73*JET,298
EC,2*(LNO-1)+40,3,.71*JET,298
EC,2*(LNO-1)+41,3,.68*JET,298
EC,2*(LNO-1)+42,3,.65*JET,298
EC,2*(LNO-1)+43,3,.62*JET,298
EC,2*(LNO-1)+44,3,.59*JET,298
EC,2*(LNO-1)+45,3,.56*JET,298
EC,2*(LNO-1)+46,3,.52*JET,298
EC,2*(LNO-1)+47,3,.48*JET,298
EC,2*(LNO-1)+48,3,.44*JET,298
EC,2*(LNO-1)+49,3,.4*JET,298
EC,2*(LNO-1)+50,3,.35*JET,298
EC,2*(LNO-1)+51,3,.3*JET,298
EC,2*(LNO-1)+52,3,.24*JET,298
EC,2*(LNO-1)+53,3,.19*JET,298
EC,2*(LNO-1)+54,3,.12*JET,298
EC,2*(LNO-1)+55,3,.05*JET,298

C*** Solution procedure
TUNIF,298       * Inital temperature
KBC,1           * Boundary condition ramping
TIME,.1 * total time to solve transient for
ITER,-200,1,1   * 200 iterations if transient (time step =time/200); if steady state need only
                * 15 iterations (blank out KBC and TIME)
```

A.2) Structural Model

```
/CORE,,,200000          * This line tells ANSYS how much memory it can use
/PREP7                  * Commands that follow are from the PREP7 module
/TITLE, Localized Heating of Aluminum 6010
RESUME                          * Tells ANSYS to start where the thermal model left off
KAN,0                           * This is a structural analysis

KTEMP,,,0.0015          * inputs the temperatures found at .0015 secs
C*** KTEMP,1,15             * alternatively, if steady state, inputs temps at iteration 15
```

```
C*** STRUCTURAL ANALYSIS
ET,1,42,,,1                    * Use an structural 2D axisymmetric element
R,1,1                      * Sets constants to one.
MP,EX,1,100.4E9,-.065E9        * Material property functions (E,ν,and α)
MP,NUXY,1,.3
MP,ALPX,1,11.18E-6,.0049E-6
KNL,1                          * Signifies that plasticity should be considered
NLTAB,1,2                      * Defines bi-linear stress-strain curve
NLY,DEFI,,298,282E6,54E6
NLY,DEFI,,450,241E6,23E6
NLY,DEFI,,500,193E6,23E6
NLY,DEFI,,750,22E6,22E6
NLY,DEFI,,800,8.3E6,9E6
NLY,DEFI,,1000,3E6,9E6

RAD=.2              * Radius of plate
D=.001/3                    *Thickness of element, assumes 3 elements thick
LNO=100                     * Number of nodes along radius in primary portion
INN=1                       * Increment nodes from 1 to LNO by INN
INL=LNO                     * Increment nodes in next thickness layer by INL
MAXN=4*LNO          * Last node in primary portion of plate
CEN=MAXN+1          * First node is secondary portion
CENL=CEN+9          * Last node on top surface of secondary portion
ECEN=3*(LNO-1)+1       * Last element on top surface of secondary portion
TREF,298                    * Reference temperature, ΔT=T-TREF
SP=20                       * Spacing factor between nodes of primary portion
                            * Allows finer meshing; matlab program determines
                            * boundary condition placement using this value.


C*** Primary portion of beam
C*** The primary portion of the beam consists of the all nodes elements after the first
C*** millimeter of the radius. Node 1 starts at the plate top and at a radius of 1 mm.
C*** The plate is three elements thick. This value should not be changed. If it is more
C*** nodes need to be generated and all references to maximum nodes need to be
C*** changed.

N,1,0.001                   * Location of first node
N,LNO,RAD                   * Node LNO located at distance RAD
FILL,1,LNO,,,,,,SP          * Create nodes between 1 and LNO spaced by SP
NGEN,2,LNO,1,LNO,INN,,-D    * Generate nodes for 1st thickness
NGEN,2,2*LNO,1,LNO,INN,,-2*D        * Generate nodes for 2nd thickness
NGEN,2,3*LNO,1,LNO,INN,,-3*D        * Generate nodes for 3rd thickness


E,1,2,2+INL,1+INL                   * Create first element in 1st thickness
E,1+INL,2+INL,2+2*INL,1+2*INL       * Create first element in 2nd thickness
E,1+2*INL,2+2*INL,2+3*INL,1+3*INL * Create first element in 3rd thickness

EGEN,LNO-1,1,1                      * Create elements along 1st thickness
EGEN,LNO-1,1,2                      * Create elements along 2nd thickness
EGEN,LNO-1,1,3                      * Create elements along 3rd thickness
```

```
C*** Secondary portion of beam.
C*** The secondary portion of the beam consists of the first millimeter of the plate. Each
C*** element has a width of 0.1 mm. This allows a fine mesh to be generated. A fine
C*** mesh is needed to adequately model the effect of the cooling jet.

N,CEN                          * First node in secondary portion
N,CENL,0.0009                  * Last node on top surface of secondary portion
FILL,CEN,CENL                          * Fill in nodes on top surface
NGEN,2,LNO,CEN,CENL,INN,,-D            * Nodes for 1st thickness
NGEN,2,2*LNO,CEN,CENL,INN,,-2*D        * Nodes for 2nd thickness
NGEN,2,3*LNO,CEN,CENL,INN,,-3*D        * Nodes for 3rd thickness

E,CEN,CEN+1,CEN+1+INL,CEN+INL      * 1st element in 1st thickness
E,CEN+INL,CEN+1+INL,CEN+1+2*INL,CEN+2*INL * 1st element in 2nd thicknes
E,CEN+2*INL,CEN+1+2*INL,CEN+1+3*INL,CEN+3*INL * 1st element in 3rd thick.
EGEN,9,1,ECEN                          * Generate elements along 1st thickness
EGEN,9,1,ECEN+1                                * Generate elements along 2nd thickness
EGEN,9,1,ECEN+2                                * Generate elements along 3rd thickness

E,CENL,1,1+INL,CENL+INL            * Generate last element in 1st thickness
E,CENL+INL,1+INL,1+2*INL,CENL+2*INL * Generate last element in 2nd thickness
E,CENL+2*INL,1+2*INL,1+3*INL,CENL+3*INL  * Generate last element in 3rd thick.

WSORT,X,0                                      * Resorts elements; reduces computing time
WSORT,Y,0

ITER,-15,1                                     * Number of iterations; need since non-linear

C*** Edge Conditions for fixed plate

D,CEN,UX,,,,,ROTZ                              * Fix displacements at edge
D,CEN+INL,UX,,,,,ROTZ
D,CEN+2*INL,UX,,,,,ROTZ
D,CEN+3*INL,UX,,,,,ROTZ

C*** Boundary conditions at plate center
D,LNO,ALL                                      * Fix center since axisymmetric
D,LNO+INL,ALL
D,LNO+2*INL,ALL
D,LNO+3*INL,ALL

C***  Edge conditions for simply supported plate
C*** D,LNO,UY
C*** D,LNO+INL,UY
C*** D,LNO+2*INL,UY
C*** D,LNO+3*INL,UY

C*** Jet Pressure load in MPa
EP,ECEN+2,3,4.7E6      * Pressure term for each element in 1st millimeter
EP,ECEN+19,3,4.02E6
EP,ECEN+20,3,3.1E6
EP,ECEN+21,3,2.1E6
EP,ECEN+22,3,1.3E6
```

```
EP,ECEN+23,3,.71E6
EP,ECEN+24,3,.35E6
EP,ECEN+25,3,.16E6
EP,ECEN+26,3,.06E6
EP,ECEN+29,3,.02E6

C*** Plot of model with boundary conditions
/PBC,ALL,2
SBCTRA
/VIEW,1,1,1,1
EPLOT
```

B) Uniform Heating of Aluminum 6010

There are two parts to this model. The first, determines the temperature distribution in an aluminum plate subjected to a uniform heat flux load. The second program uses the temperature distribution to determine the stresses in the plate. Chapter 7 elaborates on the details.

The commands "C***" and "* " signify comments. Geometry and boundary condition variables which can be changed by the user are **bolded**. Read ANSYS instructions in Appendix C if geometry changes are necessary.

Only the models for aluminum are shown here. To consider other materials, the material properties need to be changed.

B.1) Thermal Model

```
/CORE,,,200000 * ANSYS memory use
/PREP7         * Commands from PREP7 module
/TITLE, Uniform heating of Aluminum 6010

KAN,-1 * thermal analysis
ET,1,55,,,1        * thermal axisymmetric element
R,1,1              * set constants to one
MP,KXX,1,257.9,-.047          * Material properties (k,ρ,Cp)
MP,DENS,1,3010.6,-5.7879,.0033
MP,C,1,347.3,2.683,-.0039,2.25E-6

C*** MP,KXX,1,242             * Material properties for small transients
C*** MP,DENS,1,1579
C*** MP,C,1,860

RAD=.005                      * Plate Radius
D=.001/3                      * Element thickness
LNO=25                        * Last node on top surface
INN=1                         * Increment nodes from 1 to LNO by INN
INL=LNO                       * Increment nodes per thickness by INL

C*** Node and Element Generation
N,1                           * Node 1
N,LNO,RAD                     * Last node on top surface
FILL,1,LNO,,,,,SP             * Create nodes between 1 and LNO on top surface
```

```
NGEN,2,LNO,1,LNO,INN,,-D      * Generate nodes for 1st thickness
NGEN,2,2*LNO,1,LNO,INN,,-2*D      * Generate nodes for 2nd thickness
NGEN,2,3*LNO,1,LNO,INN,,-3*D      * Generate nodes for 3rd thickness


E,1,2,2+INL,1+INL                 * 1st element in 1st thickness
E,1+INL,2+INL,2+2*INL,1+2*INL     * 1st elment in 2nd thickness
E,1+2*INL,2+2*INL,2+3*INL,1+3*INL *1st element in 3rd thickness

EGEN,LNO-1,1,1                    * Generate elements in 1st thickness
EGEN,LNO-1,1,2                    * Generate elements in 2nd thickness
EGEN,LNO-1,1,3                    * Generate elements in 3rd thickness

WSORT,X,0                         * Resort elements to reduce computing time
WSORT,Y,0

C*** Boundary conditions

FLU=100E6                 * heat flux value
EC,1,1,1,FLU              *  heat flux along top surface, use convection term to get q"
EC,4,1,1,FLU,LNO+1,1

JET=5E5                           * Convection on bottom surface
EC,3,3,JET,298
EC,2*(LNO-1)+2,3,JET,298,3*(LNO-1),1


C*** Solution procedure
TUNIF,298       * Inital temperature
KBC,1           * Boundary condition ramping
TIME,.1 * total time to solve transient
ITER,-200,1,1   * 200 iterations if transient (time step =time/200); if steady state need only
                * 15 iterations (blank out KBC and TIME)
```

B.2) Structural Model

```
/CORE,,,200000 * ANSYS memory usage
/PREP7         * commands from PREP7 module
/TITLE, Uniform heating of Aluminum 6010
RESUME                  * begin where thermal model left off
KAN,0                   * structural analysis
KTEMP,,,.001            * Use temperature data at .001 secs as input (transient)
C*** KTEMP,1,15         * Use temperature data at iteration 15 as input (steady state)
ET,1,42,,,1             * use structural 2D axisymmetric element
R,1,1                   * set constants to one
MP,EX,1,100.4E9,-.065E9         *Material properties
MP,NUXY,1,.3
MP,ALPX,1,11.18E-6,.0049E-6
KNL,1                   * Consider plasticity
NLTAB,1,2               * Define plastic properties
NLY,DEFI,,298,282E6,54E6
NLY,DEFI,,450,241E6,23E6
NLY,DEFI,,500,193E6,23E6
```

```
NLY,DEFI,,750,22E6,22E6
NLY,DEFI,,800,8.3E6,9E6
NLY,DEFI,,1000,3E6,9E6

RAD=.005                          * Plate Radius
D=.001/3                          * Element thickness
LNO=25                            * Last node on top surface
INN=1                             * Increment nodes from 1 to LNO by INN
INL=LNO                           * Increment nodes per thickness by INL

C*** Node and Element Generation
N,1                               * Node 1
N,LNO,RAD                         * Last node on top surface
FILL,1,LNO,,,,,,SP                * Create nodes between 1 and LNO on top surface
NGEN,2,LNO,1,LNO,INN,,-D      * Generate nodes for 1st thickness
NGEN,2,2*LNO,1,LNO,INN,,-2*D      * Generate nodes for 2nd thickness
NGEN,2,3*LNO,1,LNO,INN,,-3*D      * Generate nodes for 3rd thickness


E,1,2,2+INL,1+INL                 * 1st element in 1st thickness
E,1+INL,2+INL,2+2*INL,1+2*INL     * 1st elment in 2nd thickness
E,1+2*INL,2+2*INL,2+3*INL,1+3*INL *1st element in 3rd thickness

EGEN,LNO-1,1,1                    * Generate elements in 1st thickness
EGEN,LNO-1,1,2                    * Generate elements in 2nd thickness
EGEN,LNO-1,1,3                    * Generate elements in 3rd thickness

WSORT,X,0                         * Resort elements to reduce computing time
WSORT,Y,0

ITER,-10,1


C***    Edge conditions if  fixed

D,1,UX,,,,,ROTZ
D,1+INL,UX,,,,,ROTZ
D,1+2*INL,UX,,,,,ROTZ
D,1+3*INL,UX,,,,,ROTZ

C*** Edge boundary conditions if simply supported
C*** D,LNO,UY
C*** D,LNO+INL,UY
C*** D,LNO+2*INL,UY
C*** D,LNO+3*INL,UY

C*** Center conditions; fixed since axisymetric

D,LNO,ALL
D,LNO+INL,ALL
D,LNO+2*INL,ALL
D,LNO+3*INL,ALL
```

```
C*** Jet Load, see matlab program
PRESS=5E6                    * Maximum pressure
EP,3,3,PRESS
EP,2*(LNO-1)+3,3,.804*PRESS
EP,2*(LNO-1)+5,3,.42*PRESS
EP,2*(LNO-1)+7,3,.142*PRESS
EP,2*(LNO-1)+9,3,.032*PRESS

C*** plot model
/PBC,ALL,2
SBCTRA
/VIEW,1,1,1,1
EPLOT
```